UNIVERSITY OF SOUTHAMPTON

ATRIAL ARCHITECTURE AND ELECTRICAL ACTIVATION

By Dr Timothy Rider Betts, MBChB MRCP

Doctorate Of Medicine

FACULTY OF BIOMEDICAL SCIENCES
SCHOOL OF MEDICINE

August 2002

UNIVERSITY OF SOUTHAMPTON

ABSTRACT

FACULTY OF BIOMEDICAL SCIENCES

SCHOOL OF MEDICINE

Doctorate Of Medicine

ATRIAL ARCHITECTURE AND ELECTRICAL ACTIVATION

By Dr Timothy Rider Betts

Previous researchers have investigated the origin and subsequent spread of sinus rhythm through the atria, but until recently these studies have been limited by the electrical mapping techniques available. A detailed appraisal of the literature is presented in Chapter 1. The thesis describes high-density, global right and left atrial activation patterns during sinus and paced rhythms in the porcine and human heart and when possible, correlates the findings with underlying atrial architecture. Central to the thesis methodology (Chapter 2) is the use of a novel electrophysiological mapping system. The EnSite 3000 system creates a three-dimensional reconstruction of cardiac chamber geometry. Onto this are superimposed high-density isopotential or isochronal maps. Sampling of the entire endocardium occurs 1200 times a second. A locator signal allows identification of anatomical structures and guiding of mapping catheters to specific sites of interest.

In Chapter 3, non-contact mapping of sinus rhythm and sinus tachycardia in the porcine heart revealed an unpredictable shift in earliest endocardial activation during changes in heart rate. These findings are contrary to previous reports and have implications for techniques used to treat arrhythmias such as inappropriate sinus tachycardia.

In Chapter 4, the spread of activation through the right atrial endocardium during sinus rhythm was correlated with endocardial dissection after the hearts were excised. A novel finding was the presence of conduction delay or block in the cavotricuspid isthmus, terminal crest and Triangle of Koch, which corresponded with changes in direction of myofibre orientation. The site of onset dictated the subsequent pattern of right atrial activation.

In Chapter 5, left atrial mapping in patients with a history of atrial fibrillation was performed during sinus rhythm and coronary sinus pacing. Areas of conduction block and delay were seen in the inferior septum and posterior left atrium. Left atrial and coronary sinus activation patterns were often dissociated. This is an important finding as coronary sinus electrograms are often used as a surrogate for left atrial activation.

In Chapter 6, right atrial mapping was performed in the porcine heart during coronary sinus pacing. This demonstrated that left to right conduction occurred at Bachmann's bundle during distal coronary sinus pacing and at the coronary sinus os during proximal pacing. The pattern of right atrial activation changed depending upon the site of left-to-right conduction. Activation was delayed or blocked as it traveled through the cavotricuspid isthmus. This was more apparent during proximal coronary sinus pacing. The lateral right atrium was activated by a wavefront that traveled posterior to the inferior caval vein. This has implications when assessing ablation of the cavotricuspid isthmus during treatment of atrial flutter.

In Chapter 7, the results of the preceding chapters were combined to design a catheter-based left atrial disconnection procedure using radiofrequency ablation. Successful atrial disconnection was performed in 10 out of 13 animals, although left atrial disconnection with intact right atrium to ventricular conduction was only achieved in 5 animals. This reduced the inducibility of atrial fibrillation from 100% to 30% of successfully disconnected subjects. Improvements in the technique may lead to its application in the human population.

In conclusion, the findings in this thesis extend current knowledge regarding the relationship between atrial architecture and electrical activation, and have led to the design and implementation of a new catheter-based therapy for atrial fibrillation.

List of contents

List of tables and illustrations

Preface

Cardiac electrophysiology is a fascinating scientific field that has grown rapidly over the last three decades. The huge technological leaps that now seem to happen almost overnight have provided the clinician and scientist with an exciting array of tools that can be used to investigate the intricacies of the onset and spread of the cardiac impulse. The 2-year research period that was undertaken to produce this thesis provided an opportunity to learn about research methodology, discover the basic principles of cardiac electrophysiology and use a novel and unique research tool. Southampton University Hospitals was one of the first centres in the world to gain a non-contact mapping system, and it soon became apparent that this particular technology was ideal for examining the relationship between cardiac activation and cardiac anatomy. We have watched this technology expand and become an accepted tool in the clinical electrophysiology laboratory, particularly for complex cases.

This thesis began by looking at the relationship between the normal cardiac impulse in the right atrium and its relationship to muscle architecture. As the experiments progressed and our knowledge increased, our attention turned to abnormal rhythm mechanisms. Although the thesis ends with an experiment to electrically disconnect the two atria and reduce the inducibility of atrial fibrillation, the work continues. Our findings are currently being used to design a multicentre trial of the atrial disconnection procedure in patients with refractory paroxysmal or persistent atrial fibrillation.

Although great progress has been made in recent years there is still much to be learned. This is what makes electrophysiology exciting!

Acknowledgements

This work is dedicated to Margaret, my wife, who endured 4 years of personal sacrifice, brought 2 children into the world, and looked after my every need during the design, implementation and writing up of the thesis.

My thanks go to my colleague, Dr Paul Roberts, who taught me everything he knew about porcine anatomy, physiology and anaesthesiology. I am also grateful to Dr Siew Yen Ho and Professor Robert Anderson of the National Heart and Lung Institute, who performed the anatomical dissection procedures and taught me cardiac anatomy. I would also like to acknowledge the British Cardiac Society who supported me during the 2-year research period.

Finally, I am indebted to my supervisors, Dr John Morgan and Dr Patrick Gallagher, whose constant support, knowledge, and constructive criticism guided me through the entire process.

Chapter 1: Introduction

The heartbeat is governed by the spread of an electrical impulse through the myocardium. Under normal circumstances, this impulse arises from the natural pacemaker, the sinoatrial node. The controlled and coordinated spread of the electrical impulse is vital for optimal cardiac function. Many previous researchers have investigated the origin and subsequent spread of sinus rhythm through the atria, but until recently these studies have been limited by the electrical mapping techniques available. An accurate, detailed description of the spread of the electrical impulse through the right and left atrial endocardial surface in the intact, beating heart has remained elusive.

Similarly, the relationships between heart rate, the site of impulse origin and the subsequent spread of activation has only been examined using epicardial or endocardial mapping techniques that have examined incomplete portions of the atrial surface. The precise relationship between the spread of the electrical impulse and the underlying myocardial architecture also remains to be defined. Previous studies have concentrated on isolated sections of cardiac muscle, but no study has yet described global right atrial endocardial activation in the intact, beating heart and subsequently compared this to the underlying endocardial architecture.

Electrical stimulation of the atria through pacing electrodes is now widely utilised as a therapy for brady- and tachyarrhythmias, as well as providing diagnostic information during electrophysiological procedures. The spread of electrical activation within and between the atria and its relationship to myocardial architecture during pacing has not been described in detail.

A greater understanding of the spread of the electrical impulse under natural and unnatural conditions is required to improve our understanding of atrial arrhythmias and help design preventative or therapeutic strategies. One such arrhythmia, atrial fibrillation, affects a significant proportion of the population and leads to increased morbidity and mortality. There is huge body of work that has examined the multitude of mechanisms that underlie the initiation and perpetuation of atrial fibrillation, yet an effective therapy remains elusive. To date, approaches that involve open-heart surgery, such as the Maze procedure, are the most effective, but have a limited application due their surgical nature. Catheter-based emulation of a surgical approach may present a less aggressive yet equally efficacious solution with reduced morbidity and mortality.

This thesis undertakes to provide a description of the spread of the electrical impulse through and between the atria during sinus rhythm and pacing using a new technology that provides

detailed three-dimensional mapping. Endocardial dissection of the atria will provide an anatomical correlate with the electrical activation pattern. Using the information gained from the initial studies, the feasibility of a novel trans-catheter ablation procedure to emulate a surgical therapy for atrial fibrillation will be tested.

Atrial anatomy

Gross anatomy of the human atria

In order to understand the relationship between atrial architecture and electrical activation, a detailed appreciation of atrial anatomy is required. Gross anatomical dissection of the human atrium provides us with a basic understanding.[1] Each atrium has three components – the appendage, the venous part and the vestibule, together with a septum separating the two atria. The posteriorly placed venous component has smooth walls and receives the superior caval vein in its upper and the inferior caval vein in its lower margins. The venous component also receives the coronary sinus, which drains the venous returns from the coronary circulation. The appendage is usually anatomically distinct, its internal surface corrugated by the folds of the pectinate muscles. The pectinate muscles themselves originate from a very prominent muscle bundle, the terminal crest that marks the junction of the appendage with the venous component. The appendage and the venous component border on the vestibule, which supports the leaflets of the tricuspid valve. The characteristic feature of the vestibule is that the pectinate muscles of the appendage surround it.

The septal surface of the right atrium contains the oval fossa. This structure marks the site of the fetal oval foramen. The oval foramen has an obvious rim that separates the foramen from the coronary sinus and the vestibule. The rim of the fossa for most of its extent is formed from infoldings of the walls of the atria. The floor of the oval fossa represents the true atrial septum. During fetal life a prominent fibromuscular fold, which extends as a continuation of the inferolateral margin of the terminal crest, directs blood from the inferior caval vein into the oval foramen. This persists after birth as the Eustachian valve or ridge.

The structure of the human left atrium is much simpler than that of the right. It also has three components. The venous component is the dominant part, receiving one of the four pulmonary veins at each of its corners. The appendage is much smaller, with a characteristic

tubular appearance, and a narrow junction with the venous component. The pectinate muscles are less prominent, being confined to the appendage, and there is no terminal crest marking the junction with the venous component. The flap valve marks the septal surface of the left atrium.

This basic introduction introduces the key components of atrial morphology. Before examining the various components of each atrium and their relevance to electrical activation in more detail, it is important to understand the muscular architecture of the chambers and establish morphological terms and references.

Myocardial Architecture

Much of our recent understanding of atrial architecture has been a result of the dissection studies by Professor Anderson's group at the National Heart and Lung Institute, London. In their paper published in 1995, they reported on 9 necropsied human hearts, all from patients who died from non-cardiac disease.[2] Each atrial chamber was dissected, with the endocardial layer removed in order to identify the arrangement of the internal musculature. The terms used in their paper will also be applied in this thesis. "Muscular bundle" or "band" is used to refer to bundles that can be seen with the naked eye simply by removing the endocardium or epicardium. The orientation of "circumferential" bundles is parallel to the atrioventricular ring, while "longitudinal" fibres run parallel to the interatrial groove and at right angles to the atrioventricular junction.

The atrial walls consist of intermingled muscular bundles orientated circumferentially and longitudinally (Figure 1). The largest, most prominent bundle in the right atrium is the terminal crest. It originates from the anterior aspect of the septum, passes in front of the orifice of the superior caval vein, and continues downwards on the right of the orifices of both caval veins, diminishing in size and merging inferiorly into the sub-Eustachian sinus near the orifice of the coronary sinus. Along its course it gives rise to 15-20 pectinate muscles that incline towards the vestibule and attach directly to the tricuspid ring at right angles. The lowermost pectinate muscle encircles the coronary sinus orifice and joins the sinus septum.

The interatrial band, commonly referred to as Bachmann's bundle, extends from the right of the orifice of the superior caval vein, crosses the atriocaval junction in front of the vein and spreads across the anterior wall of the left atrium transversely until it reaches the left atrial

Figure 1. Atrial musculature after removal of the epicardium

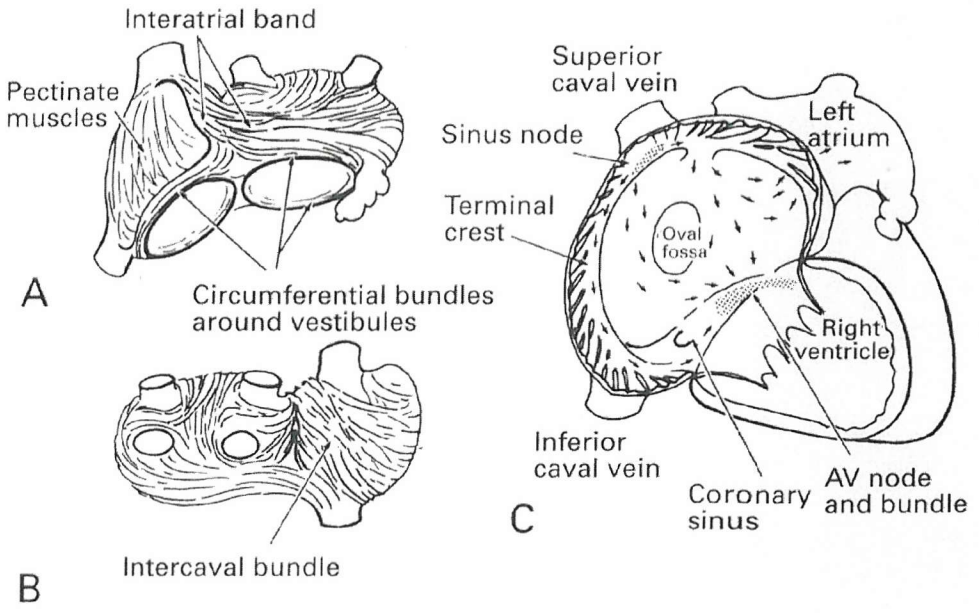

Diagrammatic representation of the (A) front and (B) back views of the overall arrangement of the atrial musculature after removal of epicardium. (C). Right atrium and the landmarks to the Triangle of Koch. Arrows represent the orientation of the major muscle bundles.

appendage, where it divides into upper and lower branches that encircle the narrow mouth of the appendage. The upper branch extends from the entrance of the orifices of the left pulmonary vein to the lateral wall. Its lower branch extends inferiorly to the atrial base, encircles the vestibule, and attaches to the mitral ring.

The infolded atrial walls form the rim of the oval fossa. The other principal bundles of the atria attach to it. The superior part of the rim is formed by an infolding of muscular fibres between the venous sinus of the right atrium and the right pulmonary veins of the left atrium. The intercaval bundle of the right atrium together with the septopulmonary bundle of the left atrium originate from this part of the rim and extend towards the right or left sinus components. The anterior part of the rim is an extensive folding of atrial musculature in the vertically orientated interatrial groove from which the terminal crest originates. The inferior part of the rim overlies the central fibrous body and continues backwards as the sinus septum, separating the orifice of the coronary sinus from the inferior caval vein. The Tendon of Todaro, an important fibrous structure, courses through the sinus septum at the site of fusion of the Eustachian valve (guarding the orifice of the inferior caval vein) and the Thebesian valve (guarding the orifice of the coronary sinus).

The anatomy around the vestibule of the tricuspid valve and the mouths of the inferior caval veins and coronary sinus is complex. In a study of 28 hearts obtained from patients who died from non-cardiac causes, Cabrera et al focused their attention on the posteroinferior part of the right atrium ("the cavotricuspid isthmus"), bordered by the extension of the terminal crest and Eustachian ridge posteriorly, the hinge line of the septal leaflet of the tricuspid valve anteriorly, a line traced between the superior extent of the Eustachian valve ridge and the tricuspid valve orifice at the base of the triangle of Koch superomedially, and a line from the terminal crest towards the vestibule of the tricuspid valve inferolaterally.[3] They described the Tendon of Todaro as a fibrous continuation of the Eustachian ridge that coursed intramyocardially through the sinus septum to insert into the central fibrous body. The Eustachian valve spanned about half the circumference of the inferior caval vein. It was thin and membranous in 21 hearts, and thick and muscular in 7 hearts. When the Eustachian valve was muscular, it formed a prominent ridge that adjoined the Thebesian valve of the coronary sinus. Marked variability was found in the ramifications of the terminal crest as it extended into the cavotricuspid isthmus. In most hearts the prominent body of the terminal crest became less marked at a more inferior site, as it approached the orifice of the inferior caval vein. From there, broad muscle bundles radiated and passed inferiorly and laterally, terminating inferior to the orifice of the inferior caval vein or else in the vestibule of the tricuspid valve. In the majority of specimens, the area immediately anterior to the inferior

caval vein was composed mainly of fibrous and fatty tissue, with very few muscular fibres coursing through. Those few fibres that did pass through headed medially towards the orifice of the coronary sinus. In 7 specimens however, the Eustachian valve was hinged to a thick muscular band that extended from the terminal crest and continued into the Eustachian ridge. In three specimens, muscular bundles from the terminal crest filled the entire isthmus.

The middle of the cavotricuspid isthmus was made up of muscular trabeculations that originated either from the wall of the coronary sinus or else were continuous with the bundles of the terminal crest. Histologically, they consisted of several layers of muscular fibres separated by fibrous tissue. In some specimens there were fewer muscular trabeculations in this sector. In the anterior sector, bordering the tricuspid valve, the musculature was smooth, with myocardium filling the full thickness of the atrial wall. Following removal of the endocardium, the arrangement of muscle fibres was remarkably similar in 6/14 specimens examined. The muscle fibres ran obliquely from the thick muscles that ramified from the distal part of the terminal crest, some terminating on the hinge line of the septal leaflet of the tricuspid valve, others continuing superiorly beneath the orifice of the coronary sinus, extending into the Triangle of Koch, where they became circumferential. These fibres were crossed at acute angles by fibres from the inferior trabeculations and vestibule.

Sanchez-Quintana et al performed a detailed examination of the muscular architecture of the Triangle of Koch.[4] As first described by Koch in 1909, the atrial border of the triangle is formed by the Tendon of Todaro, the ventricular border by the hinge of the septal leaflet of the tricuspid valve, and the coronary sinus os as the inferior border.[5] In the posterinferior area (behind and beneath the coronary sinus os), muscle fibres ran longitudinally from the pectinate muscles extending from the terminal crest, and passed directly to the vestibule of the tricuspid valve. At this site, they turned sharply to become circumferential. The sinus septum (Eustachian ridge area, separating the inferior caval vein from the coronary sinus) was made up of circumferential fibres that entered the septal area having encircled the oval fossa, becoming oblique at the level of the tendon of Todaro. Within the vestibule, fibres were circumferential, beginning as continuations from the pectinate muscles, and spiraling around the coronary sinus os before extending anterosuperiorly to join with the fibres of the sinus septum. The anterosuperior area contained both circumferentially arranged fibres, passing anterior to the oval fossa, and longitudinal fibres that ran over the site of the compact node at the vertex of the triangle, to insert into the attachment of the septal leaflet of the tricuspid valve. Overall, the arrangement of fibres in this area was complex. In a number of specimens, changes in fibre direction were observed, i.e. in the isthmus, where longitudinal

fibres turned to become circumferential, and in the posteroinferior area just behind the coronary sinus os. Changes were also seen at the apex of the triangle.

As it can be seen, the right atrium is a complex chamber, containing many separate components and structures with an intricate arrangement of muscle fibres and bundles. Much less has been published regarding the left atrium. Ho and Anderson from the National Heart and Lung Institute have provided a report based on gross examination of 26 adult heart specimens.[6] The endocardial and epicardial surfaces were dissected away to reveal the major muscle bundles. Again, they highlighted the fact that the true extent of the interatrial septum is much less than initially anticipated. The flap valve of the oval foramen marks the site of the true septum. The remaining septal structures are composed of the infolded right atrial wall superiorly and inferiorly, and the fibrofatty sandwich of atrial and ventricular musculature anteriorly. The "sandwich" comprises the atrial myocardium of the vestibules overlying the tissues of the inferior AV groove that in turn rests on the crest of the muscular ventricular septum. The muscular fold of the oval foramen itself is also filled with fibrofatty tissues of the epicardium. Muscular continuity can be traced from the folded rim into the left atrial wall. The septal raphe is bridged by a variable number of muscular strands that provide interatrial connections (Figure 2).

The vestibule of the left atrium is a smooth walled circumferential area surrounding the orifice of the mitral valve. Posteriorly, the atrial wall is thin, and directly overlies the great cardiac vein that lies in the left AV groove. The posterior portion of the vestibule directly apposes the wall of the coronary sinus. The major part of the left atrium is the venous component receiving the pulmonary veins. In the majority of hearts there were four openings of the pulmonary veins, with the left upper pulmonary vein orifice located just superior to the mouth of the atrial appendage. A sleeve of myocardium surrounded the proximal portion of the pulmonary veins, the length varying from heart to heart.

Epicardially, the basic pattern of muscle bundle orientation was the continuation of Bachmann's bundle, parallel to the AV groove that could be traced rightward to the junction between the right atrium and the superior caval vein. In the left atrium, Bachmann's bundle was joined inferiorly at the septal raphe by fibres from the anterior rim of the oval foramen. Superiorly, it blended with a broad band of circumferential fibres that arose from the anterosuperior part of the septal raphe to sweep leftward into the left lateral wall. These fibres passed circumferentially to either side of the neck of the appendage and reunited as a broad circumferential band around the inferior part of the posterior wall to enter the posterior septal raphe. Frequently, small tongues of fibres were seen extending from this band to insert into

Figure 2.

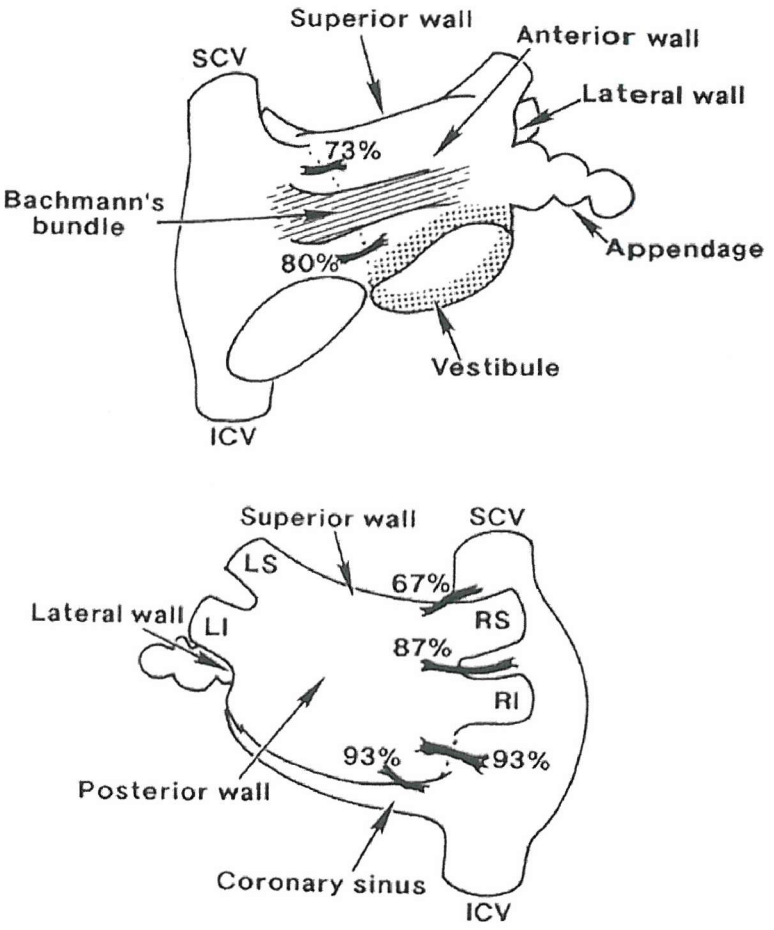

Schematic representation of the interatrial muscular bridges and their percentage of occurrence in 15 human hearts. The dotted line represents the septal raphe.

the wall of the coronary sinus. The coronary sinus was seen to have its own muscular wall that increased in thickness closer to its mouth in the right atrium.

The pulmonary veins arose from the posterior and superior walls of the atrium (the "dome"). The superior wall was composed of longitudinal fibres, arising from the anterosuperior septal raphe, beneath Bachmann's bundle. As they ascended the dome they fanned out to pass in front, between and behind the pulmonary vein openings. At the pulmonary vein openings these fibres encircled and intermingled with longitudinal fibres. On the posterior wall the septopulmonary bundle often bifurcated to become two oblique branches. The leftward branch fused with the circumferential fibres of the anterior and lateral walls, whereas the rightward branch turned into the posterior septal raphe. Often, extensions from the rightward branch passed over the septal raphe to blend with the right atrial fibres. In 10 specimens the fibres on the dome ran laterally instead of longitudinally or obliquely. In two specimens the fibres of the dome had no dominant orientation.

The pattern of endocardial fibres was relatively consistent among their specimens. The dominant fibres in the anterior wall were those taking origin as the septoatrial bundle, ascending obliquely from the anterior interatrial raphe and combining with longitudinal fibres arising from the vestibule. They passed between the right and left pulmonary veins, blending with the longitudinal fibres of the septopulmonary bundle from the subepicardial layer. The septoatrial bundle also passed leftward, superior and inferior to the mouth of the atrial appendage to reach the lateral and posterior walls. Some of these fibres encircled the mouth of the appendage, continuing into the pectinate muscles. The subendocardial fibres around the openings of the pulmonary veins were usually loop-like extensions from the longitudinal fibres, and were continuous with the subepicardial fibres.

Musculature of the Coronary Sinus

Having examined in detail the myocardial architecture of the right and left atrial chambers, attention must now be paid to the muscular structure of the coronary sinus. This venous structure lies in the left atrioventricular groove. It is formed by the continuation of the great cardiac vein. The valve of Vieussens often marks the site of transition. The coronary sinus receives tributaries as it passes round the mural leaflet of the mitral valve, and then receives the middle cardiac vein and the small cardiac vein at the crux. Von Ludinghausen et al performed a detailed anatomical study of the coronary sinus musculature in 240 human hearts.[7] In all sections, the coronary sinus was enclosed in a myocardial coat; the fibres usually arranged in spirals, or occasionally, longitudinal bundles. The fibres were seen to

originate from the posteroinferior wall of the left atrium. The terminal part of the great cardiac vein was also covered to a variable degree. The length of the myocardial sleeve varied between 6 and 11 mm. The distal portion (left myocardial edge) was formed in 4 different ways. In 58% of cases, fibres headed obliquely towards the posterior left atrial wall. In 19% they crossed the great vein at right angles. In 9% a crescent-like shape was seen. In the remaining 14% the myocardial edge was ill defined. Towards the mouth of the coronary sinus the myocardial bundles continued into the posteroinferior wall of the right atrium.

In 9% of cases, separate, small myocardial belts were seen around the terminal cardiac veins. In 8% of cases, one to several small myocardial cords were seen separate from the myocardial sleeve covering the inferior wall of the coronary sinus, passing freely through the adipose tissue of the posterior coronary groove. After traveling for 9-12 mm they inserted into the posterolateral left atrial wall.

The authors concluded that the coronary sinus was an intramural structure, based on the need for dissection and division of "left atrial" fibres during the study. In common with the study by Ho et al, myocardial strands were seen bridging the gap between the myocardial sleeve of the coronary sinus and the posterior wall of the left atrium. Ho et al did not describe the relationship between the myocardial sleeve itself and the posterior left atrial wall.

Chauvin et al examined the relationship between the coronary sinus and left atrium.[8] Although they only dissected 10 adult human hearts, sections contained the full coronary sinus and surrounding 2 cm of tissue (including the immediately adjacent regions of the left atrium, the mitral valve, and the left ventricle), together with the coronary sinus ostium, including the Triangle of Koch, Eustachian ridge, tricuspid valve annulus, and contiguous parts of the interventricular and interatrial septum. Sections of 4 μm thickness were made at 20-100 μm intervals in the plane of the mitral valve annulus, containing the full length of the coronary sinus. They described a continuous cuff of striated muscle completely surrounding the venous wall of the coronary sinus. The cuff was continuous with the ostial right atrial myocardium and extended along the coronary sinus for 25-51 mm (mean 40+/-8 mm). In this study, they stated that the cuff was not continuous along its long axis with the left atrial myocardium. The cuff was thicker towards the ostium. In some cases the fibres coiled in a helical fashion around the coronary sinus.

Importantly, they described the left atrial myocardium and coronary sinus muscle cuff as being separated by adipose tissue. In all hearts, this fatty compartment was bridged by striated muscle fibres that provided connections between the two muscular structures (Figure 3). The muscle bridges were orientated obliquely and leftward towards the left atrial

Figure 3. Muscular connections between the coronary sinus and left atrium

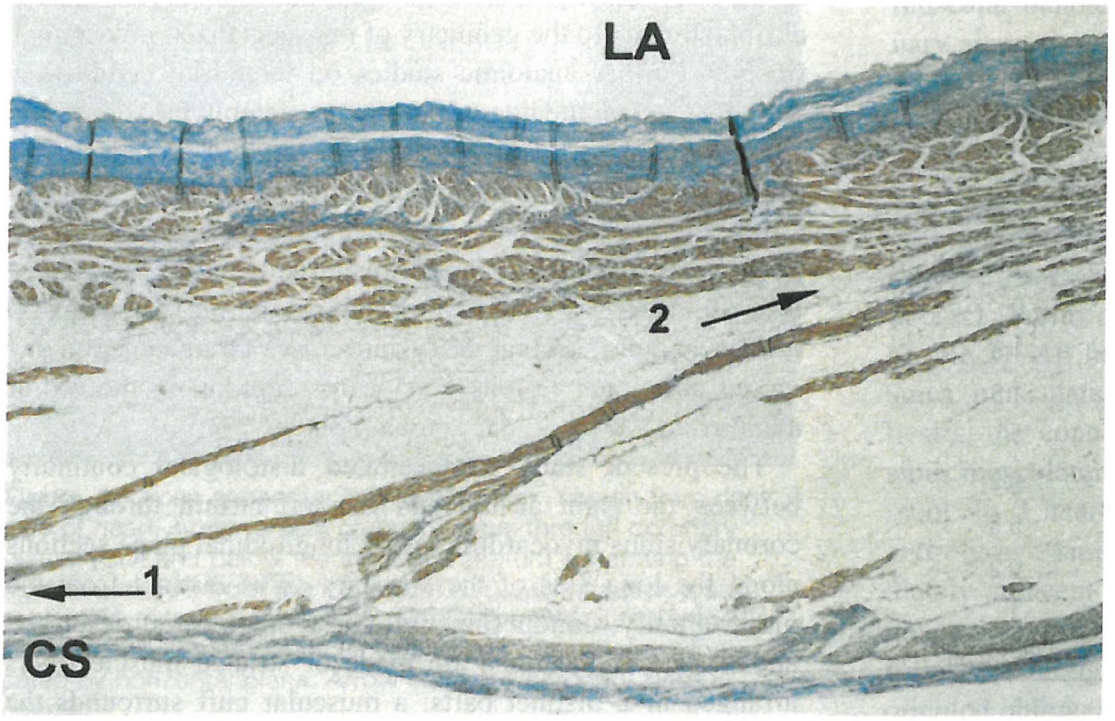

Thin and discrete muscular connections between pericoronary sinus muscle and left atrium myocardium. The coronary sinus ostium is on the left side of the figure and the great cardiac vein is on the right side. The arrows indicate the coronary sinus (1.CS) and left atrial (2.LA) ends of the muscular connection, which is 10 mm long and formed of a few thin fibres of myocardium. Masson's Trichrome stain.

myocardium, and varied greatly in size and location. They could appear as 1 or 2 discrete fascicles, or as wide muscle bands. In one heart the coronary sinus musculature and left atrial myocardium intermingled. The connections originated 4 - 20 mm from the ostium of the coronary sinus; their left atrial implantation extended for 5 - 40 mm. Although there is agreement on the presence of myocardial bridges that allow muscular communication between the wall of the coronary sinus and the posterior left atrium, their presence was described in all hearts by Ho et al and Chauvin et al, but only in 9% of hearts examined by von Ludinghausen. However, von Ludinghausen believed the coronary sinus to be an intramural structure, with the myocardial cuff originating from the left atrial wall. In contrast, Chauvin described the coronary sinus and its muscular cuff as being separated from the left atrial wall by a layer of adipose tissue, the only communication being through the myocardial bridges. Ho et al did not comment of this relationship. All three studies suggest that the coronary sinus provides a muscular communication between the right and left atria, a fact that will be related to electrical communication later in this Introduction.

The anatomy of the interatrial septum

An additional muscular connection between the two atria is the interatrial septum. The structure of this area has been described above. In particular, it has been highlighted that the "true septum" is smaller than anticipated, with much of the septal walls resulting from infolding of the right and left atrial walls, separated by a fatty layer. Sweeney et al studied the shape and margins of the atrial septum.[9] Dissections were performed in 90 human hearts and transillumination from both atrial sides was used to identify the margins. They described the shape of the septum as blade-like, with the tip directed towards the orifice of the superior caval vein. The concave anterior margin outlined the curvature of the adjacent ascending aorta and began just medial to the inferior side of the entrance of the superior caval vein. From this point the margin extended anteriorly and inferiorly to terminate in the fibrous trigone posterior to the membranous ventricular septum. The right atrial appendage was separated from the anterior septal margin by a strip of smooth muscular wall that was loosely adherent to the ascending aorta. The posterior margin extended from the tip of the blade though a convex curvature posterior to the oval fossa, terminating at the coronary sinus os. The inferior caval vein was separated from the posterior margin by a narrow expanse of free wall of the right atrium. The short inferior margin extended from the os of the coronary sinus to the fibrous trigone posterior to the membranous ventricular septum. At no point did it coincide with the tricuspid annulus.

The oval fossa was located midway between the tip of the blade and the inferior margin. In the adult hearts there was a 5 mm wide strip of muscle between the oval fossa and anterior margin of the septum. In one-third of adults, there was also a strip of muscle posterior to the fossa, approximately 6 mm in width. The area of the septum averaged 890 mm^2 in adults. The oval fossa was an average of 240 mm^2, making up 28% of the total septal area. In those hearts with a posterior strip of muscle, the oval fossa made up 15% of the total septal area.

In a review of the developmental anatomy of the atrial septum, Anderson et al again pointed out that when viewed from the right atrium, there is an extensive area of musculature potentially interposed between the two chambers, extending from the orifice of the inferior caval vein to the right atrial appendage, and from the mouth of the superior caval vein to the hinge of the septal leaflet of the tricuspid valve.[10] However, as they state, very little of the musculature can be removed without opening the right atrial wall and arriving outside the heart. This is their criterion for distinguishing folds from "true" septal structures (Figure 4). It is only the flap valve of the oval fossa and its immediate muscular inferoanterior rim (the lower limbus), which, when removed, create a communication between the right and left atrial chambers. They state that this is due to the larger part of the muscular border of the oval fossa being two-layered, formed by folding of the atrial walls. This infolding incorporates extracardiac adipose tissue.

The above papers all provide descriptive observations of atrial anatomy with particular reference to the muscular architecture, and individual structures such as the caval veins, atrioventricular valves, coronary sinus, Eustachian ridge, oval fossa, terminal crest and pectinate muscles. To relate the anatomy to the spread of electrical activation, attention must now be paid to the specialized conduction system.

Figure 4. Septal continuity between the left and right atria

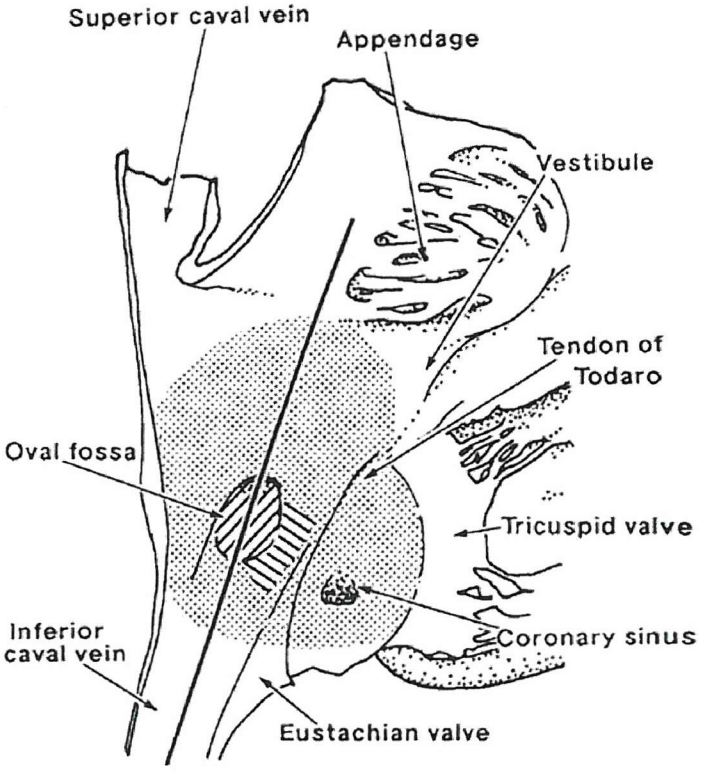

Diagram of an adult human heart opened through a cut made posteriorly through the smooth-walled portion of the right atrium. The stippled area is composed of infolded atrial walls, whereas the hatched areas, marking the floor of the oval fossa and its inferior rim, can be resected without leaving the cavities of the heart.

Reproduced with permission from Wiley-Liss Inc: Clinical Anatomy 1999;12(5):362-374.

Anatomy of the conduction system

The two components of the specialized conduction system that are directly related to the atria are the sinus node and atrioventricular node. Both Anderson[11] and Opthof[12] have reviewed the history of the discovery of the sinus node. The intrinsic automatic activity of the heart had first been recognized by both Galen (129-200) and Leonardo da Vinci (1452-1519); however, it was not until 1906 that Keith and Flack discovered the histological sinus node in the mole heart, lying in the sulcus terminalis.[13] Its appearance was similar to that of the atrioventricular node that had previously been discovered by Tawara.[14] Subsequent studies, to be reviewed further on in this chapter, confirmed the sinus node to be the origin of the cardiac impulse.

The anatomy of the sinus node

Many studies have confirmed the anatomical position of the sinus node in a number of animal species. In the late 1970s, Anderson et al performed histological analysis on 25 human infant hearts.[15] The sinus node was easily identified in all hearts examined. In 22/25 hearts the node lay in the groove between the right atrial appendage and the lateral atrial wall (terminal groove, or sulcus terminalis). The anterosuperior "head" was situated between 2 and 4 mm below the crest of the right atrial appendage. The posteroinferior "tail" was up to 10 mm below this level. The head was subepicardial, the body mainly intramyocardial, and the tip of the tail was in contact with subendocardial tissue. In 3/25 hearts the sinus node straddled the crest of the atrial appendage so that the anterosuperior head was to the left of the crest and the body and tail were to the right of the crest, in a "horseshoe" arrangement. The histological node (not including the transitional zone) measured between 4 and 6 mm in length, 2 and 3 mm in width, and less than 1 mm in thickness.

Tongues of nodal tissue extended outwards from the centre of the node, although the authors reported that these tongues did not become connections between the node and the surrounding atrial myocardium, as they remained surrounded by connective tissue. They found it difficult to identify cell-to-cell contact between sinus node specialized cells and atrial myocardium. A transitional zone was identified where the sinus node was in close proximity to the terminal crest.

He et al examined 95 adult and 30 child hearts with the aim of further delineating the margins of the sinus node.[16] They identified it as a pale structure of firm consistency, lying in the upper part of the terminal groove. A sinus node artery penetrated the node from its head or

tail, further aiding identification of the structure. They found the head of the node to lie in the terminal groove slightly below the junction between the superior caval vein and the right atrial appendage, approximately 6.5 mm from the crest of the right atrial appendage. It was found just beneath the epicardium, occupying around one-third of the terminal groove. They found a small muscle bundle crossing over the tail, so that the tail was buried in the myocardium adjacent to the endocardium. This bundle originated from the level of the upper edge of the superior right upper pulmonary vein and extended to the right atrium. They reported the shape of sinus node to complement the shape of the terminal groove. The length of the node was found to be inversely proportional to the breadth.

In their study they found the size of the node to be generally larger than those in the study by Anderson et al. Nodes measured 10.1 by 2.5 mm in children and 16.7 by 4.5 in adults. Unlike the previous study, they did not report difficulties in identifying the relationship between the sinus node and the surrounding myocardium. In some hearts, at the head of the node, a few muscle bundles coursed towards the wall of the superior caval vein to mingle with the circular muscle around the orifice of the vein. In other hearts, bundles extended directly from the head, over the caval-appendage junction, to merge into Bachmann's bundle. In a third variation, fibres were directed into the right atrial appendage. Fibres leaving the body of the node either diverged posteriorly into the wall of the superior caval vein and the interatrial septum, or diverged over the anterior aspect of the right atrium. Many muscle bundles from the tail arched posteriorly towards the interatrial septum, ran along the terminal groove to enter the terminal crest, or diverged into the right atrium.

The architecture of the atrioventricular conduction axis was first described by Tawara in 1906.[14] Shortly after, Koch described the landmarks that define its anatomical position.[5] In histological terms, the atrioventricular node, composed of specialized cardiac muscle cells, has zones of transitional cells formed from the atrial myocardium in the floor of the coronary sinus and the atrial septum. These transitional cells impinge on the compact node, which then gathers itself together to enter the insulating fibrous tissue as the penetrating atrioventricular bundle (the bundle of His).

Inoue and Becker reported on the posterior extensions of the atrioventricular node, based on histological study of 21 hearts at autopsy. The compact node was covered on the right atrial aspect by a transitional cell zone. Posterior extensions were described that were direct continuations of the compact node. Thirteen of the 21 hearts showed both leftward and rightward posterior extensions; 7 hearts had just rightward, whereas only 1 heart had a sole leftward posterior extension. When viewed from the right atrium, they described the leftward extension as being superior to the rightward extension. The rightward extension was the most

prominent, running parallel and in close relation to the tricuspid valve annulus, underneath the anterior margin of the coronary sinus os. The maximum length of the posterior extension was 9 mm, with a mean of 4.4 +/- 2 mm. The maximum length of the leftward extension was 4.0 mm, with a mean of 1.8 +/- 0.9 mm. The rightward extension gradually disappeared amid atrial myocardium, whilst the leftward extension eventually disappeared within the central fibrous body at the site of the mitral valve annulus.

Internodal conduction: anatomical studies

Whereas there is little debate as to the site and structure of the sinus node and atrioventricular nodes, there was initially some disagreement regarding the conduction of the electrical impulse between the two nodes. Specifically, there was debate over the presence of specialized tracts in the atria, similar to those of the ventricles (the bundle branches and Purkinje system described by Tawara and others).[14,17] A review of the important literature that initially fuelled, and then resolved this debate, will be presented.

In 1907, Wenckebach described a specialized pathway of Purkinje-like fibres that extended from the base of the superior caval vein down the posterior wall of the right atrium adjacent to the atrial septum, fanning out along the AV ring and entering the atrioventricular node.[18] In his review of the literature, Anderson believes that following the discovery of the sinus node by Keith and Flack, Wenckebach realized that this bundle had no functional significance.[11] Subsequently, Thorel described a pathway of specialized tissue between the sinus and atrioventricular nodes, which was located in or near the terminal crest and connected with the AV node near the coronary sinus.[19] However, Anderson could not find any evidence that Thorel published unequivocal documentation of the existence of this tract. The existence of specialized tracts was debated at the German Pathological Society in 1910, concluding that histologically specialized pathways had not been proven.

In 1916, Bachmann described the interatrial band that has subsequently taken his name (Bachmann's bundle).[20] Within his report, Bachmann pointed out that it was the packing of ordinary atrial muscle fibres within the bundle was likely to be the cause of rapid conduction through it.

Debate continued over the next few decades, with some authors presenting evidence of specialized cell or tracts within the atria, and others reporting that such tracts did not exist. It was the work published by James in 1963 that once again inflamed the controversy.[21] His anatomical study of the human heart was inspired by the recent publication of Paes de

Carvelho, who had described the existence of the sinoatrial ring in the rabbit heart, running alongside the terminal crest.[22] Paes de Carvalho felt this structure was a specialized pathway responsible for internodal conduction. James' theories were based entirely on anatomical study, with no electrophysiologic testing. He described 3 bundles of myocardium that were demonstrated histologically to connect the sinus node to the AV node. The bundles corresponded to the tracts described by Bachmann, Wenckebach and Thorel (see above). He commented that all three bundles had abundant fibres that displayed Purkinje-like characteristics, although none of the tracts consisted exclusively of such fibres.

In their 1968 paper reporting findings of the dissection of 7 human hearts, Meredith and Titus described 3 internodal pathways.[23] The anterior pathway originated at the anterior sinoatrial node. At the anterior and superior margins of the septum a large branch diverted away from Bachmann's bundle to turn inferiorly and posteriorly into the thick portion of the atrial septum, anterior to the fossa ovalis. Although fibres tended to be subendocardial on the right side of the septum, some were nearer the left atrial surface. The pathway coursed inferiorly, connecting with the superior and anterior aspects of the AV node.

The middle pathway began at the posterior aspect of the sinoatrial node, passing to the right, posterior to the SVC, to enter the superior atrial septum. It passed superior and anterior to the oval fossa. Anterior to the fossa the fibres joined the anterior pathway, to pass inferiorly to the AV node. A few fibres extended posteriorly, interconnecting with posterior pathway fibres.

The posterior pathway began at the ill-defined posterior and inferior nodal fibres, passing diffusely into the terminal crest. Fibres fanned out into the pectinate muscles although the bulk stayed in the terminal crest as far as the coronary sinus. At its lower end the terminal crest fanned out and the fibres passed anteriorly around the inferior caval vein and coronary sinus. Most of the fibres congregated beneath the coronary sinus in the subendocardial region of the floor of the right atrium. It is important to note in this study that the authors concluded that the bulk of the cells in the specific pathways were indistinguishable from normal atrial muscle cells, although many did have some of the features of Purkinje cells.

Anderson et al performed their own study using 22 human fetal and 32 infant hearts using light microscopy.[24] Within the internodal atrial myocardium, they were unable to find any histological evidence of specialized conduction pathways. Neither were they able to identify any Purkinje-like cells. They have subsequently concluded that the internodal atrial musculature is made up histologically of working atrial myocardial fibres. The myocardial walls themselves are divided into relatively narrow bands by the orifices of the veins entering

the right atrium, and by the oval fossa. Within these muscular areas, further potential for preferential conduction is provided by the packing and orientation of the muscle fibres.

So why has there been so much contentious debate and variation in reported findings? One inconsistency throughout the reviewed literature has been the use of the terms "pathway" and "tract". Following the 1910 German Pathological Society meeting, a clear definition was proposed by Monckeberg and Aschoff, that is still upheld today. A pathway should be histologically discrete, can be traced from section to section, and, most importantly, insulated by fibrous tissue sheaths from the adjacent working myocardium. These criteria are based on Tawara's description of the specialized ventricular conducting system. None of the above studies that have declared the existence of specialized atrial pathways have demonstrated findings that conform to this standard. In addition, the findings of Purkinje-like cells by some authors in the atrial myocardium must be treated with caution. Anderson et al found cells with this histological appearance randomly spaced throughout the atria and raised the possibility that they may represent a fixation artifact.[24]

The conclusion that must inevitably be drawn from a review of the above studies is that morphological "specialized internodal conduction pathways" are not present in the atria. However, as already suggested, the orientation of atrial muscle bundles may influence the spread of electrical activation between the two nodes.

Internodal conduction: electrophysiological studies

There is a considerable amount of literature published describing the propagation of electrical activation through the atria. The studies vary in the species of heart studied, the recording technique, the use of in-vitro or in-vivo cardiac tissue, and whether electrophysiological mapping was performed on the epicardial or endocardial surface.

Between 1910 and 1914, soon after the discovery of the histological sinus node, Sir Thomas Lewis demonstrated that it was possible to localize the pacemaker of the heart and to map the spread of activity by recording electrical events at various points on the atrial surface.[25] Using initial negativity in the unipolar electrogram morphology as a criterion, they localized the pacemaker to the terminal groove, between the superior caval vein and the right atrial appendage. Lewis and subsequent investigators concluded that the spread of activation out from the node was more or less radial in direction and constant in velocity. Around this time, opposing views were presented by Eyster and Meek, who noted that the sinus impulse reached the atrioventricular node before it reached the coronary sinus or the body of the right

atrium.[26] They also found that discrete lesions in the vicinity of the sinoatrial node led to atrioventricular dissociation. They concluded that these observations could not be accounted for on the basis of radial spread away from the node, and that there must be specialized fibres responsible for internodal conduction.

The development of microelectrode intracellular recording technique in the 1950s brought about a revolution in electrophysiological mapping studies. Action potential recording could be used to map the precise timing of localized cell depolarization, as well as differentiate pacemaker cells from normal atrial myocardium.[27] Paes de Carvalho et al used this technique to map atrial activation in excised rabbit atria, suspended in oxygenated Tyrode's solution.[22] With the aid of a micromanipulator they positioned two microelectrodes connected to an oscilloscope at various sites within the dissected right atrium. Of note, their preparation involved cutting the terminal crest close to the interatrial septum. They also identified a whitish bundle of tissue that formed almost a complete loop around the caval veins and coronary sinus, adjacent to the terminal crest and Eustachian ridge. They called this structure the sinoatrial ring bundle, believing it to be a specialized atrial tract (see above). They found the true pacemaker to be located in nodal fibres in the wall of the superior caval vein. Propagation immediately away from this site was slow. As the excitation wave approached the periphery of the venous region, the action potentials changed and conduction velocity increased. Due to its position, the terminal crest was reached before any other atrial tissue. Activation then propagated along the terminal crest at high velocity, and then throughout the whole atrial roof. As the excitation wavefront approached the tricuspid valve the conduction velocity decreased before entering the atrioventricular node.

This study, although groundbreaking, has a number of significant limitations. Cutting the terminal crest at the septum may have affected the spread of activation within this region. Only two electrodes were used, preventing simultaneous multisite mapping. Consequently, changes in activation resulting from a shift in the site of the primary pacemaker could have affected the subsequent spread of activation, yet gone unnoticed by the investigators. Finally, as with many of the subsequent experiments, mapping was performed in excised tissue that was dissected free and mounted in Tyrode's solution. The effect of excision, atrial stretch and loss of innervation and arterial supply may have significantly influenced the results.

To overcome some of these limitations, Durrer et al performed mapping studies on the entire isolated heart of 7 individuals.[28] The hearts were excised, attached to a Langendorff perfusion apparatus and perfused with Tyrode's solution. The hearts were able to beat spontaneously. Atrial activation mapping was performed in only 2 hearts. Epicardial recording was performed using a small unipolar electrode containing 5 terminals. Although intramural

recording was performed using up to 72 microelectrodes, only a minority of electrodes was placed in the atrium.

They reported difficulties in precisely locating the sinus node. Early activity was recorded as starting over a relatively large area next to the right border of the superior caval vein. The spread of atrial activation over the rest of the surface was described as occurring within more or less concentric isochrones, i.e. radially, although a more rapid progress was documented in the region of the terminal groove. In one of the two hearts activation also appeared to be slightly advanced within Bachmann's bundle, although the velocity within the bundle was no greater than elsewhere. The last parts of the atria to be activated were the left atrial appendage and the left inferior pulmonary vein.

Again, this study was limited by the use of an explanted heart, as well as the small number of recording sites and that only two atria were studied. Indeed, when comparing results from canine controls mapped first in situ and then after explantation, total excitation of the excised heart was more rapid than the in-situ heart, although the overall pattern was essentially the same. In common with the early findings of Lewis, but in contrast to those of Paes de Carvalho, this study reported atrial activation patterns to be more or less concentric.

Detailed in-situ mapping of human atrial activation was not performed until the development of open-heart surgery and the epicardial recording plaque. Much of this work has been performed in the St Louis laboratory of Cox and Boineau, who have pioneered the use of intraoperative electrophysiological mapping to guide arrhythmia surgery. To get beyond the limitations of a hand-held probe with single point mapping, they designed three epicardial plaques containing 156 bipolar electrodes and used them to record epicardial activation sequences in 10 patients undergoing surgical treatment of Wolff-Parkinson-White syndrome. In this paper, authored by Canavan et al, one template was placed over the posterior surface of the left atrium, beneath the pulmonary veins, extending from the left atrial appendage to the atrial septum; another template was placed posterior to the ascending aorta to contact the medial and anterior surfaces of the superior caval vein, right atrium and left atrium; and the third template was placed over the lateral surface of the right atrium and superior caval vein.[29] Activation timings during sinus rhythm were displayed as isochronal maps drawn at 10 msec intervals (Figure 5). In common with other studies, earliest activation was found in the sinus node region, at the junction of the superior caval vein and right atrium on the posterolateral epicardial surface. The wavefront was described in this paper as propagating in a radial fashion across the posterolateral right atrium to reach the posterior atrioventricular groove at 80 msec. This wavefront continued across the intercaval region to the posterior surface of the left atrium beneath the right pulmonary vein.

Figure 5. Isochronal atrial activation map of one beat of sinus rhythm

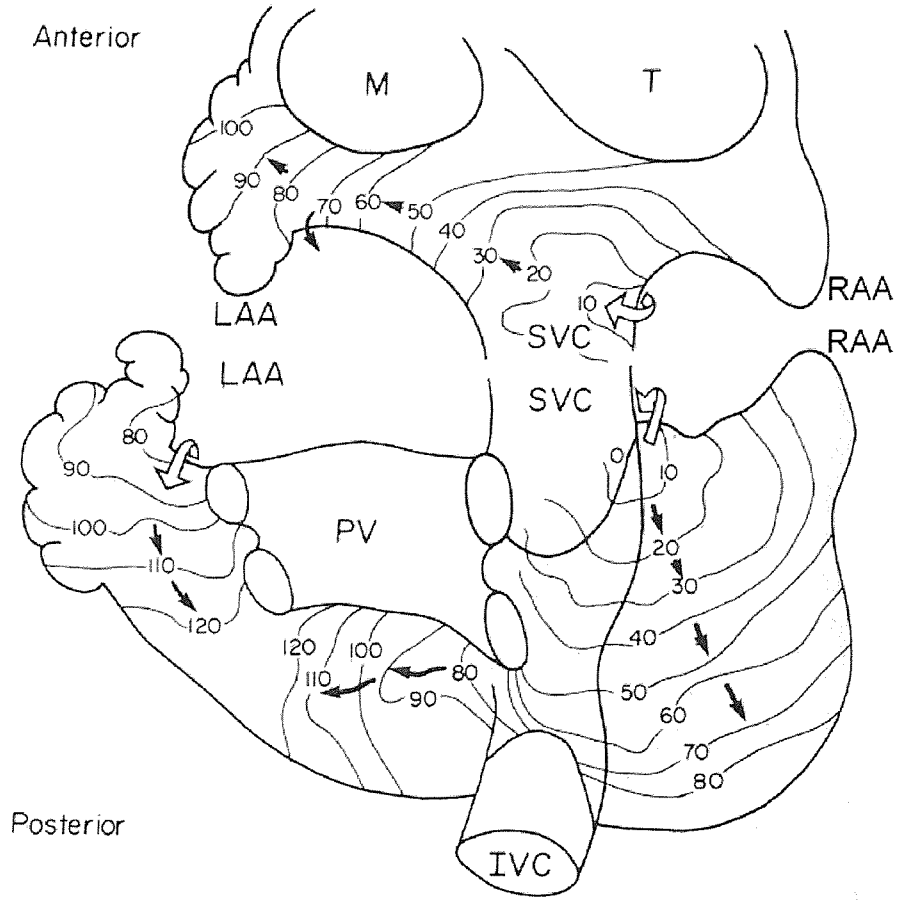

The arrows indicate the spread of activation from its origin in the superior portion of the right atrium at its junction with the superior caval vein.

RAA = right atrial appendage, LAA = left atrial appendage, M = mitral valve, T = tricuspid valve, PV = pulmonary veins, SVC = superior caval vein, IVC = inferior caval vein.

Reproduced with permission from the Society of Thoracic Surgeons: Ann Thorac Surg 1988;46:223-231

The anterior portion of the sinus wavefront reached the anterior surface of the superior caval vein at 10 msec, before penetrating Bachmann's bundle and propagating from right to left, depolarizing the anterior surface of the left atrial appendage by 100 msec. The last part to be depolarized was the area beneath the left lower pulmonary vein, at 120 msec.

The advantage of using multielectrode plaques is that simultaneous recording from multiple sites over both atria could be performed during a single beat. This removes the potential error of reconstructing activation sequences over consecutive cardiac cycles during which the activation sequence may change. The use of multielectrode templates made anatomic positioning reproducible between subjects. One disadvantage of using epicardial plaques is that no data was obtained from the interatrial septum.

The lack of information on septal activation was addressed by the same group in a study published in1990.[30] The authors studied 12 patients using the previously described epicardial plaques before inserting either a 48- or 80-bipole pair electrode plaque through an atriotomy incision in the lateral wall of the right atrium to map the atrial septum. During sinus rhythm, the earliest septal activation entered the septum below the superior caval vein in the region of the intercaval band. In 5 patients, septal activation was asymmetrical, with the wavefront propagating most rapidly along the large anterior limbic bundle around the oval fossa, and the anteromedial portion of the septum. Activation reached the inferior portion of the septum, below the coronary sinus os, 85 msec after initial sinus activation. In 2 patients, the wavefront entered the septum posterior to the oval fossa, and in two others, the wavefront entered the septum anterior to the superior caval vein.

Interestingly, in the results section of the above paper, the authors refer to their previous study authored by Canavan (see above).[29] They cite the paper as describing asymmetrical propagation. However, in Canavan's paper, activation was described as radial, implying a uniform and concentric spread with similar velocities in all directions. Uniform radial spread would be against the concept of preferential routes of conduction. Close examination of the published isochronal maps that depicted activation during sinus rhythm indeed suggest uniform spread through the right atrium, with perhaps a hint of faster conduction in the region of the terminal groove. However, in a further study by this group that was designed to investigate whether there were variations in the atrial activation sequence concordant with a multicentric origin of the pacemaker wave (reviewed later in this Introduction), isochronal maps derived from 2 epicardial plaques containing a total of 90 bipole pairs clearly demonstrate more rapid, "preferential" conduction away from the pacemaker complex along the thicker muscle bundles of the terminal crest and Bachmann's bundle. The isochronal

maps displayed irregular projections of the wavefront leftward, rightward and inferiorly. They deduced that the asymmetry resulted from the widely distributed, multicentric origin of the pacemaker complex, and preferential conduction away from the origin in the terminal crest, Bachmann's bundle and pectinate muscles.

Waldo et al have documented similar evidence for preferential conduction through the major muscle bundles of the atrium in the in situ canine heart.[31] They used small, 5-electrode epicardial plaques sutured to sites over the sinus node, terminal groove, caudal right atrium, right and left atrial appendages, Bachmann's bundle, the posteroinferior left atrium, and the base of the left atrial appendage. Activation maps and conduction times to selected sites were recorded. Discrete surgical incisions were then made in the region they described as the anterior internodal tract (adjacent to the sinus node), in Bachmann's bundle, or in the region described as the posterior internodal tract in the terminal groove. When the atrium was paced at sites believed to be the internodal tracts (i.e. Bachmann's bundle and the terminal groove), the surface P wave morphology was narrower than when the atrium was paced at sites remote from possible internodal pathways. The authors concluded that these preferential pathways conducted activation more rapidly than the surrounding atrial muscle.

When pacing was performed from the sinus node area, subsequent activation occurred earlier at sites on Bachmann's bundle and the terminal groove than at the electrodes attached to the caudal part of the right atrium and right atrial appendage. Conduction to Bachmann's bundle was always shorter than to other left atrial sites. The authors believed that this could not be explained solely on the basis of distance from the stimulus site, and that it supported the work by Wagner[32], Spach[33] and Goodman[34] who had previously identified rapid conduction in this structure. Following an incision in the anterior internodal area, the surface P wave duration lengthened (although with the same polarity) and low interatrial septum activation was delayed by 12-20 msec. A similar finding was observed when the incision was made in Bachmann's bundle, this time with a change in P wave polarity. An incision in the posterior internodal pathway had almost no effect on activation timings.

These findings led Waldo et al to conclude that the incisions must have interrupted specialized internodal pathways or tracts that played an important role in the activation sequence of the atria. They believed that the anterior internodal pathway was primarily responsible for rapid activation between the sinus and atrioventricular nodes. Their conclusions were identical to those reported earlier by Eyster and Meek.[26]

In 1965, Sano and colleagues had demonstrated in isolated sections of rabbit heart that severing the lateral branch of the terminal crest resulted in a slight increase in internodal

conduction times, whereas severing the septal branch of the terminal crest did not affect internodal conduction.[35] If both the lateral and septal branches were cut, internodal conduction times increased dramatically. Hiraoka and Adaniya later confirmed these findings.[36] Unfortunately, all of these studies were reported at a time where there was still a body of opinion championing the concept of specialized atrial conduction tracts. None of them were performed in conjunction with histological examination of the specimens. As discussed previously, the weight of evidence is now against specialized conduction tissues and is instead in favor of preferential conduction dictated by the orientation and structure of the major muscle bundles. Cutting the appropriate muscle bundles, such as the terminal groove, may still account for the observed effects if the muscle bundles themselves behaved as preferential conduction routes, with activation spreading along their longitudinal axis more rapidly than in surrounding atrial myocardium.

Studies that support the concept of preferential conduction along muscle bundles include those of Hayashi[37] and Goodman.[34] Hayashi performed epicardial mapping with plaques containing 60 electrodes on open-chest dogs. After the mapping procedure the heart was excised and prepared to allow identification of the terminal crest and pectinate muscles. Diagrams of the major muscle bundles were made and compared to the activation maps. They found that a smooth wavefront emerged from the sinus node during the first 5 msec, but by 10 msec, several regions of rapid, preferential activation could be identified. These corresponded to the terminal crest (heading in the direction of the inferior caval vein), the region extending from the sinus node to the atrioventricular groove, and a third region extending from the sinus node to the junction of the atrial appendage and the atrioventricular groove. These areas all corresponded with the site of major pectinate muscle branches. Rapid conduction was also noted to occur in the region identified as Bachmann's bundle. The authors concluded that atrial activation was non-uniform, with rapid conduction occurring along the longitudinal axis of major muscle bundles, such as the terminal crest, the pectinate muscles, and Bachmann's bundle.

Goodman et al performed their study in excised, Langendorff-perfused canine hearts.[34] The unique feature of this study was the combined use of epicardial and endocardial mapping. Epicardial recordings were initially made using a hand-held 5-pole electrode. The right atrium was then opened, the incision some distance from the terminal groove, and endocardial mapping performed. Epicardial mapping confirmed earliest activation to be present at the sinus node area in the high terminal groove. They found that activation was faster down the terminal groove than in adjacent atrial muscle. In the remainder of the atrium there was a slight preference for activation to be faster in the direction of the muscle fibres.

Activation was reported to travel along Bachmann's bundle more rapidly in the longitudinal axis than in a direction at right angles to it.

With their endocardial mapping they described three distinct routes or "pathways". One was from the anteromedial limb of the terminal crest to the upper part of the septum, corresponding with overlying epicardial activation. Activation sometimes slowed or was interrupted at the junction of the thick muscle bundle with the septum. Another was from the posterolateral portion of the terminal crest, descending in front of the os of the inferior caval vein inferior to the area posteroinferior of the coronary sinus. The third was in branches from the middle part of the terminal crest, descending along the upper limb of the oval fossa (an inconsistent finding). The anterosuperior side of the coronary sinus region and the rest of the interatrial septum were activated by lateral spreading of the excitation focus. The oval fossa received activation from its posterior side; there was no conduction across the upper and lower limb.

Importantly, epicardial and endocardial maps showed near identical activation patterns. Activation was also reported as synchronous down each side of the interatrial septum. However, many of the limitations of this study have previously been highlighted. Mapping was not simultaneous at multiple sites, but sequential. Thus, changes in the activation sequence from beat to beat may have dramatically affected the results. Additionally, endocardial mapping was performed through a significant right atrial incision. It is quite possible that such an incision could have affected atrial conduction patterns.

The current consensus of opinion, based upon the above literature, is that preferential conduction routes that correspond to the underlying myocardial architecture govern atrial conduction, rather than the presence of specialized tracts similar to those found in the ventricles. Much of our understanding of the mechanisms of preferential conduction along muscle bundles has evolved from the work of Spach and colleagues at Duke University. In their early experiments in the late 1960s and early 1970s they performed microelectrode studies of the canine heart to answer the debates on atrial activation that have been discussed in great detail above. They initially demonstrated that different conduction velocities in different parts of the atria made the concept of radial spread untenable.[38] Importantly, they agreed with the previously cited reasoning of Anderson, based on the original debate at the 1910 German Pathology Society, that a clear definition of "tract" or "pathway" must include insulation from surrounding muscle, a feature that had never been documented in the atrium. Interestingly, in their studies of activation in the canine heart, they demonstrated differences between adult and infant hearts that could be attributed to subtle changes in architecture. In the infant canine heart, wavefronts propagated directly from the terminal crest into the

adjacent area of venous atrium. In the adult canine heart, activation did not cross this area; rather, wavefronts continued to propagate inferiorly on the upper septal terminal crest and then to the mid-septum via the limbus connections. An ingrowth of connective tissue in the adult heart was identified along the junction between the terminal crest and venous atrium that was accountable for this block in electrical conduction.

The preceding anatomical and electrophysiological studies have provided a huge amount of information regarding the propagation of the cardiac impulse through the atria. There is no evidence for specialized tracts for conduction; rather, the electrical impulse is thought to spread through the myocardial fibres, with "preferential" spread in the longitudinal direction of large muscle bundles. To date, almost every study has been performed in isolated specimens of animal heart, using microelectrode techniques; and in open-chest subjects using epicardial plaques. No studies have been performed using global, high density, real-time mapping of the entire endocardial surface of the right atrium in the intact heart of a closed chest subject, with direct assessment of the relationship between the patterns of activation and the myocardial architecture of the endocardial surface. Such a technique is required to account for the beat-to-beat variations of electrical conduction during normal sinus rhythm, and provide a true picture of real-time endocardial activation and its relationship to right atrial anatomical structure. Real-time, high-density mapping allows analysis of wavefront direction and velocity as well as identifying sites of slow conduction or conduction block.

Propagation of the electrical impulse

The relationship between myocardial architecture and electrical impulse propagation

Workers in Spach's laboratory have published extensively on the propagation of the electrical impulse through cardiac muscle. At the beginning of the 20th century the propagation of electrical excitation was presumed to be uniform as though it occurred in a continuous structure. Rapid conduction occurred in specialized fibres that had unique membrane properties (such as Purkinje cells). This idea was challenged with the simple observation by Spach and coworkers that there is rapid activation in the longitudinal direction of the terminal crest (a large muscle bundle with a parallel orientation of fibres), and slow conduction in the transverse direction.[39] The maximum longitudinal velocities were between 0.9 and 1.2 m/sec and the maximum transverse velocities were 0.05 to 0.12 m/sec. The pattern of propagation within the terminal crest was determined by the stimulus site and fibre orientation. In a subsequent experiment, the conduction properties of the fetal, infant and adult canine terminal crest were compared.[40] In the fetal dogs, there was uniform transverse conduction in the terminal crest and the limbus of the oval fossa, a phenomenon labeled uniform anisotropy. By one week post-birth, the terminal crest still showed uniform anisotropy but the limbus started to demonstrate irregular transverse wavelets. This was explained by differences in the distribution and arrangement of collagenous tissue between the muscle bundles. By adulthood, many muscle bundles demonstrated connective tissue septa (similar to the newborn limbus) dividing the muscle bundle up into fascicles. Recordings showed that inter-fascicle conduction was complex, with multiple crossover points and negative velocities (retrograde conduction) in adjoining fascicles. Pacing techniques showed minimal conduction delays along the longitudinal axis of the terminal crest. However, at junctions with other separate muscle bundles, there was slow conduction across the transverse barrier, which demonstrates decremental properties and eventually functional block.

In a further experiment, they demonstrated rapid conduction in the longitudinal direction and slow conduction within the transverse direction within individual fibres in Bachman's bundle.[41] Again, this was attributed to non-uniform anisotropy, as there was no histological evidence of specialized conduction cells to be found.

Hocini et al investigated anisotropic conduction in the Triangle of Koch.[42] Langendorff-perfused pig and dog hearts were excised and the right atrium opened to expose the Triangle of Koch. A 96-pole unipolar electrode plaque was used to map the spread of activation during

pacing from multiple sites around the triangle. The area under examination was then carefully dissected to display fibre orientation.

There were 2 patterns of fibre orientation. Those between the coronary sinus os and the tricuspid valve annulus were circumferential (parallel to the TVA). As they approached the anterior portion of the triangle they turned 90 degrees in the direction of the interatrial septum (i.e. longitudinal). Fibres in the far anterior region were also circumferential and contacted the fibres arriving from the TVA at a sharp angle, running underneath the perpendicular fibres. In the second pattern, the posterior fibres were also circumferential but the anterior fibres were longitudinal and did not appear to be in communication with the fibres from the posterior area. The change in direction of the fibres tends to be smooth rather than abrupt. Non-uniform anisotropic conduction was easily demonstrated. Stimulation from the coronary sinus and the oval fossa led to slow conduction in the posterior part of the triangle (Figure 6).

The relationship between the sinus node and the site of origin of the pacemaker impulse

The origin of the electrical impulse that governs pacemaker function, and its relationship to the sinus node and surrounding myocardial architecture, has stimulated a great deal of research. As with the previous electrical propagation studies, it was the advent of the microelectrode technique of recording intracellular and extracellular action potentials that opened the door for many scientists. In excised specimens of rabbit and canine heart, Horibe et al discovered that activation began within the tail part of the sinus node.[43] Conduction velocity within the node itself was slow in all directions. It was not until electrical depolarization reached the terminal crest that conduction velocity increased. In an almost identical study, Miyauchi reported activation in the true histological sinus node region to propagate very slowly apart from in the direction of the terminal crest.[44] Once it entered the terminal crest it moved rapidly. Using the same techniques, Sano and Yamagishi reported that sites of impulse formation were found over a relatively large area, ranging from points very close to the terminal crest to approximately 2 mm away from it.[35] Importantly, theirs was one of the earliest reports of frequent pacemaker shift. Although conduction spread out from the node in a radial fashion, conduction velocity was not equal in every direction. Initially there was radial spread from within the sinus node. Once activation penetrated into the terminal crest it spread rapidly along its longitudinal direction. There appeared to be an area that showed faster conduction in the basal wall of the superior caval vein. Activation appeared to travel in an oblique direction and arrive in the terminal crest at a point slightly

Figure 6. Anisotropic conduction in the Triangle of Koch

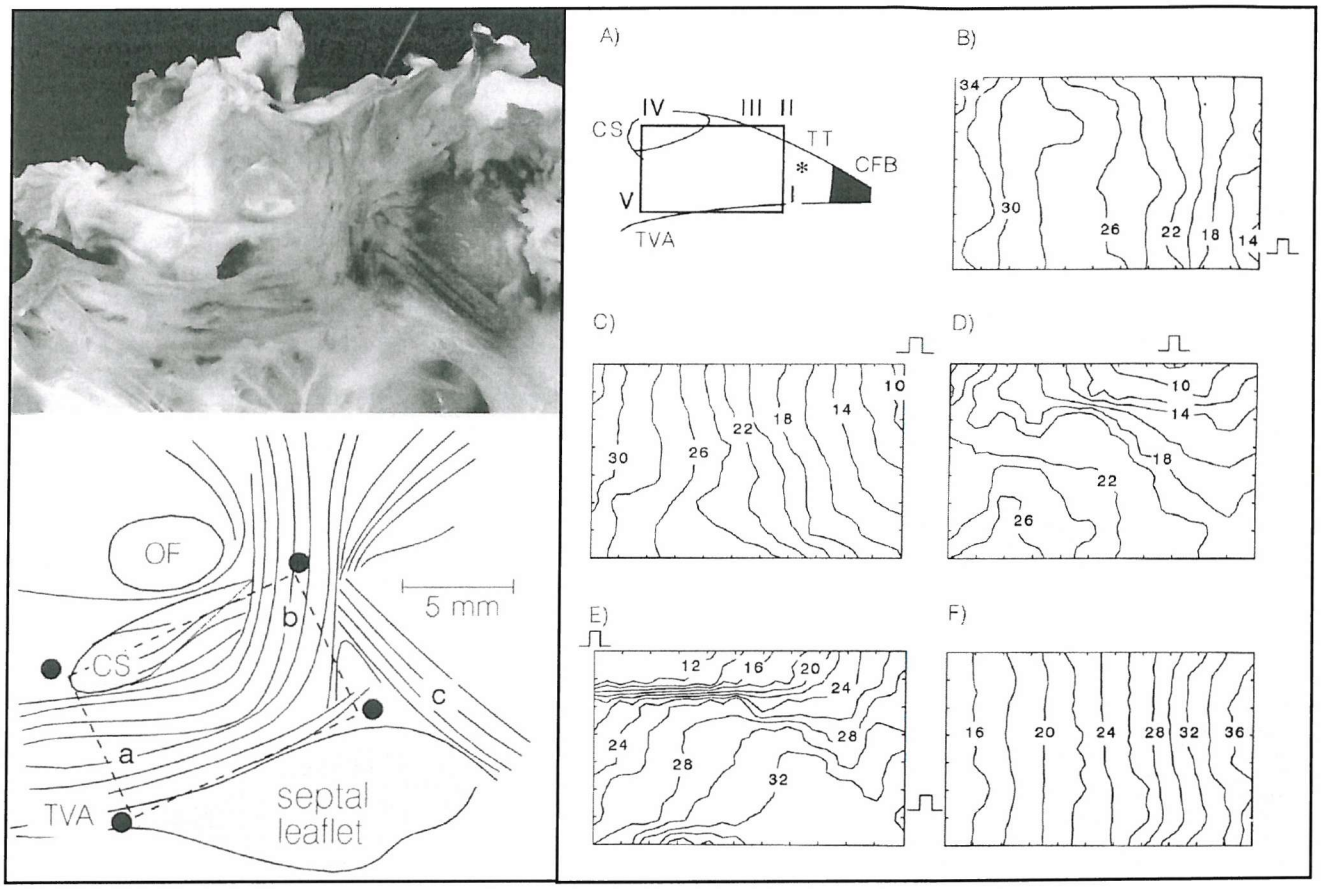

Photograph of the junctional area of a porcine heart showing the geometric pattern of the myocardial fibres in and near the Triangle of Koch. Below is a schematic drawing of the photograph, highlighting the main pattern of the fibre direction. The 4 dots mark the position of recording electrode.

A) Schematic drawing of the Triangle of Koch; the rectangle marks the position of the electrode. Pacing stimulation sites are marked I-V. B) to F): Isochronal maps with lines drawn every 2 ms. The position of the stimulation electrode is indicated by the markers adjacent to the maps.

Reprinted with permission from the American College of Cardiology: J Am Coll Cardiol 1998;31:629-636

away from the site closest to the sinus node. The node appeared to be functionally enclosed from behind and on its lateral sides by tissue that conducts very slowly. In this way activation headed preferentially towards the terminal crest.

In their study of isolated rabbit sinus nodes, Bleeker at al found the earliest action potential to be recorded in the intercaval region, 0.5 – 2.0 mm away from the terminal crest.[45] It propagated preferentially in an oblique cranial direction towards the terminal crest, as a consequence of cell orientation. In other directions, conduction was slower, and it appeared to be blocked in the direction of the atrial septum. This phenomenon has been reported in a number of species, expertly reviewed in a paper by Opthof.[12] In the sinus node of larger species, the area of slow conduction at the septal side of the node (where action potentials with poor excitability are recorded) also becomes larger. He postulated that shielding of the sinus node from one side appears to be a protective mechanism against reentry, and may result from poor electronic coupling or low excitability.

As previously mentioned, the introduction of open-chest mapping with epicardial multielectrode plaques produced dramatic findings, often contradicting the results of studies performed using microelectrodes. In 1978, Boineau et al used epicardial plaques to examine beat-to-beat variations in the origin of the pacemaker complex in the canine heart.[46] Significantly, they reported that 3 separate points of origin were consistently noted, 2 of which were outside the sinus node region. Changes in the sites of origin, brought about through manipulation of the autonomic nervous system, were associated with different activation patterns. The three sites of origin were at high, mid and low parts of superior caval vein – right atrial appendage junction. Only the mid point was positioned over the terminal crest. The points were typically 12-20 mm apart. The authors suggested that all 3 points depolarized (the surrounding areas are always activated later) even though one site might depolarize before the others. They concluded that there was a multicentric origin of sinus rhythm. All 3 sites could depolarize simultaneously, or sometimes one would be first, most often the mid site over the terminal crest. At faster rates the inferior site would not take part, and that area would depolarize late. This gave the impression that faster rates came from a more cranial origin (Figure 7). Slowing the heart rate using vagal stimulation resurrected the lower site, which then depolarized as part of the pacemaker complex.

In a continuation of this study, they performed epicardial mapping on 70 dogs, of which 10 also had limited endocardial mapping.[47] They identified 3-6 sites of origin over a large area of the terminal groove. They described subtle 3-4 mm shifts at each separate site of origin. Each site dominated at a particular range of rates. A progressive hierarchy existed, but with considerable individual variation. The lowest point was separate from the histological sinus

Figure 7. Isochronal maps of different sinus rates

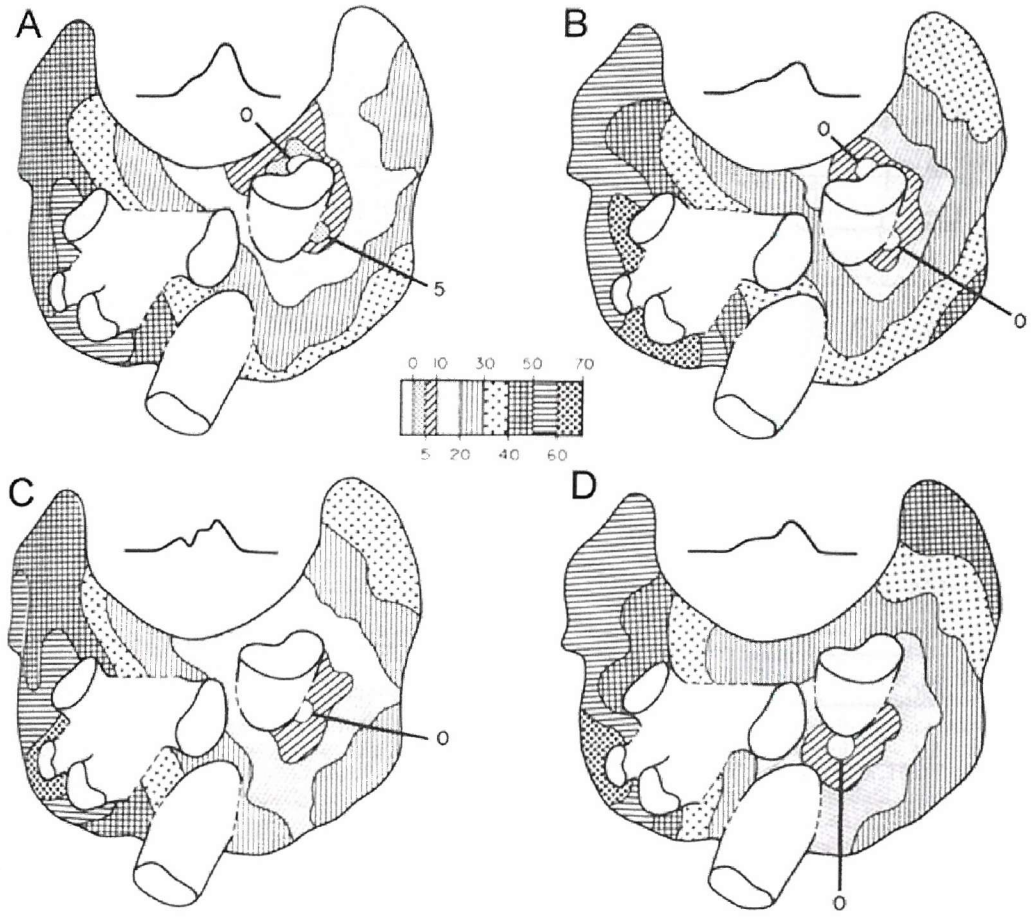

The activation maps A-D are recorded during increasingly longer cycle lengths. There is variation in P wave morphology, position of earliest depolarization and changes in overall activation pattern.

Reproduced with permission from Lippincott Williams & Wilkins: Circulation 1978; 58:1036-1048

node and continued to function even after an incision between it and the sinus node. At faster rates, higher areas dominated. At slower rates, lower areas dominated. At intermediate rates, 2 or 3 origins would fire simultaneously, activating a large area relatively quickly. Endocardial and epicardial activation patterns were similar and there was a close correlation between the points of impulse origin at the two surfaces.

The same group went on to repeat their studies in the human heart, drawing similar conclusions. They performed epicardial mapping studies in open-chest patients undergoing surgical therapy for Wolff-Parkinson-White syndrome.[48] Their activation maps demonstrated patterns ranging from a unifocal sinus node impulse origin, unifocal extranodal impulse origin, and multicentric impulse origin from 2 to 4 widely distributed atrial pacemaker sites. The extranodal pacemaker sites were found anterior and inferior to the sinus node region. They hypothesized that earlier studies may have only noted single sites of origin due to the limited mapping capabilities of the microelectrode technique. They concluded that the human atrial pacemaker complex is 75 x 15 mm in size, whereas the histological sinus node is 4-20 mm in length.

When reviewing the above studies, it becomes apparent that microelectrode studies suggest a unifocal type of impulse generation, whereas studies with multiple electrodes give contradictory results. Also, in vitro studies may not reflect in vivo patterns due to the loss of autonomic influences. However, one must also be aware that recordings made with multielectrode plaques are epicardial recordings and the true origin of the sinus impulse may be intramyocardial, hence the plaques only measure the first site of epicardial breakthrough. The literature would also suggest that pacemaker shifts occur much more in situ than in isolated preparations.

A further discrepancy between action potential recordings and epicardial electrode plaques was discovered in the study published by Bromberg et al.[49] In 6 anaesthetised, open-chest dogs, epicardial mapping was performed using a plaque with 250 unipolar electrodes. In common with other unipolar studies the maximal negative slope of the unipolar electrogram (dV/dT) was taken to indicate local depolarization.[50] The fibrous layer of epicardium was then peeled away and a "floating" microelectrode used to record action potentials from cells that corresponded to known electrode positions. The dominant pacemaker action potentials, defined as occurring >20 msec before activation in any epicardial electrogram, were seen in a 0.5 mm^2 area, usually at the junction between the lower and middle third of the sinus node. These cells were only 2 mm medial to the terminal crest that contained normal myocytes. Latent pacemaker cells (defined by their action potential occurring >20 msec after the earliest

activation of any surface electrogram) were seen in the superior portion of the node. They also formed the medial margin of the node, lying adjacent to the septum. The action potentials in these latent cells occurred 40-160 msec after the earliest electrogram and as late as 200 msec after the earliest dominant action potential. Subsidiary pacemaker sites lay between the dominant sites and the terminal crest. They extended longitudinally over half the length of the node along a tract 1-2 mm wide. In conclusion, they found a large spatial discrepancy between the timing of pacemaker cell action potentials and local electrograms. The time from the earliest action potential to the earliest electrogram was 56+/-25 msec (range 20-101). The spatial difference between the sites was 12+/-6 mm (range 6-21 mm).

Kalman et al performed Endocardial recording of extracellular electrograms in the intact, beating heart.[51] In anaesthetised dogs a decapolar catheter (2 mm bipole spacing, 10 mm inter-bipole spacing) was positioned transvenously, with the aid of fluoroscopy and intracardiac ultrasound, along the terminal crest, with the tip lying in the superior caval vein. Bipolar electrograms of localized activation during sinus rhythm were recorded during autonomic manipulation. In common with the previously reported studies, they found that increasing sympathetic or removing vagal tone resulted in a faster rate coming from a higher position along the recording catheter. They went on to examine the effects of radiofrequency ablation of the pacemaker area. Extensive ablation at the superior caval vein/right atrial junction (3.8 +/- 1.8 lesions) was required to reduce the basic underlying rate by 30%. A 2-3 cm lesion was required to reduce sinus rate by 30%. A 3-4cm lesion was required for total SAN ablation (almost the entire distance from superior to the inferior caval vein. In their study the spatial distribution of the physiological pacemaker complex exceeded the histologically defined SAN by 3-4 times.

The same group went on to perform a similar study in 16 patients referred for electrophysiological study and radiofrequency ablation of inappropriate sinus tachycardia.[52] Again, a multipolar catheter with 5-10 bipole pairs (2 mm interelectrode distance, 5 mm interbipole distance) was positioned along the posterolateral right atrial wall, adjacent to the terminal crest, with the tip in the superior caval vein. The aim of the study was to reduce the intrinsic resting rate of the sinus node and prevent excessive sinus tachycardia from occurring, by ablating the cranial portion of the sinus node complex (believed to be responsible for the faster rhythms). They found that the majority of the sinus node region was capable of producing sinus tachycardia, hence large lesions were required, extending a long way down the terminal crest, before there was a significant fall in baseline rate. Extensive ablation led to a high need for permanent pacemaker implantation. They reported that searching for the site of earliest endocardial electrogram around the sinus node area was of

limited usefulness, as multiple sites showed similar activation times. Although they were able to decrease the intrinsic rate after sinus node ablation they could not conclude whether this was due to destruction of nodal cells or ablation of sympathetic innervation.

As can be seen from the previous discussion, there has been an abundance of literature published on the activation patterns of the sinus node and its relationship to the surrounding atrial myocardium. These studies have used a variety of recording methods, including intracellular action potential recording with microelectrodes, epicardial multisite recording with multielectrode plaques, and intracardiac recording with transvenous catheters. No study has been able to take into account the effect of beat-to-beat variations in the site of earliest activation on the endocardial surface of the right atrium. The data presented regarding the effect of rate change on the site of earliest endocardial activation is based on very limited mapping techniques. Modern electrophysiological mapping techniques require knowledge of endocardial activation characteristics, as almost all procedures are catheter-based using transvenous access to the right atrium. Studies are required that can identify the earliest site of endocardial activation and relate it to right atrial anatomy and the site of the histological sinus node. Such studies require high-density real-time endocardial mapping on a beat-to-beat basis, in the intact, beating heart of a closed-chest subject.

Electrophysiological properties of the terminal crest

Attention will now be directed towards the few studies that have examined the muscular structures in the internodal myocardium, including the atrial septum, the terminal crest, the coronary sinus, the left atrium and the interatrial connections.

Earlier in this introduction we reviewed some of the literature detailing the discovery of non-uniform anisotropy. Spach et al. demonstrated that conduction velocity in the canine terminal crest was 10 times as fast in the longitudinal plane than in the transverse direction.[39] The few recent studies that specifically set out to examine in-vivo conduction properties of the human terminal crest have used bipolar intracardiac recordings. As will be discussed further on in the introduction, the anisotropic properties of the terminal crest may result in the formation of a barrier to conduction. Such a barrier could contribute to the substrate of macroreentrant atrial arrhythmias such as atrial flutter. Consequently, the few studies that have investigated the transverse conduction properties of the human terminal crest have been performed in patients undergoing electrophysiological studies and radiofrequency ablation for atrial flutter.

Critical to the understanding of these studies is the interpretation of double potentials seen in recording electrodes. A double potential is defined as two discrete electrograms or potentials separated by an isoelectric period (flat line). The two potentials represent disparate activation times either side of a line of conduction block, recorded by a single bipole pair that overlies the line of block or is close enough to detect both wavefronts. If two wavefronts run parallel to the line of block at identical times, or approach at right angles to the line but collide at the same time, only a single potential will be recorded.

The correlation of anatomical structures, such as the terminal crest, with the presence of electrogram characteristics, has been investigated by a number of authors. Many have reported the presence of double potentials in the posterior or posterolateral right atrium during atrial flutter.[53-58] Yamashita created a model of atrial flutter in the canine heart by running tight sutures along a short segment of the lateral terminal crest, effectively ligating it.[58] During sinus rhythm, this had the effect of delaying conduction from the high to the low right atrium. Prior to terminal crest ligation, atrial flutter was not inducible. By creating a line of conduction block at that site, atrial flutter became inducible. Double potentials were recorded from this region during the arrhythmia. Interestingly, during flutter, conduction ran perpendicular to the non-ligated margins of the terminal crest. Conduction across these regions was slow, and double potentials were seen.

This study suggests a number of important points. Firstly, ligation of the terminal crest slows longitudinal conduction from the high to the low right atrium. Secondly, a vertical line of conduction block is necessary for the maintenance of atrial flutter. During atrial flutter, this line of block is represented by double potentials. Finally, slow transverse conduction across the upper and lower margins of the terminal crest is possible in the canine heart, and may also result in double potentials.

Olgin et al studied 8 patients with atrial flutter, using intracardiac ultrasound to identify structures such as the terminal crest and Eustachian ridge, and allow accurate positioning of recording catheters alongside them.[54] In 7 out of 8 patients, double potentials were recorded along the terminal crest and Eustachian ridge during flutter, suggesting that these structures provided lines of conduction block.

Tai et al set out to determine the conduction properties of the terminal crest in 24 patients with and without atrial flutter.[59] Again, recording was performed using a 24-pole catheter along the terminal crest, this time identified only with the aid of fluoroscopy and the site of double potentials in the electrograms. Incremental pacing was performed at a site in the low right atrium posterior to the terminal crest. In every patient, pacing eventually resulted in the

appearance of double potentials, indicating conduction block. The principle finding was that double potentials appeared in the flutter group at a pacing cycle length close to sinus rhythm (640 msec). Double potentials did not appear in the non-flutter group until the pacing cycle length was reduced to 214 msec. These results suggest that the transverse conduction properties of the terminal crest vary dramatically between individuals, and may be responsible for the development of atrial flutter in some patients.

Using a similar methodology, Arenal et al investigated whether conduction block across the terminal crest in patients with atrial flutter was functional or fixed.[60] They noted that no double potentials were seen along the terminal crest during sinus rhythm. In 6/24 patients, block was present at the slowest pacing rates, suggesting that it was fixed. In the remainder, block occurred at one or more sites but was pacing rate dependent. They found that it was easier to demonstrate block when pacing from the posterior wall or coronary sinus os.

Schumacher et al studied patients with a history of atrial flutter and atrial fibrillation, using two decapolar catheters placed either side of the terminal crest with the aid of intracardiac echocardiography.[61] They used the presence of double potentials to indicate conduction block, and continuous, fractionated potentials to indicate slow transverse conduction across the terminal crest. At slower pacing rates, continuous activation was seen in all bipoles indicating slow transverse conduction. Double potentials, suggesting conduction block, coincided with changes in activation patterns. They were not necessarily found along the entire extent of the terminal crest.

These studies all provide further evidence of non-uniform anisotropy in the terminal crest. Longitudinal conduction within this major muscle bundle is rapid. Where demonstrable, transverse conduction is slow, and may be indicated by continuous, fractionated electrograms, or possibly double potentials. In the majority of patients with atrial flutter, transverse conduction block is functional, occurring over a wide range of cycle lengths.

The spread of electrical activation through the left atrium

With regard to the left atrium, there is a paucity of information available on the spread of electrical activation. Anatomically, we have described the muscular connections between the right and left atrium. The principal sites of communication are the interatrial band (Bachmann's bundle), the musculature of the coronary sinus, and the "true" interatrial septum. We have already discussed the epicardial recordings by Boineau and others that have

confirmed Bachmann's bundle as a "preferential" route of conduction between the atria.[20,30,41,46]

Attention will now be turned to the few published studies investigating the electrical connections between the two atria, including the coronary sinus musculature.

Electrophysiological properties of the coronary sinus musculature

Antz and colleagues designed their study to examine whether the coronary sinus musculature provided electrical connections to the right and left atria.[62] They used excised Langendorff-perfused canine hearts, with a 20-pole catheter placed in the coronary sinus and great cardiac vein, and another 20-pole catheter positioned along the low posterior wall of the left atrium at the site adjacent to the coronary sinus. After initial mapping studies, the coronary sinus was opened and microelectrodes were implanted into the musculature adjacent to the catheter to validate the extracellular electrogram recordings with intracellular action potential recordings.

During lateral left atrial pacing, double potentials were seen in the coronary sinus catheter. The first component were far field potentials going from lateral to septal left atrium. The second component consisted of sharp, local coronary musculature spikes, seen only in those electrodes adjacent to coronary sinus musculature. The earliest coronary sinus spikes started at a site 26+/-7 mm from the coronary sinus os, with later activation heading septally and laterally along the coronary sinus musculature.

Right atrial pacing at the coronary sinus os resulted in spikes in the coronary sinus catheter going from septal to lateral, closely followed by farfield electrograms from the overlying left atrium. From this finding it was concluded that activation entered the left atrium through a low septal connection. The timing of the coronary sinus musculature and far-field left atrial components of the electrograms in the coronary sinus catheter were confirmed by the electrograms seen in the left atrial catheter and action potential recordings performed in the coronary sinus.

This study presents some important findings. A catheter positioned in the coronary catheter records electrograms from two sources. High frequency, sharp spikes represent activation in coronary sinus musculature. Low frequency, far-field electrograms represent activation from the left atrial muscle adjacent to the coronary sinus. The key message to note is that

activation in the coronary sinus and overlying left atrium is not necessarily synchronous. However, there are electrical communications between the two, occurring 2-3 cm inside the coronary sinus. The right atrium connects electrically to the coronary sinus at the os. Thus, the musculature of the coronary sinus provides a conduit for electrical activity to spread from the left to right atrium, and vice versa.

Dissociation of the left atrial activation from that in the coronary sinus has recently been demonstrated by Kasai et al. Paced extrastimuli were delivered at proximal and electrodes of a decapolar catheter positioned in the coronary sinus in patients undergoing electrophysiological studies. Double potentials were assumed to represent a combination of local coronary sinus muscle activation and separate overlying left atrial myocardial activation. During distal coronary sinus pacing, double potentials with increasing interpotential interval from proximal to distal coronary sinus as a function of extrastimulus prematurity were detected in 9/30 patients, suggesting block in a discrete local pathway distally connecting the coronary sinus to the left atrium and leading to a reversal of the low posterior left atrial activation sequence.[63]

Ndrepepa et al examined the relationship between coronary sinus and left atrial electrograms in 9 patients with atrial flutter or fibrillation.[64] They positioned a 64-pole basket catheter in the left atrium and a 16-pole catheter in the coronary sinus os. Again, the methodology relied upon interpretation of double potentials in the coronary sinus catheter. During atrial fibrillation the sharper, initial component of the double electrograms maintained a constant relationship with right atrial activation times. The second, blunted component was discordant with left atrial posterior wall electrograms recorded from the basket catheter. Thus the coronary sinus electrograms did not depict left atrial activation during atrial fibrillation. During atrial flutter, activation of the posterior wall was delayed compared with activation of the coronary sinus. In some instances, the direction of activation in the left atrium was different from that in the coronary sinus. During sinus rhythm, activations patterns in the coronary sinus and posterior left atrium were either proximal to distal (septal to lateral) or the combination of two wavefronts that approached from proximal and distal and collided in the middle. In 2/9 patients the coronary sinus and left atrial patterns were dissimilar, and apparently similar in 7/9.

Electrophysiological characteristics of the interatrial septum

Electrical activation may also spread between the atria though the interatrial septum. Sun and colleagues performed simultaneous mapping of the right and left atrial septum in intact,

beating canine hearts.[65] Mapping was performed using 64-electrode basket catheters positioned in the right atrium through a femoral vein, and in the left atrium through a small incision in the left atrial appendage. At best, between 17-19 electrodes were in contact with each septal surface. During sinus rhythm, the right septum activated from the superoposterior margin, 20+/-8 msec after the onset of right atrial activation. The resulting wavefront propagated inferiorly across the septum, taking 48+/-7 msec to reach the inferoanterior region. Left septal activation initiated in the superior middle anterior region, 37+/-8 msec after the onset of right atrial activation (17+/-7 msec after the initiation of right septal activation). This site corresponded with the left atrial insertion of Bachmann's bundle in the left septum. Activation spread inferiorly along the left septum, taking 62+/-8 msec. In 2/10 dogs, a second site of early activation was also seen in the inferior left septum. Therefore, although the direction of activation was similar on both sides of the septum during sinus rhythm, activation on the left side was delayed. During pacing from different sites around the periphery of the septum, activation on the two sides was discordant. Interatrial connections were identified at both the inferior and superior margins of the septum. During inferior right septal pacing and right ventricular pacing, although the right septum was activated from inferior to superior, the left septum was activated by 2 distinct wavefronts that propagated from the superior and inferior regions towards the middle of the septum.

The spread of electrical activation from the left atrium to the right atrium

Preferential routes of conduction from the left atrium to the right atrium were examined by Roithinger et al. Eighteen patients were investigated using electroanatomic mapping (for a more detailed discussion on electroanatomical mapping, see later on). Pacing at cycle lengths of 450-600 msec was performed at the distal coronary sinus (distal electrode at the 2:30-4:00 position when viewed in the left anterior oblique angle) or the posterior left atrial wall via a transseptal puncture. Isochronal maps with 30 msec isochrones were constructed of right atrial activation. In the 11 subjects where pacing was performed from the distal coronary sinus, the earliest site of right atrial activation was at the coronary sinus os in 9, the oval fossa in 1 and Bachmann's bundle in 1 other. In the 10 patients who had pacing performed in the posterior left atrium, the earliest site of right atrial activation was Bachmann's bundle in 3, the oval fossa in 2, simultaneously at Bachmann's bundle and the oval fossa in 1, simultaneously at Bachmann's bundle and the coronary sinus in 2, and simultaneously at Bachmann's bundle, the oval fossa and the coronary sinus in 1. The mean time from pacing stimulus to earliest right atrial activation was similar for all 3 sites of breakthrough (58-68

msec). The total right atrial activation time was significantly longer with coronary sinus pacing than right atrial pacing.

This study did not assess the differences between proximal, mid and distal coronary sinus pacing on the site of earliest right atrial activation. The role of the three structures (coronary sinus, Bachmann's bundle and oval fossa) and their relationship to subsequent activation patterns has not been determined. Coronary sinus pacing is a common component of diagnostic electrophysiological procedures, and may have a role in permanent atrial pacing modalities, yet the relationship between the site of pacing and subsequent activation patterns has not been examined. The electrical connections between the left and right atria may have a critical role in arrhythmogenesis, yet this aspect of atrial conduction is poorly understood.

The role of anatomy in the genesis of atrial arrhythmias

Much has been discussed so far on the relationship between electrical propagation and myocardial architecture. Many studies have demonstrated the occurrence of non-uniform anisotropic conduction in areas of the right atrium such as the terminal crest, Eustachian ridge, cavotricuspid isthmus, Triangle of Koch, and interatrial septum. The anisotropic properties of these structures allow them to function as regions of conduction block, manifest as double potentials in recording electrodes. Conduction block may be fixed or functional, occurring at different rates. In many circumstances, conduction block only becomes apparent when the wavefront approaches the structure at right angles to its orientation. During electrophysiological studies, this is demonstrated by pacing at different sites within the cardiac chamber. Much of what would appear to be functional electrophysiological properties of the atrium is therefore derived from its anatomic structure. Consequently, the mechanism of atrial arrhythmias may be directly related to the properties of the atrial architecture.

The anatomy of atrial flutter

This has already been reviewed to some extent in a preceding section with particular reference to the role of the terminal crest in the atrial flutter circuit. It has been demonstrated by many authors that the atrial flutter circuit is macroreentrant and contained within the right atrium, with an area of slow conduction in the cavotricuspid isthmus.[66-69] The anatomical components of the atrial flutter circuit were identified by Olgin et al using intracardiac ultrasound.[54] They demonstrated in 7/8 individuals that the terminal crest and Eustachian

ridge provided a critical posterior barrier to conduction in the right atrium, characterised by double potentials. The tricuspid valve annular provided the anterior barrier. Knowledge of the arrhythmia circuit allows an anatomical approach to the treatment of atrial flutter using radiofrequency ablation. A linear lesion that crosses from the posterior to the anterior barrier will interrupt the arrhythmia circuit, preventing the arrhythmia from occurring. In the case of atrial flutter, this site is the cavotricuspid isthmus.

The anatomy of atrial fibrillation

Atrial anatomy may also play a significant role in the genesis and maintenance of atrial fibrillation. Endocardial mapping of the right and left atria has revealed that the trabeculated right atrium has more organised activation during atrial fibrillation than the smooth walled right atrium.[70-72]Within the right atrium the disorganised posterior region and the organised lateral wall appeared to be separated by the crista terminalis. With regard to interatrial connections, Bachmann's bundle has been identified as a critical crossroads between the two atria during atrial fibrillation.[73]Using epicardial plaques in the sterile pericarditis dog model of atrial fibrillation it has been shown that the majority of reentrant circuits involved Bachmann's bundle. Following ablation of Bachmann's bundle they were unable to sustain induced atrial fibrillation for longer than 5 seconds.

The identification of the boundaries that make up the common flutter circuit has lead to a successful anatomic approach to its treatment with radiofrequency ablation. The isthmus between the inferior caval vein and tricuspid valve annulus is a critical site in the circuit, with a relatively narrow gap between the two easily identifiable structures. If a line of radiofrequency energy burns is drawn from the valve annulus to the inferior caval vein, creating a line of conduction block, the arrhythmia terminates and becomes non-inducible.[67,74]. Confirmation of the presence of complete conduction block at this site is conventionally achieved by pacing from the coronary sinus os and noting the pattern of activation around the septum and right atrial free wall, as well as measuring the time delay from the pacing stimulus to activation in a bipole electrode in the low lateral right atrium.

During atrial fibrillation, electrical activation of the atria is far more complex. It has been recognized that the atria fibrillate as a consequence of multiple reentrant circuits, continuously shifting in a chaotic fashion.[75] There may be a spatial heterogeneity, with organisation patterns differing between the atria. Atrial fibrillation is believed to initiate from triggers, such as ectopic beats or a rapidly firing focus of electrical activity. Much attention has recently been focused on the pulmonary veins as a source of such triggers.[76] Areas of

fixed and functional conduction block provide the substrate for reentry, as well as the perpetuation of the arrhythmia. Adverse conditions in the atrium, such as stretch, pressure overload, myocardial disease and alterations in the electrophysiological properties of the cell membrane, may all increase the atria susceptibility to fibrillation.

Anatomically-based therapies for atrial arrhythmias

The consequences of atrial fibrillation are numerous, including a reduction in cardiac output, an uncontrolled ventricular rate, and thromboembolism. Pharmacological therapy is generally ineffective, and usually limited to control of the ventricular response. Consequently, alternative, more invasive therapies have been attempted over the last 3 decades, with the principle aim of restoration of sinus rhythm together with adequate ventricular rate control.

The left atrial isolation procedure

One of the earliest surgical operations developed to treat atrial tachycardia was the left atrial isolation procedure. Specifically aimed at treating focal left atrial tachycardias, Williams et al performed their operation on 10 dogs, using rapid left atrial pacing to simulate left atrial tachycardia.[77] During cardiopulmonary bypass, they dissected out the interatrial groove to locate the septal portion of the left atrium. A standard left atriotomy incision was performed, which was then extended anteriorly across Bachmann's bundle and down to the mitral valve annulus. The atriotomy was extended posteriorly, parallel to the interatrial septum, to the mitral valve annulus and coronary sinus. Cryoablation was then performed at the mouth of the coronary sinus to destroy any remaining interatrial communications.

Following left atrial isolation, most animals initially had electrically silent left atria, although the majority developed a slow escape rhythm after a few hours, dissociated from right atrial activity. Sinus rhythm, with normal right atrium to ventricle conduction, was present in every animal. Rapid left atrial pacing was contained within the left atrium, the remainder of the heart staying in sinus rhythm, without any deleterious effects on haemodynamic function.

Graffigna et al published the only series of human left atrial isolation in 1992.[78] They performed a left atrial isolation procedure on 100 patients with atrial fibrillation who were undergoing mitral valve repair or replacement. Again, the procedure required extension of the usual left atrial atriotomy around the left atrial margins of the interatrial septum, reaching the anterior and posterior mitral valve annulus. Cryoablation was performed at the junction

between the incision and the mitral valve annulus, and over the adjoining coronary sinus (Figure 8).

Left atrial isolation was effectively performed in 88%, as detected by left atrial pacing techniques. Sinus rhythm was restored in 79 patients (81.4%). The isolated left atrium continued to fibrillate in 48 patients (55.8%), showed an intrinsic escape rhythm in 27 cases (32.5%) and was electrically silent in 11 (12.7%). Sinus rhythm persisted in 70 (72.1%) patients who survived until hospital discharge. In a comparable group of patients who underwent mitral valve replacement without left atrial isolation during the same period, 80% remained in atrial fibrillation postoperatively.

This study demonstrated that isolation of the left ventricle restored sinus rhythm in the right atrium ventricles in the majority of patients with atrial fibrillation and mitral valve disease. It is likely that the left atrium played a key role in the initiation and maintenance of fibrillation in these patients as mitral valve disease leads to left atrial stretch, dilatation, a rise in pressure and subsequent fibrotic change. An important point however is the continuation of fibrillation, or electrical silence, in the left atria of the majority of patients. In this situation the risk of thromboembolism remains, necessitating anticoagulation. Cerebral embolism accounted for three late postoperative complications.

The Maze procedure

The most established surgical therapy for atrial fibrillation is the maze procedure (also known as the Cox-Maze procedure). Once it was recognized that a critical mass of atrial myocardium was required for reentrant wavelets to circulate and maintain fibrillation, James Cox and colleagues devised their procedure to compartmentalize the atria.[79] They effectively created a "maze" by placing incisions within the two atria, connecting anatomical barriers, based on two premises: 1) The atriotomies must be positioned so that it is impossible for an electrical wavefront to originate in any one area of the atrium, propagate around major orifices (or regions of functional conduction block) in the left or right atria or both, and then return to (reenter) the original site of origin (thereby establishing a complete reentry circuit) without crossing one of the incisions; and 2) The atriotomies must be placed close enough so that there is not enough room for even the smallest reentry circuit to form between them. The maze must also leave the heart in a post-operative rhythm that is generated in the atrium, activates all parts of the atrial myocardium and then propagates through the AV node to the ventricles. Therefore the atriotomies must be placed such that the sinus node impulse will

Figure 8. The left atrial isolation procedure

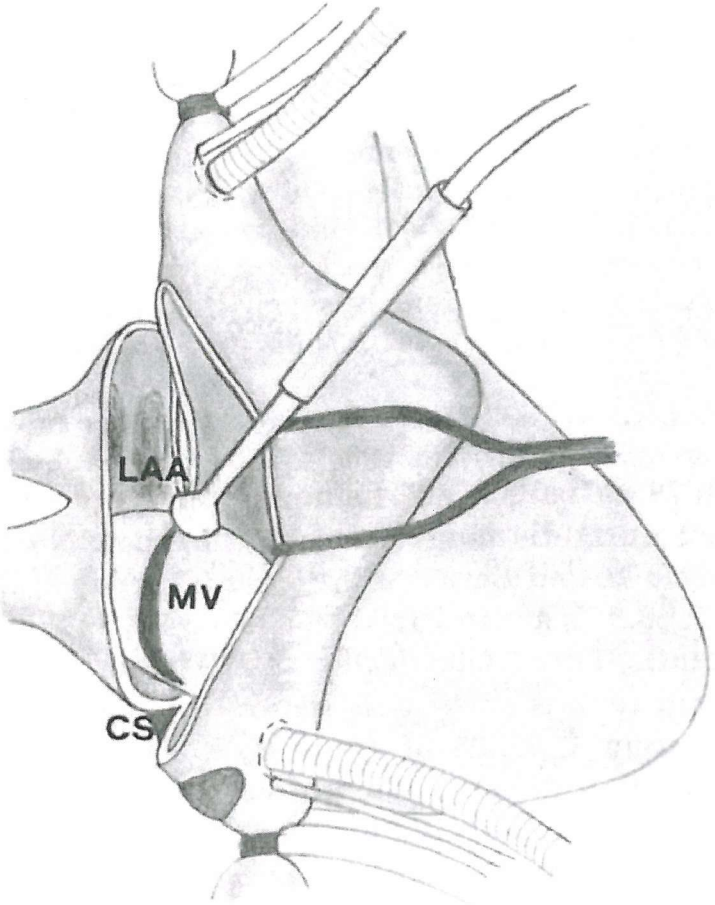

Surgical technique of left atrial isolation. CS = coronary sinus, LAA = left atrial appendage, MV = mitral valve

propagate throughout both atria in a predetermined manner and within a specified time before passing through the AV node. Finally, it is important that the multiple atriotomies, even if they restore sinus rhythm, do not affect effective atrial contraction.

It soon became clear that the position of the atriotomy incisions dramatically affected sinus node function and atrial contractility, with many of the earliest patient requiring pacemaker therapy and continued anticoagulation. There have been many modifications to the Maze procedure in an attempt to overcome these limitations.[80,81] In the modern era, the Maze procedure can be performed with low morbidity and mortality, yet it is still a major undertaking requiring open heart surgery and cardiopulmonary bypass, and there are doubts about the long-term effects on atrial contractile function.

Many groups have attempted to emulate the surgical maze procedure using transvenous endocardial radiofrequency catheter ablation techniques. Such a procedure would avoid the need for open-heart surgery. However, catheter ablation techniques have encountered many obstacles. Left atrial lesions require trans-septal access, which can be accompanied by procedural morbidity. The most effective set of lesions has yet to be elucidated. Most significantly, it appears to be exceptionally difficult to create long, contiguous, full-thickness linear lesions. Gaps in lesions are not uncommon and may be proarrhythmic, leading to atypical forms of atrial flutter. Initial results in animal models of atrial fibrillation appeared to be encouraging, with high initial success rates.[82-84] It was noted in these studies that success often required left atrial lesions in addition to right atrial lesions. The difficulty with animal models of atrial fibrillation is that it is not known how they relate to fibrillation in the human patient.

There have been many reports of catheter maze procedures in human subjects.[85-91] Success rates vary between 0% and 67%, although it should be noted that many "successful" patients required continuation of their drug therapy. Right-sided linear lesions alone are ineffective and procedures are extremely long, taking up to 14 hours.[87,91]. At present, despite recent advances in mapping and navigation technology, plus advances in catheter design, the transcatheter Maze procedure has very high recurrence rates and is technically challenging.

The ideal catheter-based procedure for the treatment of atrial fibrillation would be simple, effective, avoid left atrial lesions, and not affect atrial contractility. The surgical left atrial isolation procedure had many of these qualities, although the left atrium remained electrically silent in many subjects. There has been no attempt to perform a catheter-based left atrial isolation procedure. If the interatrial connections could be identified during right atrial mapping, and severed using radiofrequency ablation, similar results may be achievable

without the need for surgery. Biatrial pacing using a coronary sinus lead could maintain coordinated left atrial contraction.

Transcatheter endocardial electrophysiological mapping techniques

Until recently, the only available approach to electrophysiological mapping of cardiac activation was a sequentially-based method of placing a catheter with single or multiple electrodes in contact with the heart tissue to view the resultant local activity, displayed as intracardiac electrograms. By placing multiple catheters at different positions, and moving steerable catheters from site-to-site, a gradual pattern of the sequence of activation could be built up, providing the rhythm remained stable. There are a number of obvious limitations to this approach, namely the limited number of simultaneous electrograms obtained (usually a maximum of 10-20 sites within a chamber) and the requirement for good tissue contact. Although electrograms offer information on the precise timing of local activation, data regarding wavefront direction, and consequently, velocity, is speculative. Data is presented as a non-intuitive, two-dimensional display that may be difficult to relate to underlying cardiac anatomy. Although the 64-pole basket catheter has been used for arrhythmia mapping for the past 4-5 years, good tissue contact is still required, and the mapping electrode density is still limited.[65]

Electroanatomic mapping using the Biosense CARTO system has provided a significant breakthrough in the approach to electrophysiologic assessment.[92] The addition of an electromagnetic navigation signal, triangulated by 3 external sensors, allows the position of a customised mapping catheter to be detected by the computer software. When the catheter tip is in contact with the endocardial surface, its position is logged by the computer, together with the electrogram from the catheter tip. The timing of local activation, referenced to a standard catheter electrogram in a fixed position, is noted. As the mapping catheter is moved around the endocardial surface, up to 1-200 points may be collected, together with their local activation times. This allows the construction of a three-dimensional model of the chamber geometry, over which an isochronal map may be superimposed. Although this technology has become established for the mapping and ablation of cardiac arrhythmias, a number of limitations apply. Catheter contact with the endocardial surface is required for each point. Each point is collected individually, limiting the total number of sites samples to usually no more than 1-200 and leading to long procedure times. Most importantly, an accurate map requires a constant, stable rhythm, as beat-to-beat variations will not be noticed or accounted for.

Computerised epicardial mapping, using multielectrode plaques, has allowed the presentation of data as isochronal maps that may be superimposed on images of cardiac anatomy. Until now, however, high-density endocardial mapping on a beat-to-beat basis has not been possible. The development of the EnSite 3000 non-contact mapping system has now made this achievable (Figure 9). A review of the EnSite system and the validation studies are presented in the Methods section. The non-contact mapping system is a vital component of this thesis methodology as it allows global endocardial mapping of high-enough resolution to pinpoint the onset of endocardial activation and identify spatial shifts in that may occur on a beat-by-beat basis. The three-dimensional reconstruction of chamber geometry facilitates direct comparisons with chamber anatomy. Variations in activation patterns that occur as a result of changes in heart rate or pacing site may be recorded instantly and applied to the original model of chamber geometry. In contrast, electroanatomic mapping with the CARTO system requires a stable rhythm, and any change in site of onset or activation pattern requires complete remapping to collect new geometry and electrograms, a time consuming process. The locator signal also allows positioning of any conventional catheter at sites of interest within the mapped chamber, thus guiding ablation therapies.

Figure 9. A comparison of endocardial mapping techniques

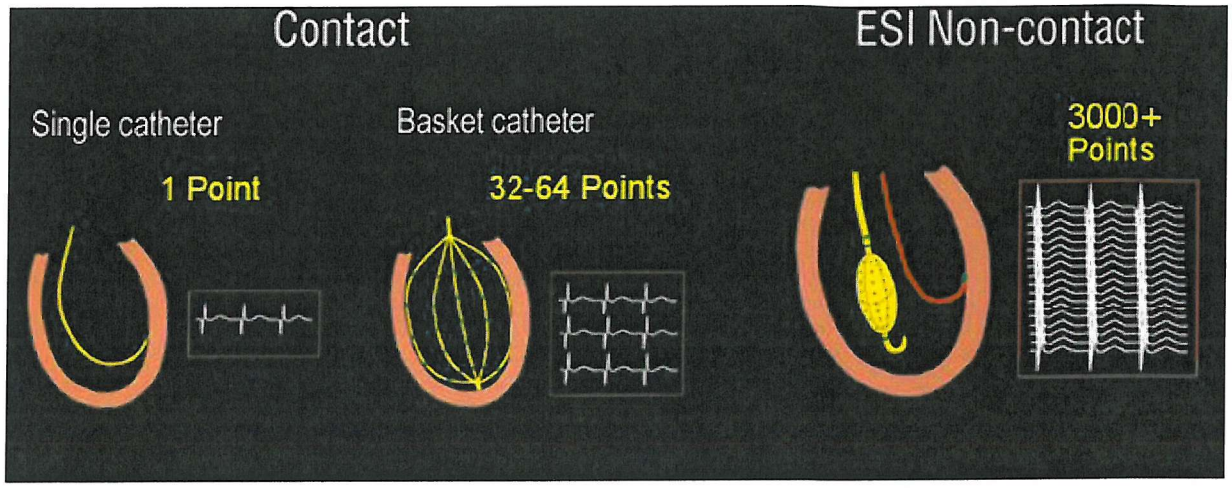

Thesis Aims and Research Questions

The preceding literature review identifies the important relationship between anatomical structures, the architecture of the myocardial fibres, and propagation of the electrical impulse. A number of questions have also been raised, based on gaps in our knowledge and the limitations of previous methodology. This thesis sets out to address some of these questions:

Electrophysiological mapping using microelectrodes or epicardial plaques has provided most of our current knowledge regarding the site of onset of sinus rhythm and its spatial relationship to the sinus rate. Modern electrophysiological procedures are catheter-based and utilise endocardial recordings. To date, only single catheter endocardial mapping techniques have been used to record the site of earliest activation during sinus rhythm at different heart rates. Non-contact mapping provides high-density global endocardial mapping on a beat-to-beat basis. This technique may be used to answer the following question

Question 1: Is there a relationship between the site of earliest endocardial activation and sinus cycle length?

Previous studies have documented the spread of the electrical impulse through the right atrium using microelectrodes in excised specimens of cardiac tissue, or epicardial plaques on the surface of open-chested subjects. Other studies have suggested that the spread of electrical impulse does not use specialized conduction tracts, but is dictated by the orientation of myocardial fibres in the principle muscle bundles. Detailed endocardial mapping of the spread of the electrical impulse through the right atrium has not previously been studied, due to the limitations of single catheter mapping in the in-vivo heart.

Question 2: How does endocardial activation spread through the intact, beating, in-vivo right atrium during sinus rhythm, and what is its relationship to the underlying atrial architecture?

Although we have some understanding of left atrial anatomy and architecture, there are no published studies that have examined global left atrial activation patterns during sinus rhythm or pacing. The relationship between left atrial and coronary sinus activation patterns is also poorly understood as no studies have been able to perform simultaneous high-density left

atrial mapping and coronary sinus mapping. Positioning of a non-contact mapping catheter in the left atrium allows us to pose the question:

Question 3: How does depolarisation spread through the left atrium during sinus rhythm and coronary sinus pacing?

Anatomical interatrial connections have been identified as the coronary sinus, Bachmann's bundle and the oval fossa. There is only limited data on the electrophysiological connections between the atria, their potential role in right atrial activation during sinus rhythm and atrial arrhythmias and the relative role of these connections during pacing.

Question 4: How does electrical activation enter and then spread through the right atrium following pacing at different sites within the coronary sinus?

An appreciation of the relationship between anatomy and the spread of electrical activation may provide additional insights into the mechanisms and potential therapies for atrial arrhythmias. The surgical left atrial isolation procedure was an effective treatment for atrial fibrillation, but to date has not been emulated by catheter techniques do to the inability to identify left-to-right atrial connections. Non-contact mapping data on intra-atrial connections, plus the ability to rapidly identify such connections on a beat-by-beat basis, provides the final question for this thesis:

Question 5: Is transcatheter radiofrequency ablation of the interatrial connections feasible, and if so, does it prevent atrial fibrillation?

Justification

An understanding of the spread of electrical depolarisation through the atria under normal conditions is a basic requirement before progressing to the investigation of abnormal conduction during arrhythmias. Abnormalities of atrial conduction may result in symptomatic brady- or tachycardias. Atrial arrhythmias are common, with atrial fibrillation alone affecting 1% of the population over 60 years of age and >10% of the over 80s. Consequently, understanding the relationship between anatomy and the spread of atrial conduction may have therapeutic implications for a significant proportion of the population.

Treatment options are continuing to expand and have evolved beyond the (often ineffective) use of drugs. The information provided by diagnostic electrophysiological studies has led to the development of radiofrequency ablation techniques, with the goal of providing curative therapy without the need for lifelong drug taking. Pacing therapies are also being developed, designed to suppress abnormal atrial conduction, and create a more homogeneous electrophysiological substrate.

Palliative atrial surgery for congenital and acquired heart disease has now become commonplace. It is well recognized that surgery of this nature can create a substrate for atrial arrhythmias, particularly macroreentrant circuits (incisional flutters). The effects of surgery on atrial anatomy, and the spatial relationship between surgical incisions and natural barriers to conduction, may have an influential role in the development of these arrhythmias.[93]

Addressing the questions raised in this thesis will provide a greater understanding of the substrate for atrial arrhythmias. This could lead to development of new pacing and ablation therapies for atrial arrhythmias, such as inappropriate sinus tachycardia and atrial fibrillation, together with refinement of palliative surgical procedures for congenital heart disease. In addition, the use of a novel, non-contact mapping technology will be explored.

Chapter 2: Methodology

Methods - Myocardial architecture of the porcine atrium

In order to assess the direct relationship between myocardial architecture and electrical activation, it is necessary to pathologically examine the structure of the mapped heart. In addition novel ablation procedures, involving destruction of areas of cardiac tissue, should first be assessed in the animal subject. For this reason, 4 of the 5 experiments were performed in an animal model, allowing euthanasia and excision of the heart following the mapping procedure.

For this thesis, the pig heart was chosen as the animal model. The pig is commonly used as a substitute for human subjects in studies involving the heart. The endocardial mapping system used in this thesis requires cardiac chamber dimensions similar to that of an adolescent or adult human. This precludes the use of smaller animal species. Within the United Kingdom, experiments may only be performed on dogs in situations where other animals are not feasible. For these reasons, as well as for practicality and cost, the pig was the most appropriate animal species to use in the animal studies reported.

The similarities and differences between human and porcine hearts have been studied. Crick et al looked at the myocardial structure of 27 pigs using gross examination and dissection.[94] The pig heart lies in the chest with the classic "valentine shape". The anteroposterior radiographic view in the pig is similar to the left anterior oblique view in the human. As in man, the pig atria had a venous component, a vestibule of an atrioventricular valve, and an interatrial septum. The atrial appendages both face anteriorly towards the back of the sternum. In the pig heart, the caval veins entered the right atrium at right angles to each other, whereas in man they are directly in line. The right atrial appendage in the pig has a narrow, tubular appearance, unlike the broad based, triangular shape in the human. In both species, the appendage is lined by pectinate muscles, which extend out to surround the margins of the vestibule of the tricuspid valve.

The interatrial septum is marked by the oval fossa in both species, although in the pig it is more deep set and superior, close to the orifice of the superior caval vein. The Triangle of Koch is similarly located in both species. Whereas in the human heart the right atrium is usually larger than the left atrium, in the pig they are of a similar size. The left atrial appendage in the pig has a broader base than in the human heart. From the left atrial aspect, the interatrial septum in the pig appears longer than that in man, due to differences in atrial

morphology and the position of the aortic trunk. In both species the majority of the atrial septal region is composed of the infolded groove between the superior caval vein and the right pulmonary veins.

Bharati et al examined the conduction properties of the porcine heart.[95] They performed standard electrophysiological studies on 5 anaesthetised pigs. In their animals, the average heart rate was 132 +/- 32 beats per minute (range 91 – 167), considerably faster than in the human heart. The authors felt that this was probably a consequence of greater sympathetic tone, or less vagal tone, in this species. The intervals between electrograms in the high right atrium and low right atrium were around 10 msec, slightly faster than in human children. Histologically, the sinus node was found in the usual position, at the junction between the superior caval vein and the right atrial appendage. The atrioventricular node lay on the right crest of the interventricular septum, lower down on the septum than in man. Most strikingly, in the pig there were an immense number of nerve trunks, distributed throughout the His bundle and bundle branches.

Methods - Non-contact mapping

The EnSite 3000 non-contact mapping system consists of a catheter-based non-contact multielectrode array, a custom-designed amplifier system, and a Silicon Graphics workstation (Figure 10). The multielectrode array comprises a 7.5F balloon mounted on a 9F catheter around which is woven a braid of 64 insulated 0.003 inch diameter wires. A laser is used to remove a single spot of insulation on each wire, 0.025 inches in length, producing 64 non-contact electrodes, in a pattern of 8 rows by 8 columns. The multielectrode array is positioned in the centre of the chamber under examination, without being in contact with the endocardial surface. The raw far-field electrical data from cardiac activation are acquired and applied to a computerized multichannel amplifier and digital recording system. The unipolar multielectrode array signals are recorded using a ring electrode as a reference, which is located on the shaft of the catheter, approximately 16 cm proximal to the array. Data are sampled at 1.2 kHz and filtered with a programmable bandwidth between 0.1 and 300 Hz.

The system locates any conventional catheter with respect to the multielectrode array by sourcing a 5.68 kHz, low-current "locator" signal from the roving catheter pole, and alternately sinking the current in ring electrodes approximately 1 cm proximal and distal to the multielectrode array on the non-contact catheter shaft. Given the known position of the array electrodes and the current-sink ring electrodes, an algorithm is used to determine the

Figure 10. The non-contact mapping system

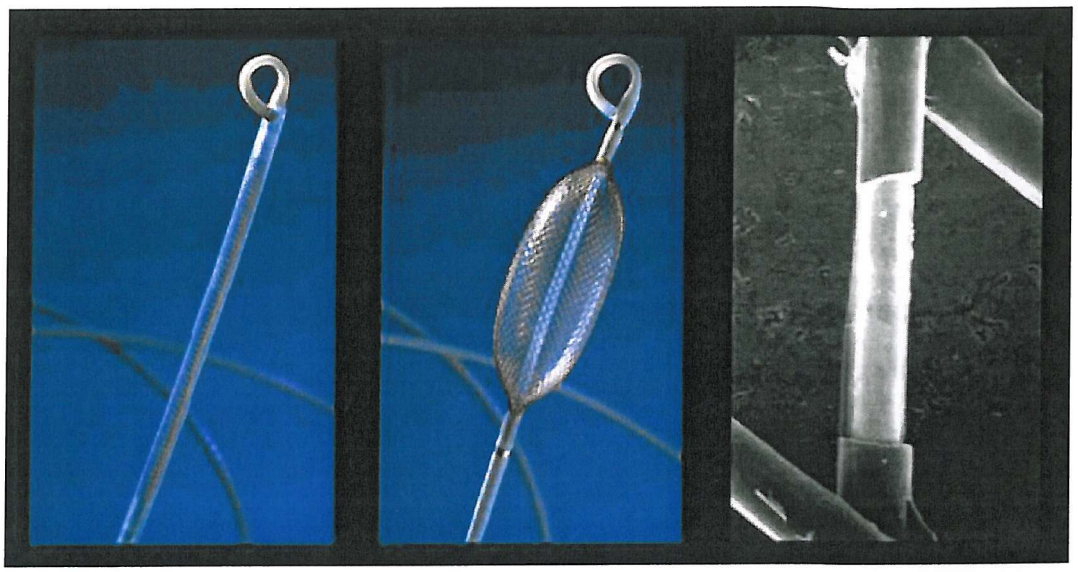

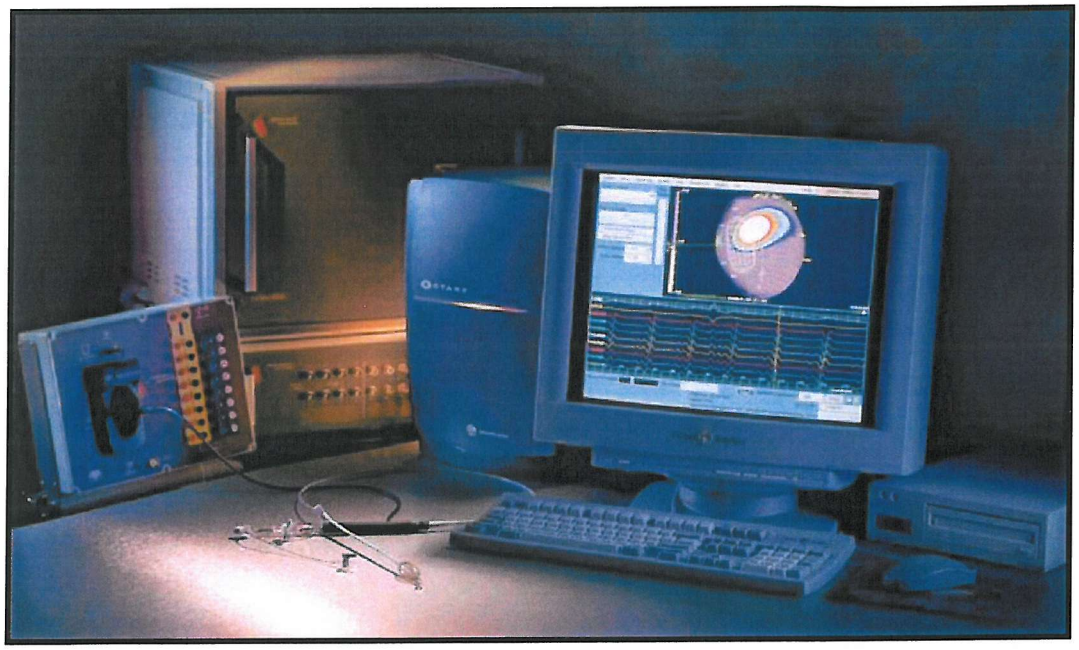

EnSite catheter (above) and system (below)

position of the roving source by demodulating the 5.68 kHz potentials on the multielectrode array (Figure 11a).

The locator signal can be used to construct a three-dimensional computer model of the endocardium, which can then be used for the reconstruction of endocardial electrograms and isopotential maps. As the roving catheter is moved around the endocardial surface, many hundreds of coordinated are collected, building up a chamber specific, anatomically contoured model of endocardial geometry. The system stores only the most distant points visited by the roving catheter in order to ignore those detected when the catheter is not in contact with the endocardial wall. Initially, the geometry forms as a polygonal representation. The sampled coordinates are then fitted to a bicubic spline surface to better estimate the actual chamber surface. The resultant geometry represents the shape of the cardiac chamber during end diastole, i.e. at full expansion. The locator signal can also be used to display and log the position of any catheter on the endocardial surface.

The potential field on the endocardial surface generates the electrical activity detected by the electrodes on the surface of the multielectrode array. A technique to enhance and resolve the actual endocardial surface potentials has been devised based on an inverse solution to Laplace's equation using a boundary element method. The potential field at any one electrode is influenced by the potentials from the entire endocardium, with the degree of influence diminishing with the distance between the electrode and each endocardial point (Figure 11b). The potential field generated on the multielectrode array surface therefore depends upon both the geometry of the multielectrode array and the endocardial surface, and their relationship in space. The multielectrode array geometry is determined at manufacture, and the endocardial geometry acquisition has been described above. With this information, it is possible to compute endocardial electrograms from the multielectrode array potentials by an inverse solution of Laplace's equation (Figure 11c). The boundary element method is applied to reduce the number of elements (and equations), thus allowing the calculations to be performed in real time (1200 Hz, or every 0.83 ms) for each instant of voltage potential measures by the multielectrode array electrodes.

Using these techniques, the system is able to reconstruct and interpolate over 3000 unipolar electrograms simultaneously over the entire virtual endocardium. These electrograms may be superimposed on the virtual endocardium to produce isopotential or isochronal maps with a colour range representing voltage or timing of onset. Electrograms may be interactively selected with the computer mouse pointer as individual points, points along a line, or points within a rectangle from anywhere on the virtual endocardium and displayed as waveforms.

Figure 11a. The locator signal

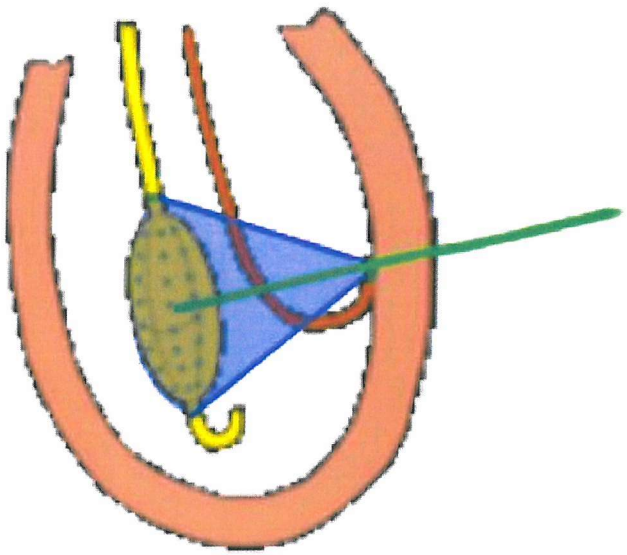

Figure11b. The potential field around the multielectrode array

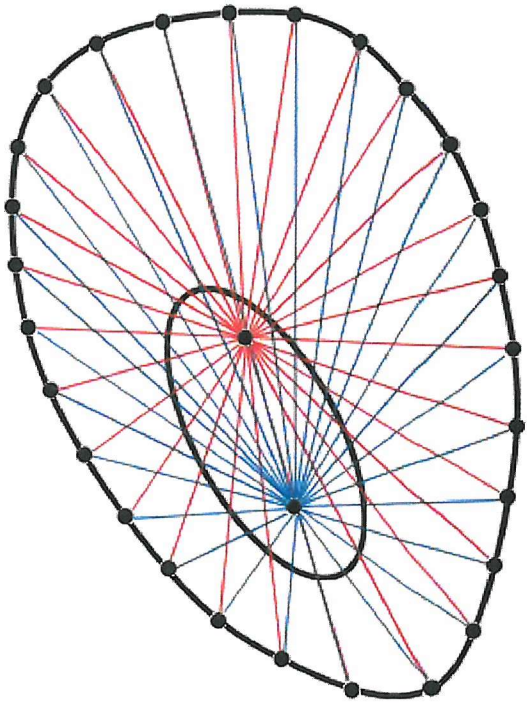

Figure 11c. The inverse solution of Laplace's equation

$$\iint_{\partial D}\left[v\frac{\partial w}{\partial n}-w\frac{\partial v}{\partial n}\right]dA=\iiint_{D}\left[v\nabla^{2}w-w\nabla^{2}v\right]dD$$

The reconstructed electrograms are analogous to those measured by a standard recording catheter in contact with the surface. Thus, the reconstructed electrograms are subject to the same electrical principles as contact catheter electrograms insofar as both contain far-field electrical information from the surrounding myocardium as well as the underlying myocardium. By allowing digital subtraction of unipolar reconstructed electrograms, bipolar electrograms may be displayed by the system.

The use of this non-contact mapping system has been validated by a number of authors. Kadish et al performed right atrial mapping in 12 anaesthetised dogs.[96] In 9 experiments, three quadripolar catheters were placed in the right atrium. Repeated episodes of atrial flutter and fibrillation were induced, and correlations between virtual and contact recordings were performed at 2 – 8 sites within each arrhythmia episode. In the second set of experiments, 2 decapolar catheters were placed within the right atrium to allow 20 simultaneous electrograms to be recorded and used for correlations. Recordings were made during sinus rhythm, atrial pacing, and induced atrial arrhythmias.

To validate the accuracy of the locator signal and the three-dimensional geometry representation, the locator signal was used to estimate distances between electrodes on a multipolar catheter positioned within the right atrium (Figure 12). To validate the accuracy of virtual electrograms, a template-matching algorithm was used to score the correlation between unipolar electrograms from a standard electrophysiology catheter and a virtual electrogram computed from the non-contact system.

A total of 210 interelectrode distances were evaluated. The mean difference between the measured and computed distance was 0.09 +/- 1.3 mm. The mean absolute value of the difference was 0.96 +/- 0.77. The distance between the balloon centre and the vertical distance from the balloon equator did not affect the accuracy of distance measurements, although the vast majority of sites were within 30 mm of the centre or equator.

During sinus rhythm the mean correlation coefficient at all sites between virtual and contact electrograms was 0.80 +/- 0.12. The mean difference in activation times between the virtual and contact electrograms was 1 +/- 4 msec. At a distance of >40 mm from the balloon centre, the accuracy of the electrogram reproduction decreased from a correlation coefficient of 0.82 +/- 0.16 to 0.72 +/- 0.16.

Similar findings have been reported in validation studies of left ventricular non-contact mapping by Schilling et al.[97] Around the equator of the multielectrode array, perfect matches in virtual and contact unipolar electrogram timing were seen up to 52 mm from the centre of the array.

Figure 12. Locator signal validation

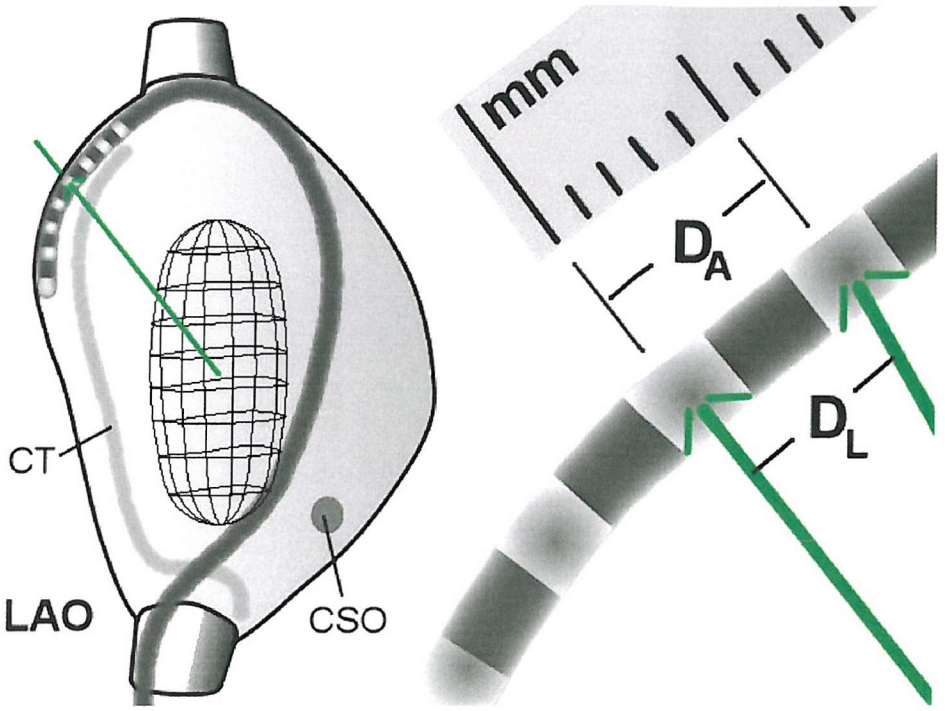

Webster Crista catheter placed in 10 positions with EnGuide switched to each electrode during recordings of sinus rhythm, AFL, and AF. The 7 inter-electrode distances (DL, figure-right) were computed from the EnGuide coordinates in mm (figure-right). Actual distance (DA) between each electrode pair was measured with a micrometer and compared to the EnGuide distances.

However, differences in timing increased gradually with distance, with a significant change beyond 34 mm. Accuracy of electrogram morphology also gradually deteriorated at greater distances.

Gornick et al using in-vitro and in-vivo studies validated the EnSite system accuracy.[98] Initially, the EnSite catheter was deployed in a foam-saline chamber. The tip of ablation catheter was guided by the EnGuide Locator signal to a focal site electrically generated on the foam "endocardial" surface. The tip was punctured into the foam, the foam was removed, and the distance was measured between the electrode generating the focal source, and the roving electrode (D_A). Distances from the EnSite array to focal site ranged from 10 to 58 millimeters. Within a range of 50 mm, D_A was 2.33 ± 0.44 mm. At distances greater than 50 mm, D_A was 7.5 ± 1.13 mm. In this test, all three key algorithms came into play, since geometry was developed, a focal site was mapped using the endocardial map generation, and the EnGuide locator was used to guide to the focal source.

In the second stage of their study, the EnSite catheter was deployed in left ventricle of 11 dogs. Four pairs of transmyocardial 'plunge' electrodes were randomly placed with the clinician blinded. A randomly chosen pair was paced and the EnSite system used to identify the focus and guide an ablation catheter to deliver RF application at the focal site (Figure 13). In 6 animals a second site was also paced, mapped, and burned. Each heart was excised and the actual distance (D_A) from the centre of the burn to centre of the pacing pair was measured. The D_A was 3.0 ± 2.9 mm. This study provided a strong validation for single-beat focal activation mapping. Pacing artifact did not contribute to results, as low-amplitude bipolar pacing was used, and maps were generated several msec after pacing. The lack of influence of pacing artifact was verified by lowering the pacing energy to just below capture, and confirming that this provided no clues as to focal origin on the map.

Figure 13. Accuracy of impulse origin identification

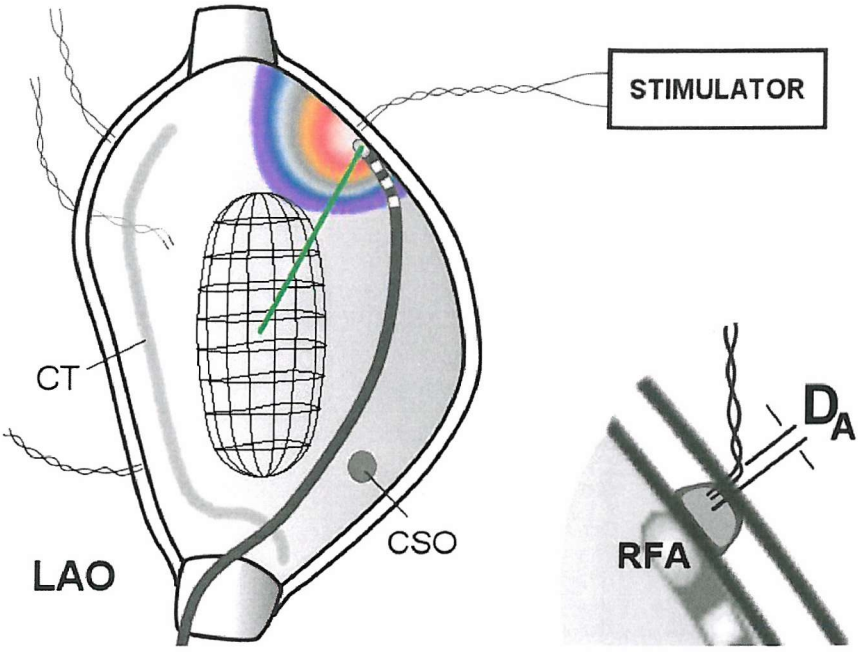

Four pairs of transmyocardial 'plunge' electrodes were randomly placed with clinician blinded. Randomly chosen pair paced, EnSite system used to identify focus and guide ablation catheter to deliver RF application at focal site. In 6 animals a second site was also paced, mapped, and burned. Each heart was excised and the actual distance (D_A, figure-right) from the centre of the burn to centre of the pacing pair was measured (figure-right).

Methods - Subjects

Animal studies

All animal studies were performed under Home Office Project licence approval. Experiments were performed on 30 young adult crossbred Landrace/Large White swine (*sus scrofa*). All animals were female sex, and were raised in the on-site animal housing facility to minimize stress and allow growth. Experiments were not performed until the weight reached at least 70 kg. Mean weight +/- standard deviation was 84.3 kg +/- 8.3 kg, range 71 – 103 kg. A minimum weight of 70 kg was required in order to ensure that the animal's heart, and in particular their right atrium, was large enough to accommodate the non-contact mapping catheter without compromising blood flow and dropping cardiac output. At this weight range, the hearts were of equivalent size to a small human adult.

All procedures were performed under general anaesthetic. The animals were starved overnight, then pre- medicated with an oral benzodiazepine. When drowsy, a large ear vein was cannulated and 10 ml of intravenous alphaxalone/alphadalone injected to induce anaesthesia. When unconscious, endotracheal intubation was performed, and anaesthesia maintained using inhaled isofluorane mixed with oxygen and room air. Bolus doses of opiates (Temgesic) were given every 90-120 minutes for additional analgesic effect. No muscle paralysis agents were used.

The animal was positioned on a radiographic screening table in the supine position and secured using limb ties. Both femoral veins were cannulated using the Seldinger technique and 9 – 11 F haemostatic sheathes inserted. A femoral artery was also cannulated to provide arterial pressure monitoring and access for blood gas analysis. Sheathes were also inserted in the left and right internal jugular veins under direct vision using a cut down approach in the neck.

Continuous 4- lead ECG and arterial pressure monitoring was performed to assess haemodynamics and the animals well being. External radiolucent defibrillation pads were positioned on either side of the chest for emergency cardioversion. A unipolar reference patch was positioned on the animal's belly, and a back plate under the animals back for radiofrequency energy delivery. An additional four ECG limb leads were placed on the animal for recording on the non-contact mapping system.

A Phillips C-arm unit provided fluoroscopic imaging. Under x-ray guidance, the coronary sinus was cannulated with either a quadripolar catheter (10 animals) or a 20 pole steerable catheter (20 animals) for pacing and recording purposes. The catheter position was adjusted

so that the distal tip was at the 2-3 o'clock position around the mitral valve annulus in the anteroposterior view. When a 20-pole catheter was used, the proximal poles were positioned across the cavotricuspid isthmus and up the lateral right atrial wall, adjacent to the terminal crest.

The non-contact mapping catheter was inserted into the right atrium over a guidewire through the left femoral vein and positioned in the mid right atrium. The guidewire was extended out beyond the catheter into the superior caval vein to provide additional stability. The balloon within multielectrode array was inflated with radio-opaque contrast to make it visible using fluoroscopy (Figure 14). Heparin was given as a bolus injection of 10,000 units and then infused intravenously to keep the ACT around 300 seconds.

A steerable mapping and ablation catheter was introduced through the right femoral vein. The three-dimensional reconstruction of right atrial geometry was created by dragging the ablation catheter around the endocardial surface. Initially, the catheter tip was advanced superiorly into the superior caval vein until the bipolar electrograms almost disappeared and fluoroscopy identified it as being within the mouth of the caval vein. The catheter was rotated around 360 degrees, collecting and labeling at least 6 points around the os. The catheter was then moved down to the mouth of the inferior caval vein until contact electrograms had almost disappeared, and the procedure repeated.

Next, the catheter was steered to the tricuspid valve annulus, using contact electrogram morphology and fluoroscopy as a guide. A minimum 6 points were collected and labeled. The coronary sinus os was identified using electrogram morphology and the position of the coronary sinus catheter. The ablation catheter was then dragged around the endocardial surface, between these landmarks, collecting many hundreds of points. The oval fossa was easily identified as a deep-set structure with a prominent limbus into which the catheter tip would catch. In 10 animals the oval fossa was patent, allowing the ablation catheter to pass into the left atrium. Additional structures, such as the Eustachian ridge and terminal crest, would also catch the catheter tip. The mouth of the atrial appendage was identified using fluoroscopy.

After chamber geometry had been created, ventricular pacing was performed at a rate 50-100 msec faster than sinus rhythm. If there was retrograde conduction through the atrioventricular node, non-contact mapping was performed and the isopotential maps examined to find the earliest site of right atrial activation, presumed to be in the vicinity of the node. If identified, the atrioventicular node was marked on the geometry.

Figure 14. Catheter positioning

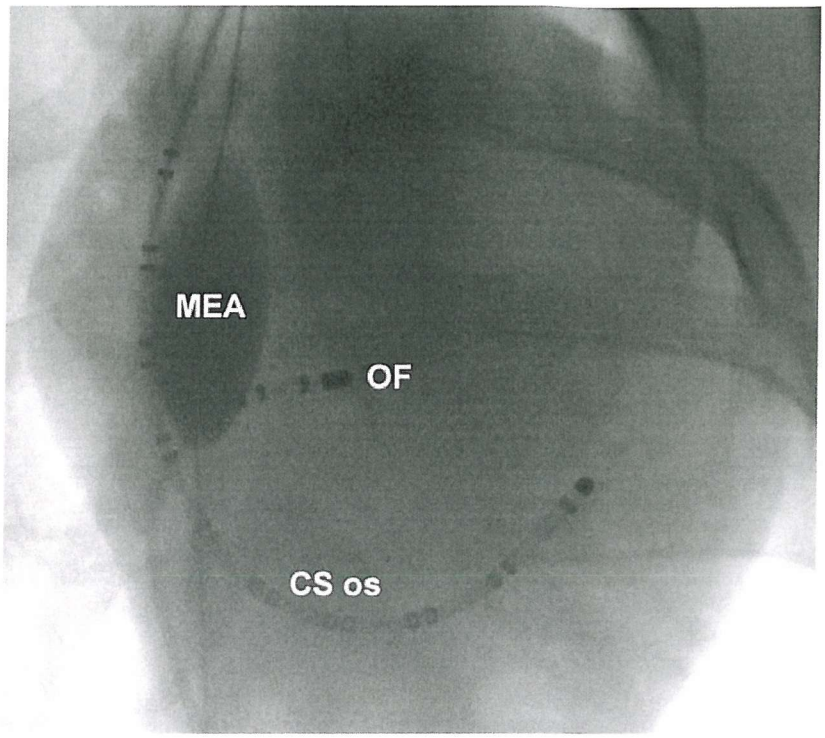

Anteroposterior fluoroscopic view demonstrating the position of the multielectrode array in the mid-right atrium. The 20-pole catheter is positioned with the distal portion in the coronary sinus and the proximal portion in the right atrium. A mapping catheter is positioned in the oval fossa.

Individual experiments were then performed according to the methodology described in each chapter. All recordings were of at least 60-second duration. All data were recorded onto the non-contact mapping system hard drive and backed up onto optical disk for later review. Data were recorded in "raw" format, allowing manipulation and adjustment by filter settings at review stage. Data analysis was performed off line once the experiment had been completed.

Pacing procedures were performed using an external stimulator at 2 msec pulse width and amplitude at twice the pacing threshold. Unless otherwise indicated, pacing cycle lengths were 50 msec faster than the underlying sinus rate. Radiofrequency ablation was performed using a Stockert radiofrequency energy generator. Power output, temperature limitation and duration of application are all described in the appropriate chapter.

At the completion of each experiment, the animal was euthanased using a phenobarbitol infusion. The chest was opened and the heart excised. Gross external and internal examination of the right atrium was performed immediately, before fixing the heart in 10% formaldehyde.

Human Study

The study using human patients was carried out under institutional guidelines after obtaining informed consent from each patient. Each patient had paroxysmal atrial fibrillation and was undergoing radiofrequency ablation of ectopic foci thought to originate from the pulmonary veins. All data was collected prior to ablation therapy or administration of drugs. All antiarrhythmic medication was stopped for 5 days prior to study. No patients were taking amiodarone.

Non-contact mapping of the left atrium was performed in the fasted, non-sedated state. Venous access was gained via the femoral veins and right subclavian vein. The non-contact multielectrode array was positioned in the left atrium via a transseptal approach through the oval fossa. The tip of the multielectrode array was positioned in the left upper pulmonary vein or atrial appendage. The steerable mapping and ablation catheter (Bard, Lowell, MA) was advanced into the left atrium via a transseptal puncture through the oval fossa, within a guiding sheath (Daig, Minnetonka, MN). A 20-pole catheter with 2-10-2 mm spacing (Bard, Lowell, MA) was positioned in the coronary sinus with the tip advanced to the 4 o'clock position when imaged in the 45^{O} left anterior oblique view. Intravenous heparin was infused to maintain the Activated Clotting Time at 300-350 seconds.

Left atrial geometry was created in the standard fashion. Anatomical structures, including the pulmonary veins, oval fossa, mitral valve annulus and left atrial appendage, were identified using a combination of electrogram characteristics and fluoroscopy. Non-contact mapping was performed initially during sinus rhythm. Then, pacing was performed on each of the bipole pairs in turn within the coronary sinus (from the distal pair to the pair at the coronary sinus os) at a cycle length of 600 ms. The position vector from the centre of the multielectrode array to the bipole pairs within the coronary sinus was marked on the left atrial geometry using the locator signal. Pacing amplitude was 1.0 mA above threshold. All data were recorded on optical disk for later analysis. Isopotential maps of left atrial activation during sinus rhythm and pacing were analyzed offline.

Additional methods used in each separate experiment are discussed in the appropriate chapters.

Terminology and Orientation

An accurate description of the onset and spread of electrical activation through the right atrium, plus reference to anatomical structures and dissection findings, requires a clear definition of the spatial orientation used in the subsequent text. As previously mentioned, the animal subjects were placed in a supine position on the operating table. Therefore, for reference purposes, anatomical orientation was based upon the radiographic views obtained in this position (Figure 15). When viewed through the EnSite system, the right atrial endocardium is displayed as a single chamber that appears as a "cast" of the right atrial geometry. The radiographic views used to image the heart fluoroscopically were also applied to the non-contact descriptions.

In human subjects, the anatomical descriptions and orientation within the left atrium are related to the left atrium rather than the anatomical view of the human body.

Figure 15. Terminology and orientation

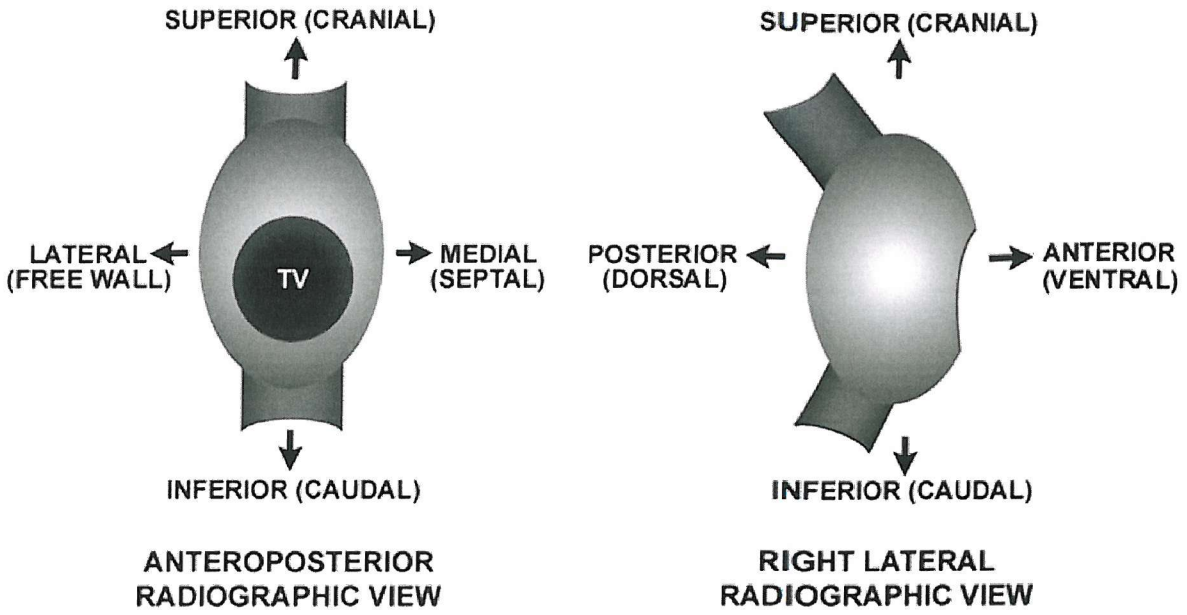

Orientation and anatomic description of the porcine right atrium, as viewed when the animal is supine and imaged radiographically.

Chapter 3: Site of earliest endocardial activation at varying heart rates of sinus rhythm and sinus tachycardia in the porcine heart

Chapter abstract

Introduction: Previous mapping studies of sinus rhythm suggest faster rates arise from more cranial sites within the lateral right atrium. In the intact, beating heart, mapping has been limited to epicardial plaques or single endocardial catheters. The present study was designed to examine shifts in the site of earliest endocardial depolarisation during sinus rhythm and sinus tachycardia using high-density mapping in the intact, beating heart.

Method: Non-contact mapping of the right atrium during sinus rhythm was performed on 10 anesthetized swine. Recordings were made during sinus rhythm, phenylephrine infusion and isoproterenol infusion. The hearts were excised and the histological sinus node identified.

Results: The mean minimum and maximum cycle lengths recorded were 355+/-43 ms and 717+/-108 ms. A median of 3 (range 2-5) sites of earliest endocardial depolarisation were documented in each animal. With increasing cycle length the site of earliest endocardial depolarisation remained stationary until a sudden shift in a cranial or caudal direction, often to sites beyond the histological sinoatrial node. Endocardial shift was unpredictable with considerable variation between animals. Overall, faster rates arose from more cranial sites ($R=0.46$, $p=0.023$). There was no difference in the mean cycle length of sinus rhythm originating from specific positions on the terminal crest ($R=0.44$, $p=0.17$). Cranial sites displayed a more diffuse pattern of early depolarisation than caudal sites.

Conclusions: In the porcine heart the relationship between heart rate and site of earliest endocardial depolarisation shows considerable variation between individual animals. These findings may have implications for clinical mapping and ablation procedures.

Introduction

The preceding literature review has described how anatomical dissections have located the histological sinus node, lying in the terminal groove at the junction between the right atrial appendage and the superior caval vein. It consists of a subepicardial head, an intramyocardial body, and a subendocardial tail. In the porcine heart it measures 18 mm in length and 3.5 mm in width.[12] There are limited connections between the nodal tissue and surrounding atrial myocardium. A zone of transitional cells has been described where the node lies in close proximity to the terminal crest.[15] Small muscle bundles leave the node and penetrate into the superior caval vein, Bachmann's bundle, the right atrial appendage, and towards the interatrial septum.[16]

Activation mapping of the sinus node using microelectrodes has demonstrated that conduction within the node is slow, and velocity does not increase until it reaches the surrounding myocardium, usually the terminal crest.[43,44] Epicardial plaque mapping studies have described the occurrence of frequent sinus node pacemaker shift.[46,47] Many points of origin of the sinus impulse can be identified, some outside the area of the histological sinus node (typically around the os of the superior caval vein and at the high, mid and low junctions between the superior caval vein and right atrial appendage). This has been described as a multicentric origin of the sinus node impulse. The different sites depolarised at slightly different times, or occasionally simultaneously, depending upon the underlying sinus rate. The relationship between the different pacemaker sites can give the impression that faster rates originate from more cranial sites. However, considerable variation exists between individual subjects. It has been suggested that the human atrial pacemaker complex is 75 x 15 mm in size, whereas the histological sinus node is only 20 mm in length.

Combined multielectrode and epicardial mapping techniques have also demonstrated that the site of earliest action potential recording (the presumed site of impulse origin) may be distant, in both time and space, from the site of the earliest electrogram, adding further confusion to our understanding of the sinus impulse.[49]

Today, the vast majority of diagnostic electrophysiological studies and therapeutic procedures are performed using endocardial contact mapping with bipolar electrograms. Basic studies using simple multipolar catheters positioned along the terminal crest indicate that faster rates originate from more cranial positions.[51] Multiple sites show similar activation times, and a significant proportion of the sinus node needs to be destroyed before radiofrequency ablation affects the upper rate that the sinus node is capable of.[52] Again, the spatial distribution of the pacemaker complex would appear to exceed the histologically

defined node by 3-4 times. These studies have been limited by the resolution of the mapping electrodes.

This experiment was designed to test the hypothesis that the site of earliest endocardial activation is related to the cycle length of sinus rhythm or sinus tachycardia, with faster rates occurring from more cranial positions. This study is unique in that it involves high-density, endocardial mapping in the intact, beating heart.

Methodology

The basic methodology was performed as described in the preceding Methods chapter. In brief, the animal subjects were cared for and grown to 75-105 kg in weight. All procedures were performed under general anaesthesia, in accordance with the Home Office Project License. Electrophysiological data were recorded using non-contact mapping techniques. The non-contact mapping catheter multielectrode array was positioned in the centre of the right atrium via the left femoral vein. A 20-pole steerable catheter was positioned in the coronary sinus, such that the catheter tip was in the 2-3 o'clock position when viewed in the fluoroscopic anteroposterior position, the distal 5 bipolar pairs (electrodes 1 – 10) were positioned in the coronary sinus, and the proximal 5 bipolar pairs were placed along the floor of the right atrium and up the lateral wall, adjacent to the terminal crest. A 4 mm tip steerable ablation catheter (Stinger, Bard, Lowell, MA) was used for the creation of chamber geometry and labelling of anatomic structures. During non-contact mapping the electrode positioned at the coronary sinus os was used as a spatial reference to look for evidence of multielectrode array movement in relation to chamber geometry. Its position at the beginning of the study was labelled on the geometry and all subsequent measurements were validated against this point.

Baseline data was recorded during sinus rhythm. The heart rate was then slowed using an intravenous injection of 400 mcg of phenylephrine. Phenylephrine is an alpha-adrenergic agonist that causes peripheral vasoconstriction and a reflex slowing of the heart rate mediated via the vagus nerve. Non-contact mapping was performed and data recorded at 2-minute intervals until the heart rate returned to baseline. The heart rate was then increased using an intravenous injection of isoprenaline (a beta-adrenergic agonist). Doses ranged from 10-20 mcg, until a heart rate of greater than 150 beats per minute was achieved. Non-contact mapping was performed and data recorded at 2-minute intervals until the heart rate again returned to baseline.

Following the mapping procedures, the animals were euathanased with 50 ml of Phenobarbitol. The hearts were excised and placed in 10% formaldehyde. The specimens were sent to the National Heart and Lung Institute, Imperial College, London, where they underwent meticulous examination. Initially, the caval veins, pulmonary veins, pulmonary artery and aorta were tied, and the chambers inflated with latex. Once this had dried, the right atrium was cut from superior tricuspid valve annulus to the tip of the right atrial appendage, and peeled open. The latex thus provided a detailed cast of right atrial geometry and was to aid identification of anatomical structures and their spatial relationships. The right atrium then underwent detailed endocardial dissection. The endocardium of the right atrium was peeled off without damaging the myocardial fibres. Watchmaker's forceps were used to follow the orientation of the fibres. Detailed sketches were made demonstrating the architecture of the endocardial layer of the musculature. Further histological examination was then performed to identify the precise location and dimensions of the histological sinus node. The sinus node was identified histologically in the subepicardium as a cluster of small, weaving myocardial cells within a dense fibrous matrix. The location was determined by marking the limits of the node on the slides. Length and width were determined by tracing from section to section from superior to inferior. Sections were cut transversely across the right atrium-superior caval vein junction.

Electrophysiologic data was assessed in a standard manner. Anatomical labels were marked on the geometry to demonstrate the margins of the caval veins, tricuspid valve annulus, coronary sinus os, right atrial appendage and oval fossa, using data recorded obtained from electrogram characteristics and fluoroscopy. The terminal crest was identified by fluoroscopy (in the anteroposterior view it is a "C-shaped" curve at the lateral margin of the right atrial silhouette), and by identifying its relationship to other anatomical structures on the latex cast, and transferring this data to the virtual geometry. For measurement purposes, during off-line review the most cranial and anterosuperior portion of the right atrium at the crest of the junction of the superior caval vein and the right atrial appendage was identified and labelled on the right atrial geometry as the vertex. This provided a fixed, static reference point from which subsequent measurements to sites of earliest endocardial depolarisation were made.

Sinus rhythm and sinus tachycardia were defined as 5 consecutive beats with a cycle length that varied by less than 10 msec with identical P wave morphology on the surface ECG (limb leads). All 5 beats had to originate from the same site on the right atrium geometry and the locator signal steered to the electrode positioned at the coronary sinus os had to be within 2 mm of the marked reference point on the geometry. Activation was traced backwards in time from the end of the surface P wave, viewing the isopotential map in 0.83 ms intervals. As the

beginning of the P wave was reached, colour sensitivity and offset were changed to keep areas of depolarisation visible (represented by a range of colours against the purple background). Virtual electrograms were constantly positioned on the geometry at the site of depolarisation. Highpass filter settings were adjusted to as low as possible (usually 1 Hz), so that the isoelectric baseline on the virtual electrogram trace was flat. The site of earliest activation was defined as the area on the geometry with the earliest onset of depolarisation (as represented by the origin of the earliest negative potential on the isopotential map) that also had a QS or qS complex in the virtual unipolar electrograms.

The site of impulse origin at different heart rates was labelled on the geometry. The distance along the terminal crest from the vertex of the right atrium to the site of impulse origin was measured using the surface tape measure facility. Recordings were analysed starting with the slowest documented rate (longest cycle length) and were repeated each time the site of earliest depolarisation shifted by more than 5mm or the cycle length changed by 5%, until the maximum heart rate was reached. Incremental fixed heart rate or cycle length intervals were not used, as an increase in 20 beats per minute from 80 to 100 beats a minute (a 25% increase) may have had a greater influence on site of impulse origin than an increase from 160 to 180 beats a minute (a 12.5% increase).

Statistical analysis was performed using a personal computer, Microsoft Excel 2000 and StatsDirect software. Data was examined using multiple linear regression and non-parametric regression analysis where appropriate. A p value of <0.05 was considered statistically significant. Data are presented as mean +/- SD unless otherwise indicated.

Results

Non-contact mapping was performed on 10 animals, mean weight 84 +/- 6 kg. The mean maximum cycle length recorded was 717 +/- 108 msec (range 600 – 950 msec). The mean minimum cycle length recorded was 355 +/- 43 msec (range 290 – 440 msec). The mean range of cycle length recorded was 362 +/- 118 msec (range 205 – 575 msec). This data is summarised in Figure 16, together with the effect of isoprenaline and phenylephrine infusion. Isoprenaline infusion resulted in a mean decrease in cycle length of 308 +/- 120 msec. Phenylephrine infusion resulted in a mean increase in cycle length of 30 +/- 23 msec

Endocardial mapping

The site of earliest endocardial activation was recorded from a median of 3 separate sites (range 2-5) consistent with the anatomical position of the terminal crest in each animal. The mean length of endocardium that contained sites of earliest depolarisation was 27 +/- 21 mm (range 5 – 65 mm). There was a positive relationship between the length of endocardium that gave rise to sinus impulses, and the number of sites of impulse origin ($R2=0.62$, $p<0.001$). There was no relationship between the range of cycle lengths mapped and the distance between the most cranial and caudal sites of earliest depolarisation ($p=0.56$), or the number of sites of earliest depolarisation ($p=0.075$).

There was considerable variation between the 10 animals studied regarding the change in site of earliest endocardial activation at different cycle lengths. Individual recordings are presented in Figure 17. A combined scatter plot of distance from the right atrial vertex for all cycle length recordings in every animal is shown in Figure 18. Although the trend was for faster rhythms to originate from more cranial sites, and slower rhythms from more caudal sites, the recordings at 900 ms cycle length made in animals 1 and 7 heavily influenced the trend line displayed. However, multiple linear regression analysis of mean endocardial distance along the terminal crest for each cycle length recorded, weighted by the number of recordings at each cycle length demonstrated a statistically significant positive correlation ($R^2=0.21$, $p<0.05$). Non-parametric linear regression analysis gives a Kendall's rank correlation coefficient of 0.14 ($p<0.05$). There was no relationship between the mean cycle lengths recorded at sites 10, 20, 30, 40 and 50 mm from the vertex (multiple regression analysis, weighted by the number of cycle length recordings at each site, $R=0.44$, $p=0.17$).

Figure 16.

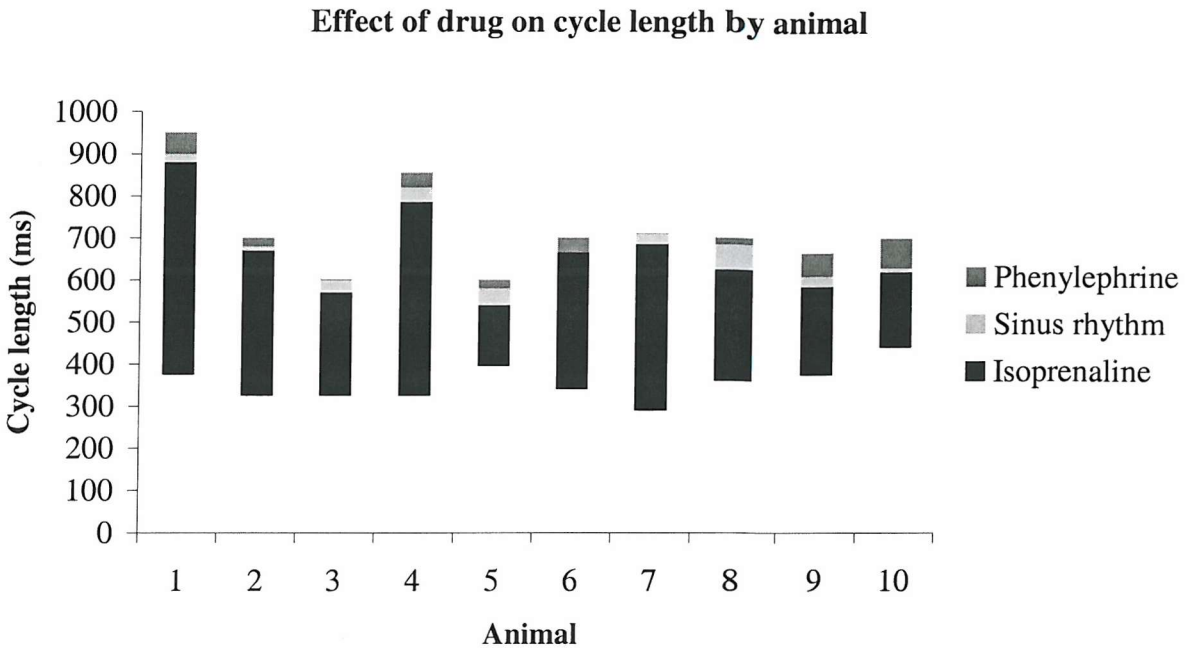

Range of recorded cycle length of sinus rhythm and sinus tachycardia for each animal. The shaded bars show baseline sinus rhythm prior to drug infusion (light grey), increase in cycle length in response to intravenous phenylephrine (dark grey) and decrease in cycle length in response to isoproterenol infusion (black).

Figure 17. Individual animals' charts of site of impulse origin by cycle length

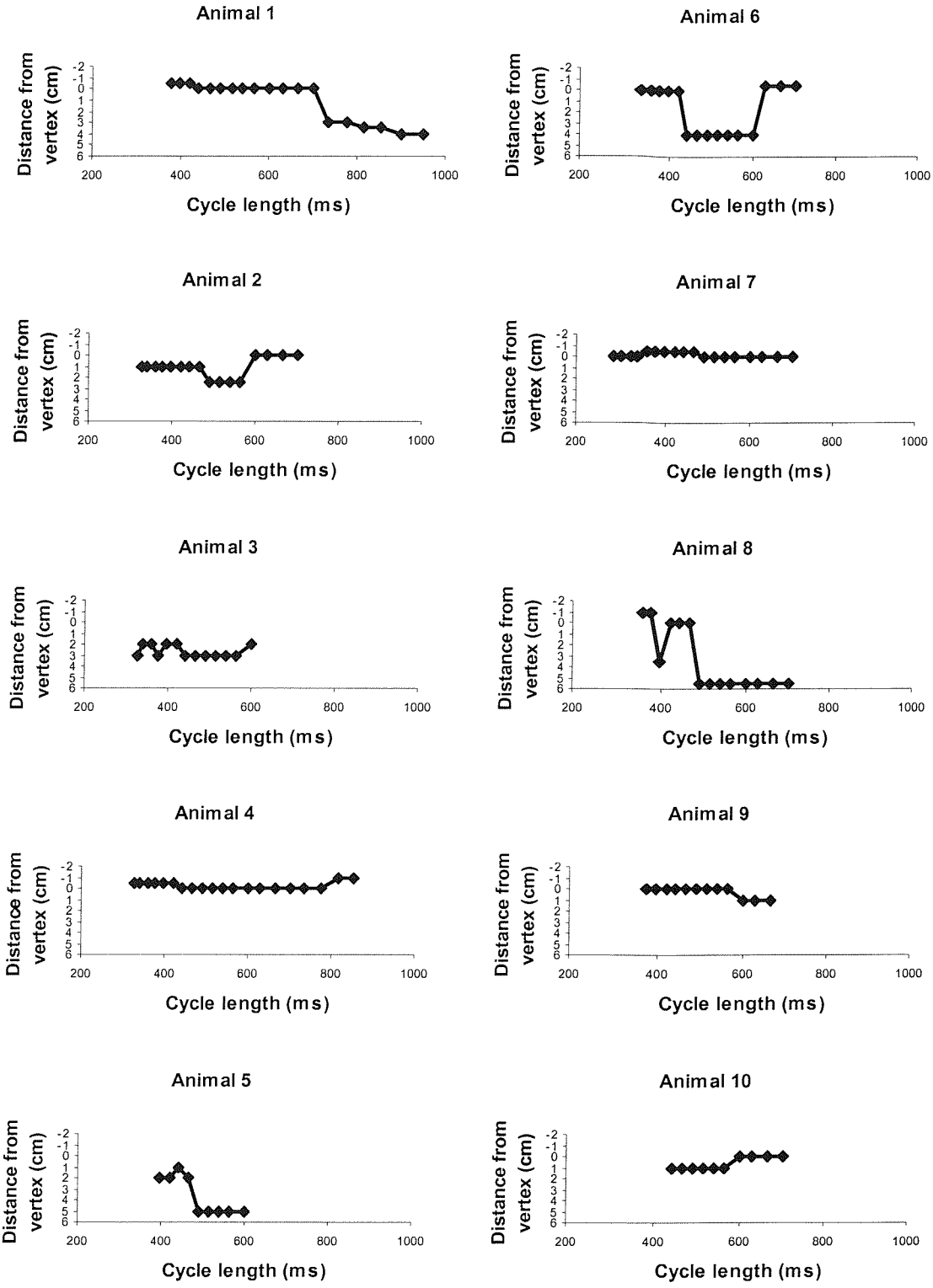

Individual charts of the site of earliest endocardial activation, measured as the endocardial distance to the vertex of the right atrium, for each cycle length recorded. Positive distances are measured down the lateral wall, whereas negative distances are measured down the medial wall.

Figure 18.

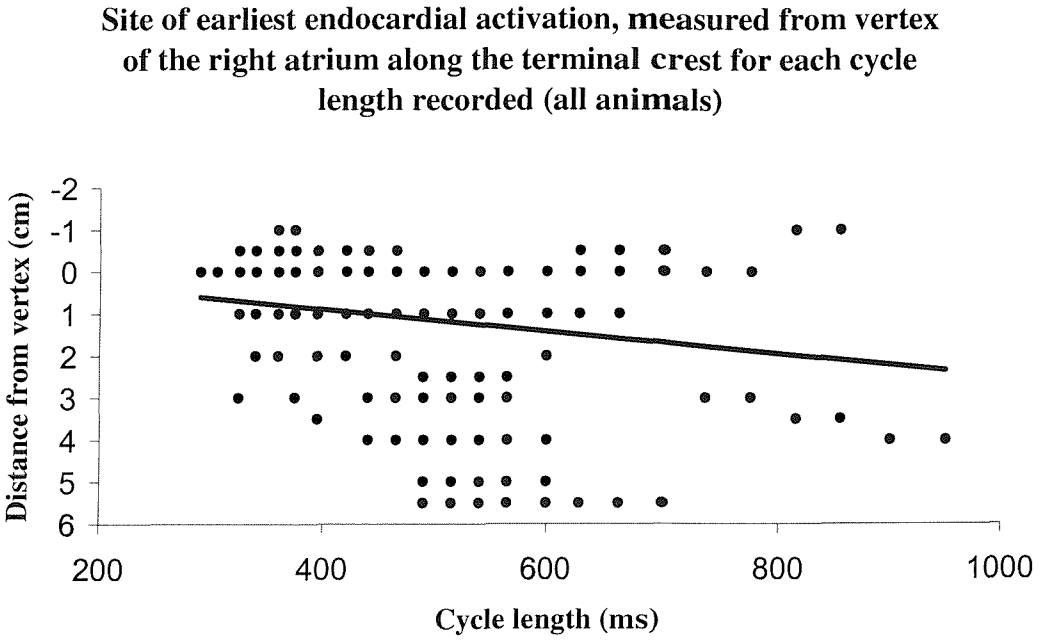

Combined scatter plot of distance from the right atrial vertex for all cycle length recordings in every animal

Changes in site of earliest depolarisation occurred in all animals following isoprenaline infusion. Only animals 1 and 9 demonstrated a stepwise cranial shift in the site of earliest depolarisation as the cycle length shortened (Figure 19). In the remaining 8 animals, the distance of the site of impulse origin from the vertex of the right atrium both increased and decreased as the cycle length shortened (Figure 20). The greatest distance between 2 consecutive sites was 55 mm, occurring over a shortening in cycle length of 25 msec (animal 8).

Characteristics of site of earliest depolarisation

The initiation and subsequent spread of depolarisation demonstrated certain characteristics depending upon the position of the site of earliest depolarisation (Figure 21). When depolarisation began at a site that was adjacent to the superior caval vein, a broad area of endocardium depolarised within the first 5 ms. Careful adjustment of the colour contrast and gain settings were required to focus the isopotential map on the precise site of earliest depolarisation. On the other hand, when the site of earliest depolarisation was in the region of the mid-lateral terminal crest, the isopotential maps demonstrated a discrete focus of earliest depolarisation during the first 5 ms with a gradual spread of depolarisation in a cranial and caudal direction.

The histological sinus node and site of earliest endocardial depolarisation

Five hearts underwent detailed dissection and histological examination. The remaining 5 hearts were not examined, as they were required intact for an alternative study (see Chapter 7). The mean length of the histological sinus node in the 5 examined hearts was 9 +/- 3mm. In 2/5 animals the histological node straddled the vertex of the right atrium, lying over the crest of the atrial appendage with the head on the medial side and the tail on the lateral side. In the remaining 3/5 the histological node lay in the lateral terminal groove with the superior portion 5–10mm from the vertex.

In 4/5 hearts the length of atrial geometry that provided sites of earliest depolarisation exceeded the length of the histological measurement of the sinus node, suggesting that in some instances earliest endocardial depolarisation was distant from the histological sinoatrial node.

Figure 19. Isopotential maps of earliest endocardial activation

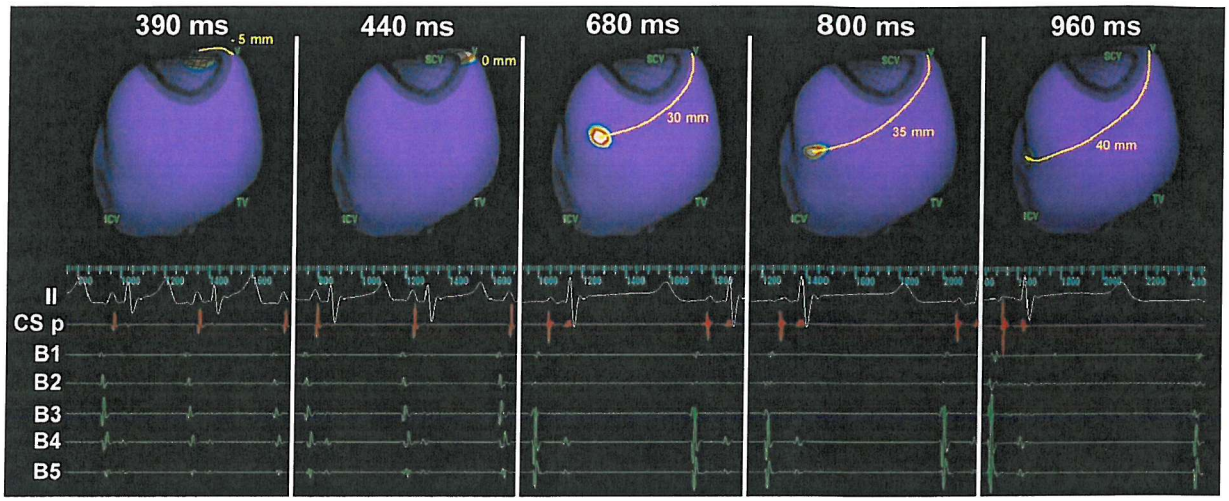

Isopotential maps demonstrating the onset of endocardial activation at five different sites and cycle lengths (taken from animal 1). In each frame the right atrial geometry is shown in an identical orientation, similar to a right anterior oblique view with extreme cranial tilt. The coloured area with white centre represents depolarisation. ECG recordings from lead II, an electrogram from the electrodes at the coronary sinus os and electrograms from the 5 proximal bipole pairs on the 20-pole catheter extending down the lateral right atrial wall adjacent to the terminal crest, are displayed.

Figure 20. Isopotential maps of earliest endocardial activation

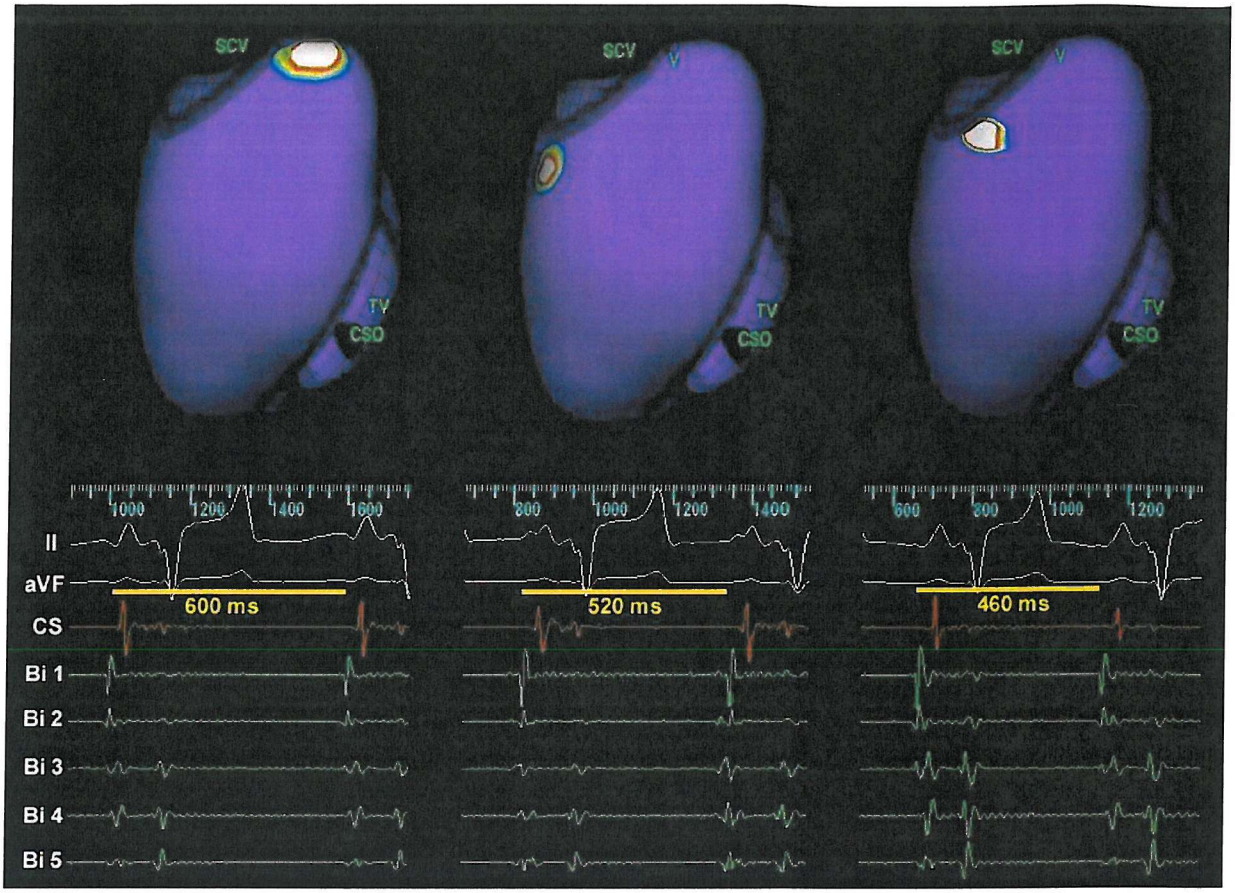

Isopotential maps demonstrating the onset of endocardial activation at three different sites and cycle lengths (taken from animal 3). In each frame the right atrial geometry is shown in an identical orientation, similar to a right lateral view with extreme cranial tilt. The coloured area with white centre represents depolarisation. ECG recordings from leads II and aVF, an electrogram from the electrodes at the coronary sinus os and electrograms from the 5 proximal bipole pairs on the 20-pole catheter extending from the superior caval vein (Bi 1) to the inferior caval vein (Bi 5) are also shown. At 600 ms cycle length the site of earliest endocardial activation is at the vertex of the right atrium. At 520 ms cycle length it arises from a site 23mm from the vertex, and at 460 ms cycle length it arises from a site 12mm from the vertex when measured using the surface tape measure facility. SCV, superior caval vein; V, vertex of RA; CSO, coronary sinus os; TV, tricuspid valve; CL, cycle length.

Figure 21. Isochronal maps of cranial and lateral sites of impulse origin

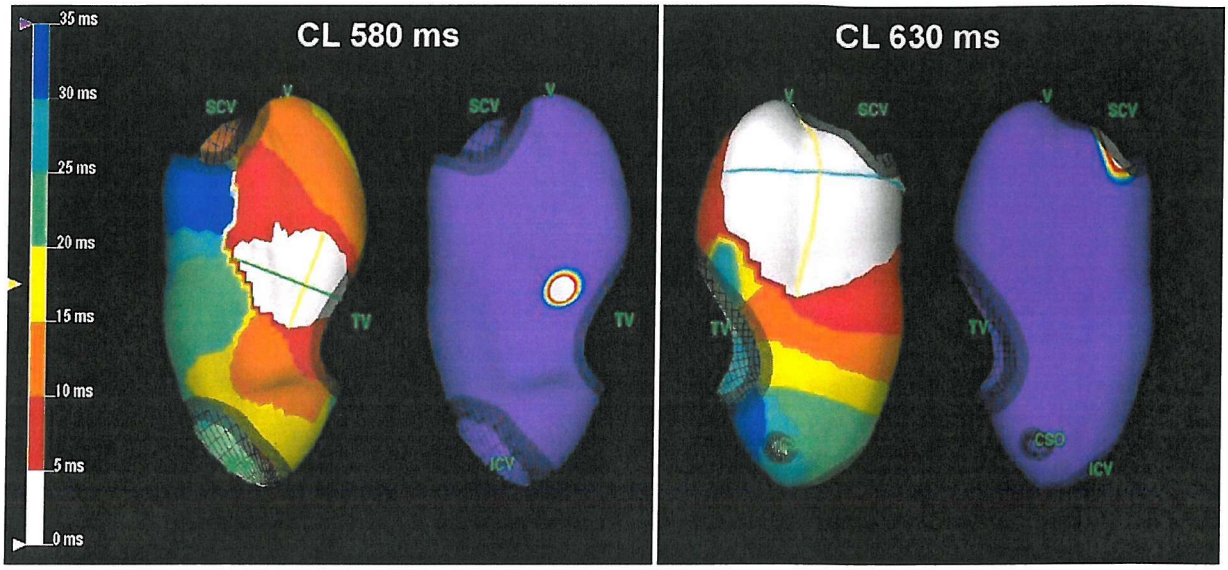

Colour isochronal maps with isochrones at 5 ms intervals taken from animal 6. At 580 ms cycle length the site of earliest endocardial activation is 50mm from the vertex at a site in the mid lateral wall consistent with the position of the terminal crest (a right lateral view is displayed). The area coloured white is depolarised within 5 ms of the onset of endocardial activation. The green and yellow surface tape measure lines are 23 and 20mm in length. At 630 ms cycle length the site of earliest endocardial activation is on the medial superior caval vein/right atrial junction, 10mm from the vertex (a left anterior oblique view is displayed). The area coloured white is depolarised within 5 ms of the onset of endocardial activation. The blue and yellow surface tape measure lines are 45 and 50mm in length.

Discussion

The present study demonstrates that in the intact, beating swine heart, earliest endocardial depolarisation over a range of heart rates during sinus rhythm and sinus tachycardia arises from a median of 3 (range 2 - 5) sites that are consistent with the position of the terminal crest. As the cycle length changed, the site of earliest endocardial depolarisation shifted from one site to another. Although overall, faster heart rates arose from more cranial positions, a graded, hierarchical pattern was only clearly demonstrated in 2/10 animals. The site of earliest endocardial depolarisation at a given cycle length varied considerably between animals and often lay beyond the margins of the histological sinus node. At cranial sites adjacent to the superior caval vein, a diffuse pattern of early depolarisation was typically seen with a broad area of endocardium demonstrating similar activation times. At more caudal sites on the lateral terminal crest, a more focal pattern was noted.

The present study is the first to use non-contact mapping to investigate the origin of the sinus impulse. As described in Chapter 2, non-contact mapping has a spatial resolution of 2-3 mm. The correlation coefficient between non-contact and contact electrogram morphology is 0.8+/-1.2 with a mean difference in activation times of 1 +/- 4 ms. In contrast to epicardial plaques and multielectrode catheters, non-contact mapping is able to provide high-density mapping of the entire right atrial endocardium. Unlike electroanatomic mapping, beat-to-beat variability can be documented and accounted for.

Pacemaker shift within the right atrium has previously been studied using microelectrodes in isolated sections of right atrium. Action potential recordings have demonstrated pacemaker shift within the sinus node that occurs in response to changes in autonomic tone, with a cranial shift associated with faster heart rates.[99,100] Unipolar and bipolar mapping studies using multielectrode plaques have revealed epicardial shifts in earliest depolarisation that occur with vagal or sympathetic stimulation.[47,101] Epicardial mapping also indicates an apparent cranial shift in the earliest electrogram with faster rates.

It is important to note that the present study identified the earliest endocardial potential rather than the earliest sinus node potential. A spatial disparity between the site of earliest action potential recording and the earliest extracellular electrogram has been described previously. A combined extracellular electrogram and intracellular action potential recording study in the canine heart showed that the earliest action potential occurs 56 +/- 25 ms before the earliest epicardial electrogram.[49] The distance between the two recording sites was 12 +/- 6mm. These findings suggest that the earliest extracellular electrogram does not necessarily occur at the site of pacemaker impulse origin. Indeed, the earliest electrogram may occur at sites

beyond the margins of the histological sinoatrial node (as also demonstrated in this study).[46,102]

The precise mechanism of pacemaker shift is poorly understood. There may be a small area within the histological node that initiates the sinus impulse with a limited number of routes out of the node into the surrounding atrial myocardium. Changes in the site of the earliest recorded electrogram may represent changes in the dominance of one exit route over another, brought about by small shifts within the node. Alternatively, a multicentric origin of the sinus impulse has been described. In open-chest canines, Boineau et al reported 3-6 epicardial sites of earliest depolarisation, arranged around the junction between the superior caval vein and right atrial appendage.[46,47] In some instances, a single site depolarised to initiate the sinus beat. In other instances, multiple sites depolarised during each beat but with one site depolarising before the others, giving the appearance of a higher or lower origin of the impulse. At faster rates, the lowest site did not depolarise. A similar phenomenon has been reported in human epicardial mapping studies.[48] The present study recorded a single site of earliest endocardial depolarisation for each heartbeat. As the sinoatrial node is a subepicardial structure, by the time that the spread of depolarisation has reached the endocardium, separate wavefronts may have merged into one confluent wavefront. With epicardial mapping the spread of depolarisation has less distance to travel and therefore separate wavefronts may remain disparate, giving a multicentric origin.

When earliest endocardial depolarisation arose at caudal sites it appeared as a discrete focus that gradually spread cranially and caudally. When earliest depolarisation arose from a cranial position around the margins of the superior caval vein, the onset was more diffuse, with a relatively large area depolarising within the first 5 ms of activation. Virtual unipolar and bipolar electrograms at sites around the superior caval vein demonstrated near identical activation times. The cranial pattern could be consistent with multiple epicardial sites of impulse origin that are in the process of merging at the point of earliest endocardial depolarisation. The caudal pattern is more typical of a single site of impulse origin that arises intramurally or subendocardially.

Endocardial mapping in the canine right atrium has been reported by Kalman et al.[51] Mapping was performed using a single decapolar catheter with 2-mm bipole spacing and 10-mm interbipole spacing, positioned along the terminal crest with the tip located in the superior caval vein. Infusion of isoproterenol caused an increase in heart rate and resulted in a gradual, stepwise shift of the site earliest depolarisation in a cranial direction. All subjects behaved in the same manner, as opposed to the considerable variety seen in our study. It is likely that the limited mapping used made localisation of the site of earliest endocardial

depolarisation an imprecise estimate, particularly as no recordings were made on the medial aspect of the superior caval vein. In the human heart, endocardial electroanatomic mapping with the CARTO system in patients with inappropriate sinus tachycardia revealed a caudal shift of 7 +/- 5 mm in the site of earliest endocardial activation during Esmolol infusion and a cranial shift of 9 +/- 4 mm during isoproterenol or aminophylline infusion. Unlike the present study, recordings were only made at 2 or 3 separate cycle lengths and were not analysed on a beat-by-beat basis, therefore shifts in the site of earliest activation over a wide range of recorded cycle lengths were not assessed.[103]

Clinical implications

Sinus node modification using endocardial transcatheter radiofrequency ablation has been used to treat inappropriate sinus tachycardia. In the present study the considerable variation between animals with regard to the site of earliest endocardial depolarisation during sinus rhythm makes endocardial identification of the sinus node and the origin of the pacemaker complex challenging. During sinus tachycardia some subject displayed earliest endocardial activation at cranial sites, whereas in others it appeared at caudal sites. With a cranial origin a relatively large area around the superior caval vein demonstrated similar early activation times, which may be a result of merging wavefronts. In the human heart early electrograms originating from a relatively wide area during sinus tachycardia have also been reported.[52,104] These findings may go some way to explain the need for ablation of extensive areas of the terminal crest and superior caval vein – right atrium junction before sinus node function is altered, often requiring the use of 8-mm or irrigated-tip ablation electrodes.[51,52,103,105] The findings in the present study are consistent with the concept that sinus node modification requires extensive destruction of the cranial portion of the sinus node complex rather than a focal ablation approach.[103,105] Successful radiofrequency ablation lesions may be distant from the site of earliest endocardial activation, a finding that would concur with the present study's suggestion that the site of earliest endocardial activation represents the endocardial exit point into the RA of an impulse that originates from sinus node cells embedded in the subepicardial layer.

Study limitations

The present study was performed in the porcine heart and the results may not be applicable to humans. The cycle length of sinus rhythm was not greater than 700 ms (85 beats/min) in 8/10

animals. No animal achieved a cycle length of greater than 1000 ms (60 beats/min). Consequently, recordings of slow hearts rates, which may have arisen from additional sites within the right atrium, were not made. If rates with a cycle length of 1000 ms or more had arisen from sites low down in the terminal crest, this may have produced a pattern more similar to that described by Kalman et al.[51] The resting rate of 85-100 beats per minute may have resulted from the high resting sympathetic tone typically seen in swine.[95]

Subtle shifts in the site of earliest endocardial depolarisation may have been artifactual due to multielectrode array movement within the right atrium. To counter this, the locator signal was steered to an electrode positioned at the coronary sinus os. The electrode position was marked on the geometry and used as a reference point for each recording. In addition, shifts of less than 5mm were ignored. However, combined movement of the reference electrode and multielectrode array cannot be ruled out.

Conclusions

During sinus rhythm and sinus tachycardia, earliest endocardial depolarisation arises from one of 2 to 5 sites in a region consistent with the location of the terminal crest. These sites may lie beyond the histological margins of the sinoatrial node. As cycle length shortens the site of earliest endocardial depolarisation may remain static or shift 5-55mm in a cranial or caudal direction in an unpredictable manner. Only a minority of subjects in this study demonstrated a stepwise shift in the origin of earliest endocardial depolarisation in a cranial direction. Depolarisation enters the endocardium over a diffuse area at cranial sites and with a more focal pattern at caudal sites. These findings suggest that endocardial mapping using single catheters may be an inadequate technique for guiding ablation of inappropriate sinus tachycardia.

Chapter 4: The relationship between right atrial architecture and the spread of electrical activation during sinus rhythm

Chapter abstract

Introduction: Previous mapping studies of right atrial activation during sinus rhythm have been limited by the use of epicardial electrode plaques in open-chest subjects or microelectrodes in the excised heart. This study describes global right atrial endocardial activation patterns using high-density mapping and compares the results with underlying endocardial architecture.

Method: Non-contact mapping of the right atrium was performed in 21 anesthetized swine. Isopotential and isochronal maps were superimposed upon three-dimensional reconstructions of right atrium geometry. Hearts were excised and endocardial dissection performed.

Results: Two patterns of right atrial activation were recorded. The site of earliest endocardial activation occurred either laterally at a position consistent with the terminal crest, or superiorly at the junction between the superior caval vein and appendage. The subsequent spread of depolarization followed the longitudinal orientation of muscle fibres. Areas of conduction delay and block were seen at the junction between the terminal crest and posterior wall, the cavotricuspid isthmus and around the margins of the Triangle of Koch. Endocardial dissection at these sites demonstrated complex fibre orientation. A lateral site of earliest activation demonstrated a more prominent display of conduction delay or block.

Conclusions: The spread of the sinus impulse follows endocardial myofibre orientation and is dictated by the site of earliest activation. Even during sinus rhythm, anisotropic conduction results in areas of conduction block or delay. These findings have implications in the development of reentrant arrhythmias and may influence surgical or electrophysiological procedures.

Introduction

In the preceding chapter, non-contact mapping in the swine heart was used to describe the relationship between heart rate and the onset of endocardial activation in the right atrium. In this chapter the study was designed to identify the subsequent spread of activation after the onset of sinus rhythm and its relationship to the underlying myocardial architecture.

The right atrium is structurally complex, consisting of a smooth venous component, the vestibule of the tricuspid valve, and the trabeculated appendage with the surrounding pectinate muscles. These areas are broken up by the insertion of the caval veins and coronary sinus, together with the Eustachian ridge, Tendon of Todaro, and oval fossa. As previously described, the myocardial architecture is organized into muscle bundles, such as the terminal crest, that are easily identifiable. Recent anatomical studies have failed to find any evidence for specialized conduction tracts within the atria, based on the criteria that a conduction tract should be histologically discrete, be traced from section to section, and, most importantly, be insulated by fibrous tissue sheaths from the adjacent working myocardium. Studies using epicardial electrode plaques in open chest subjects, or microelectrode recordings in tissue specimens, have indicated that conduction through the atria is governed by the orientation of muscle fibres. It has been shown that within small muscle bundles, such as those contained within the terminal crest, conduction may be up to 10 times faster in the longitudinal axis than in the transverse axis, a phenomenon called anisotropic conduction. Previous studies have suggested that spread of activation from the sinus node to the atrioventricular node travels preferentially through the large muscle bundles, such as the terminal crest. Spread of activation to the left atrium occurs preferentially via Bachmann's bundle.

Today, clinical electrophysiological studies are performed using endocardial mapping techniques. Other electrophysiological procedures, such as transvenous pacing, also act via the endocardial surface. Our understanding of endocardial patterns of right atrial activation in the intact, beating heart is limited. The relationship between endocardial activation pattern, site of impulse origin, and underlying myocardial architecture has not been explored. In the present study, high density, three-dimensional endocardial mapping was performed in hearts that were subsequently subjected to detailed endocardial dissection.

Methods

The basic methodology was performed as described in the Methods chapter. In brief, the animal subjects were cared for and grown to 75-105 kg in weight. All procedures were

performed under general anaesthesia, in accordance with the Home Office Project License. Electrophysiological data were recorded using non-contact mapping techniques. The non-contact mapping catheter multielectrode array was positioned in the centre of the right atrium via the left femoral vein. A 20-pole steerable catheter was positioned in the coronary sinus, such that the catheter tip was in the 2-3 o'clock position when viewed in the fluoroscopic anteroposterior position, the distal 5 bipolar pairs (electrodes 1 – 10) were positioned in the coronary sinus, and the proximal 5 bipolar pairs were placed along the floor of the right atrium and up the lateral wall, adjacent to the terminal crest. A 4 mm tip steerable ablation catheter (Stinger, Bard, Lowell, MA) was used for the creation of chamber geometry and labeling of anatomic structures.

Following the mapping procedures, the animals were euathanased with 50 ml of Phenobarbitol. The hearts were excised and placed in 10% formaldehyde. The specimens were sent to the National Heart and Lung Institute, Imperial College, London, where they underwent meticulous examination. Initially, the caval veins, pulmonary veins, pulmonary artery and aorta were tied, and the chambers inflated with latex. Once this had dried, the right atrium was cut from superior tricuspid valve annulus to the tip of the right atrial appendage, and peeled open. The latex thus provided a detailed cast of right atrial geometry and was used to aid identification of anatomical structures and their spatial relationships.

The right atrium then underwent detailed endocardial dissection. The endocardium of the right atrium was peeled off without damaging the myocardial fibres. Watchmaker's forceps were used to follow the orientation of the fibres. Detailed sketches were made demonstrating the architecture of the endocardial layer of the musculature. Further histological examination was then performed to identify the precise location and dimensions of the histological sinus node.

Electrophysiologic data was assessed in a standard manner. Anatomical labels were marked on the geometry to demonstrate the margins of the caval veins, tricuspid valve annulus, coronary sinus os, right atrial appendage and oval fossa, using data recorded obtained from electrogram characteristics and fluoroscopy. The terminal crest was identified by fluoroscopy (in the anteroposterior view it is a "C-shaped" curve at the lateral margin of the right atrial silhouette), and by identifying its relationship to other anatomical structures on the latex cast. This data was subsequently transferred to the virtual geometry during study review.

Sinus rhythm and sinus tachycardia were defined as 5 consecutive beats with a cycle length that varied by less than 10 msec with identical P wave morphology on the surface ECG (limb leads). All 5 beats had to originate from the same site on the virtual geometry. Activation was

traced backwards in time from the end of the surface P wave, viewing the isopotential map in 0.83 msec intervals. As the beginning of the P wave was reached, colour sensitivity and offset were changed to keep areas of depolarisation visible (represented by a range of colours against the purple background). Virtual electrograms were constantly positioned on the geometry at the site of depolarisation. Highpass filter settings were adjusted to as low as possible (usually 1 kHz), so that the isoelectric baseline on the virtual electrogram trace was flat. The site of earliest activation was defined as the area on the geometry with the earliest onset of depolarisation (as represented by the origin of the earliest negative potential on the isopotential map) that also had a QS or qS complex in the virtual unipolar electrograms.

The spread of depolarisation from the site of earliest activation, through the surrounding myocardium, was then examined by moving the isopotential map forward in time in 0.83 msec intervals. As the area of depolarisation increased, the sensitivity and colour offset of the isopotential map were adjusted to allow for the increasing amplitude of the electrical signal. The spread of activation and its relationship to anatomical structures was noted, with particular attention paid to areas of conduction delay or block.

Total right atrial activation time was defined as the time from the onset of endocardial activation to the time that the last site within the right atrium began depolarisation, as determined by the dV/dt max of the virtual unipolar electrograms at the appropriate sites on the geometry. The time from earliest endocardial activation to the onset of the P wave in the surface ECG was also recorded.

Statistical analysis was performed using a personal computer and Statview software. Comparison of mean values between 2 groups was performed using the student t-test. A p value of <0.05 was considered statistically significant. Data are presented as mean+/-standard deviation, unless otherwise indicated.

Results

Non-contact mapping of sinus rhythm was performed on 21 animals, mean weight 81.4 +/- 4.3 kg. The mean cycle length of mapped sinus rhythm was 548 +/- 110 ms (range 390 - 920 ms).

RA activation patterns

Two basic patterns of right atrial activation were recorded. Three animals displayed both patterns during separate recordings. 10/21 animals displayed a lateral site of earliest activation with depolarisation at a site on the lateral right atrial wall consistent with the position of the terminal crest. Activation typically spread in a cranial and caudal direction, as well as anteriorly into the right atrial appendage (Figure 22). A line of conduction block or delay prevented immediate spread into the posterior wall. The length of the line of conduction block varied between animals, but was always present at the superior portion of the terminal crest. Activation descended to the low lateral right atrium before rotating around the lower margin of the line of block to ascend and cross the posterior wall. Endocardial dissection revealed that the anatomical position of the line of block was consistent with the junction between the terminal crest and the smooth-walled venous component of the posterior atrium (Figure 23). The spread of activation followed the longitudinal orientation of fibres within the terminal crest and the pectinate branches that coursed into the right atrial appendage. In one animal a site of earliest endocardial activation was recorded in the posterior wall. A line of conduction block preventing spread anteriorly towards the right atrial appendage and TV annulus was demonstrated in the lateral wall, again consistent with the anatomical position of the terminal crest.

Fourteen animals demonstrated a superior site of earliest activation, occurring at the junction of the superior caval vein and right atrial appendage. In every case, activation descended the lateral wall, posterior wall and septum in a fairly uniform manner, appearing as a single, broad wavefront (Figure 24). Endocardial dissection in each heart showed a longitudinal arrangement of fibres in the terminal crest, posterior wall and septum, running from the superior to inferior atrium (Figure 23). Four animals showed conduction delay in the high septum, anterior and superior to the oval fossa (Figure 25). This area was consistent with the medial end of the terminal crest. Endocardial dissection revealed a horizontal spread of fibres that crossed the superior margin of the oval fossa and inserted into the TV annulus.

Figure 22. Isochronal maps of a lateral site of earliest activation

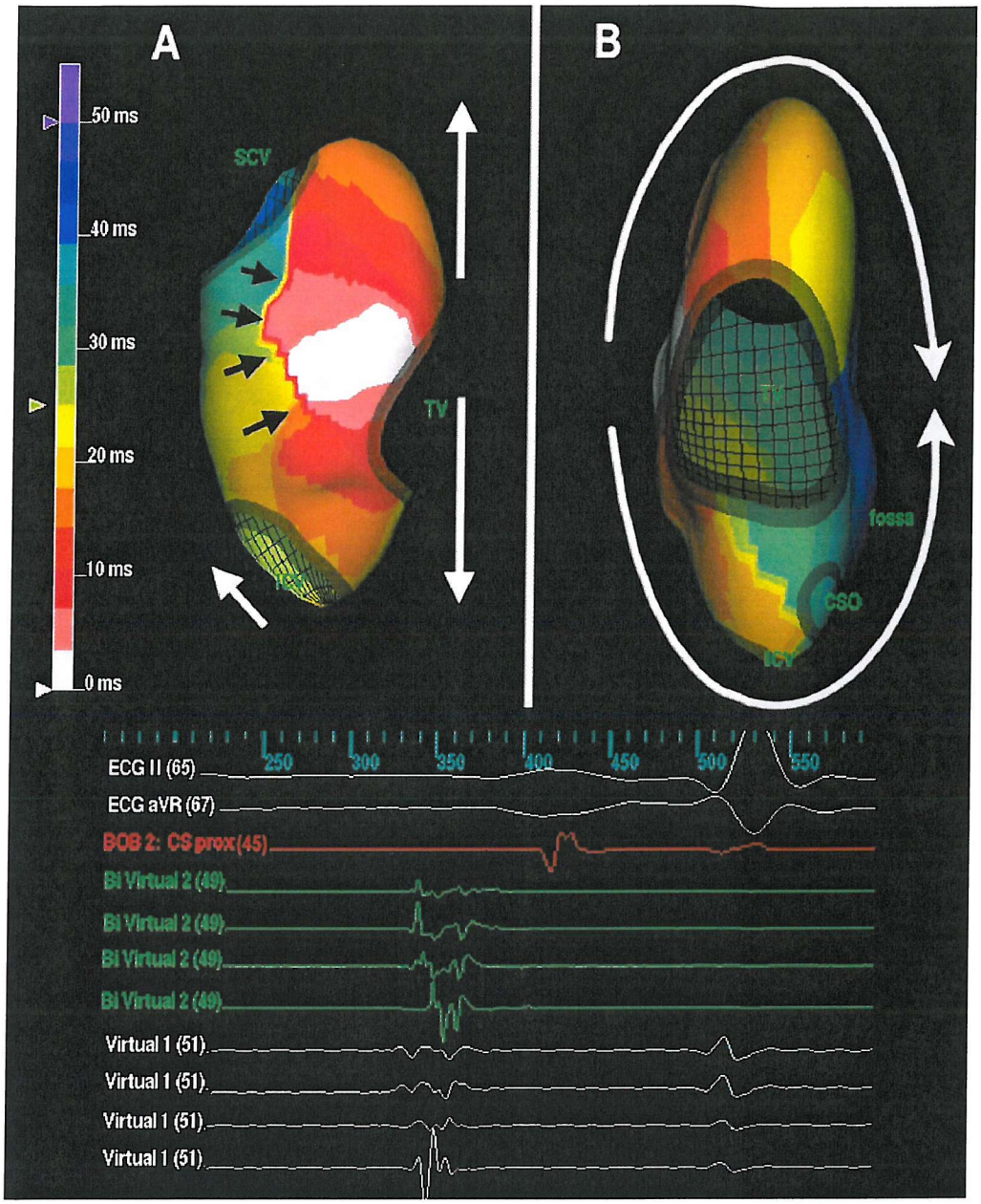

Isochronal maps with a lateral site of earliest activation. A: The right atrial geometry is viewed in a right lateral orientation. The site of earliest activation is colored white. Initial spread is superior and inferior (white arrows). A line of conduction block is present between the terminal crest and posterior wall (black arrows). B: The geometry is viewed in an anteroposterior orientation. Activation begins at the mid-lateral right atrium (white color), spreading both inferiorly and superiorly around the TV (white arrows). The two wavefronts meet in the mid-septum. Bipolar (green) and unipolar (white) virtual electrograms recorded from the TC (black arrows) are displayed demonstrating double potentials.

SCV, superior caval vein; TC, terminal crest; OF, oval fossa; ICV, inferior caval vein; CSO, coronary sinus os.

Figure 23. Endocardial dissection of the right atrium

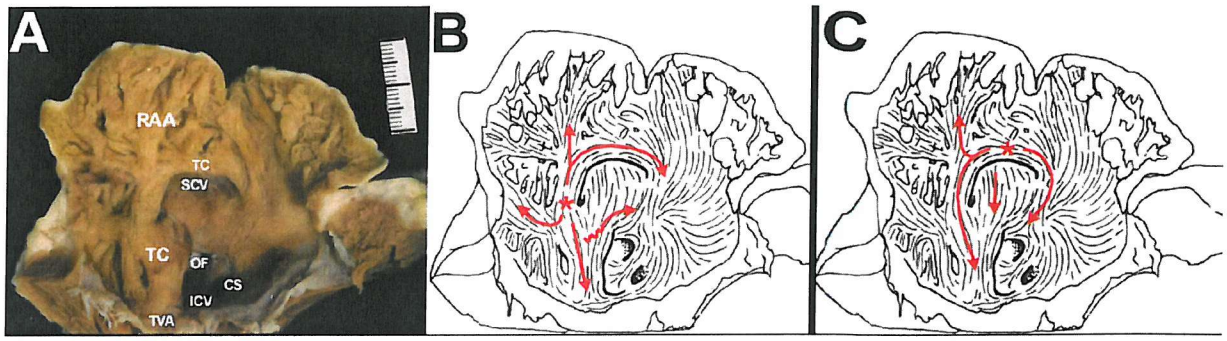

A: The right atrium has been cut from the superior TV to the tip of the right atrial appendage and spread open to display the endocardium. The prominent muscle bundle of the terminal crest is easily visualized. B: A sketch of the right atrial endocardial fibre arrangement. In this example the site of earliest activation is on the lateral terminal crest (*) with the spread of activation following the longitudinal arrangement of fibres within the terminal crest and pectinate muscles (arrows, see Figure 22). There is no immediate spread into the posterior wall, giving the appearance of a line of conduction block or delay along the posterior border of the terminal crest. Depolarisation crosses into the low posterior wall after descending the terminal crest. C: In the same animal a separate recording demonstrated a superior site of earliest activation at the anterior superior caval vein–right atrial junction. Activation followed the longitudinal arrangement of fibres, giving the appearance of a single wavefront (see Figure 24).

RAA, right atrial appendage; SCV, superior caval vein; TC, terminal crest; OF, oval fossa; ICV, inferior caval vein; CS, coronary sinus.

Figure 24. Isochronal maps of a superior site of earliest activation

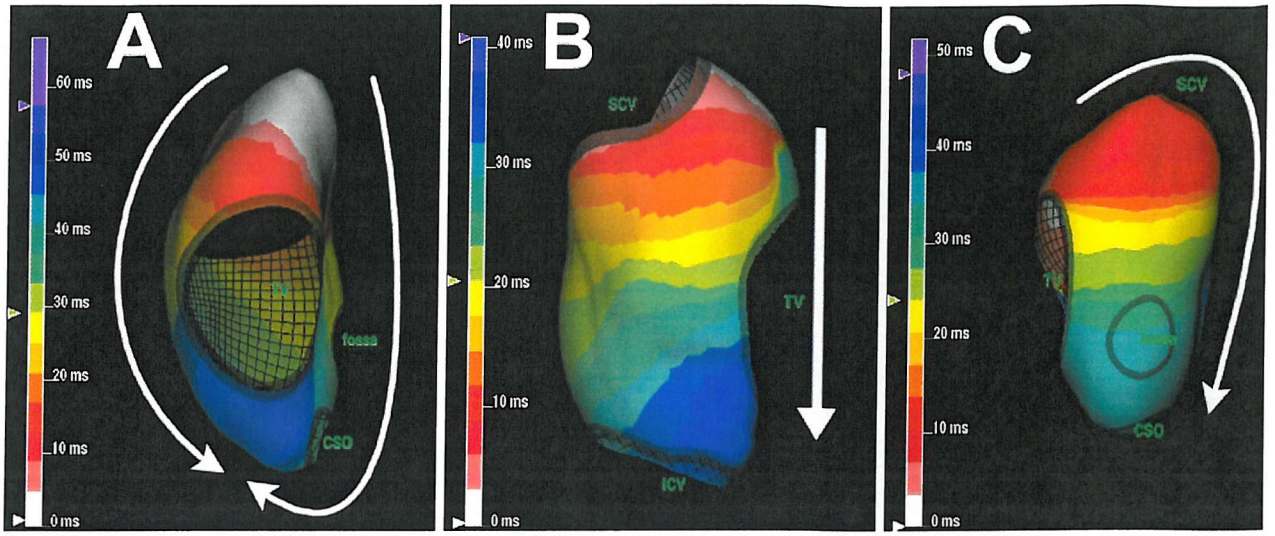

A: The right atrial geometry is viewed in an anteroposterior orientation. The site of earliest activation is coloured white and is at the junction between the superior caval vein and right atrial appendage. Activation spreads simultaneously down the lateral, medial and posterior walls (white arrows). The wavefronts collide in the cavotricuspid isthmus. B: The right atrial geometry is viewed in a right lateral orientation. Activation spreads uniformly down the lateral wall (white arrow). C: The right atrial geometry is viewed in a left lateral orientation. Activation begins at the lateral superior caval vein - right atrium junction. Spread down the septum is fairly uniform heading from superior to inferior (white arrow).

SCV, superior caval vein; TV, tricuspid valve; ICV, inferior caval vein; CSO, coronary sinus os.

Figure 25. Isochronal map and endocardial dissection of septal site of conduction delay

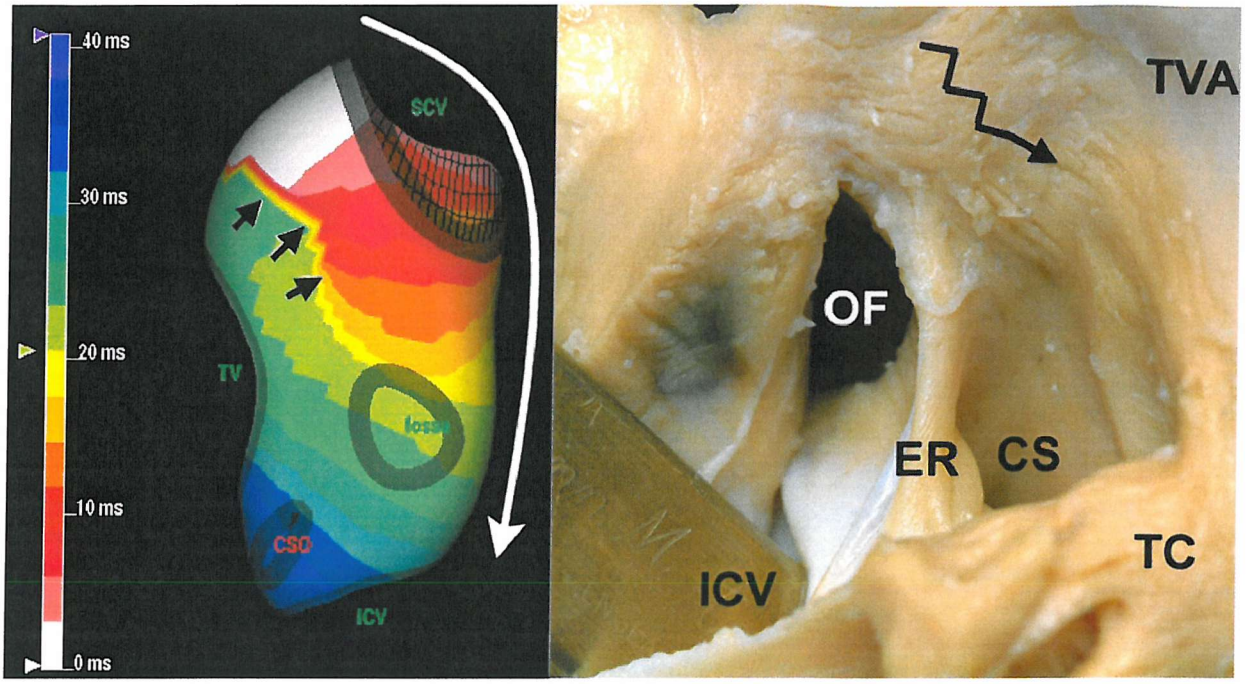

Isochronal map demonstrating anisotropic conduction during sinus rhythm. The right atrial septum is viewed in a left lateral orientation. Earliest activation is at the superior caval vein - right atrium junction. Activation spreads rapidly from superior to inferior down the mid-septum (white arrow). There is delayed or blocked conduction in the high anterior septum (black arrows) in the region consistent with the position of the medial terminal crest. Endocardial dissection of the right atrium demonstrates a horizontal array of fibres crossing superior to the oval fossa to insert into the TV annulus. Depolarisation descending from the superior site of earliest activation has to cross perpendicular to fibre orientation (black arrow).

SCV, superior caval vein; TV, tricuspid valve; ICV, inferior caval vein; CSO, coronary sinus os; OF, oval fossa.

In 7 animals there was conduction delay or block in the mid or lateral cavotricuspid isthmus (Figure 26). Delay or block was more pronounced in recordings with a lateral wall site of earliest endocardial activation. The medial isthmus was activated 20 - 30 ms later by wavefronts that had spread across the posterior wall or descended the septum. Endocardial dissection in the majority of these animals showed an abrupt termination of the terminal crest within the cavotricuspid isthmus, with the longitudinal muscle fibres and pectinate muscles inserting in a perpendicular fashion into the TV annulus. The mid-isthmus muscle fibres were sparse, with large areas of fibrous and fatty tissue immediately adjacent to the ICV. In one animal with a site of earliest activation in the lateral wall, a substantial array of muscle fibres traversed the isthmus to reach the coronary sinus os. In this animal, mapping showed only slight delay of activation as it crossed the isthmus from lateral to medial.

A slowing in conduction velocity was recorded in 5/21 animals between the coronary sinus os and the TV (Figure 27). Endocardial dissection of this area displayed a disorganized arrangement of fibres, running from posterior to anterior below the oval fossa and towards the TV. In animals with conduction delay or block at this site the muscle fibres inserted directly into the annulus. In animals with no slowing in conduction velocity, a significant proportion of the fibres turned into the isthmus to run circumferentially, parallel to the TV annulus.

RA activation times

Mean right atrial activation times were 50.6+/-7.3 ms with a lateral wall site of earliest activation and 47.5+/-7.3 ms with a superior site of earliest activation (p=0.364).

Onset-to-P wave

Mean earliest activation-to-P wave onset times were 26.6+/-6.2 ms with a lateral wall site of earliest activation and 17.1+/-9.4 ms with a superior site of earliest activation (p=0.03)

Figure 26. Isochronal map and endocardial dissection of lateral cavotricuspid isthmus site of conduction block

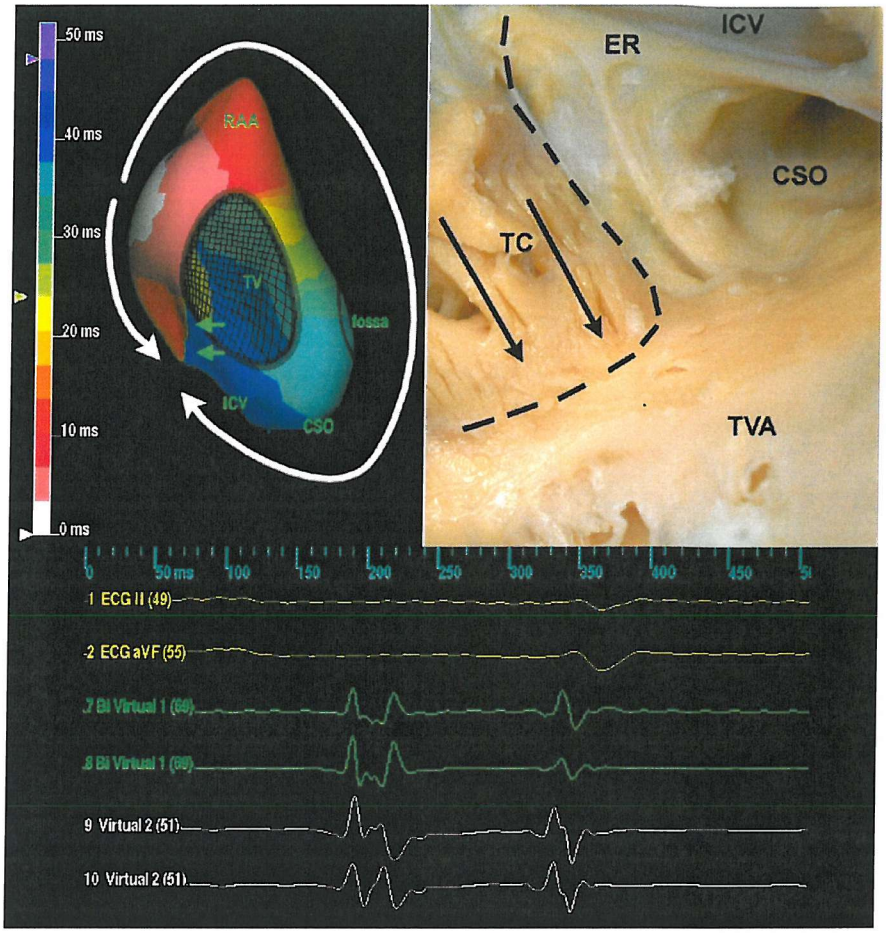

Isochronal map demonstrating conduction block during sinus rhythm. The right atrial geometry is viewed in an anteroposterior orientation. Activation begins at the mid-lateral right atrium (white colour). A line of conduction block is present at the lateral cavotricuspid isthmus (green arrows). The remainder of the right atrium and cavotricuspid isthmus is activated by the superior wavefront that rotates around the TV annulus (white arrows). Endocardial dissection reveals that the prominent terminal crest ends abruptly with the majority of fibres inserting into the tricuspid annulus. The posterior cavotricuspid isthmus is mainly composed of fibro-fatty tissue with a few fibres orientated perpendicularly to the terminal crest. Activation descends within the terminal crest (arrows) before encountering conduction block or delay (dotted line). Bipolar (green) and unipolar (white) virtual electrograms recorded from the lateral CTI (black arrows) are displayed demonstrating double potentials.

TVA, tricuspid valve annulus; right atrial appendage, right atrial appendage; ICV, inferior caval vein; CSO, coronary sinus os; TC, terminal crest; ER, Eustachian ridge.

Figure 27. Isochronal map and endocardial dissection of conduction delay in the Triangle of Koch

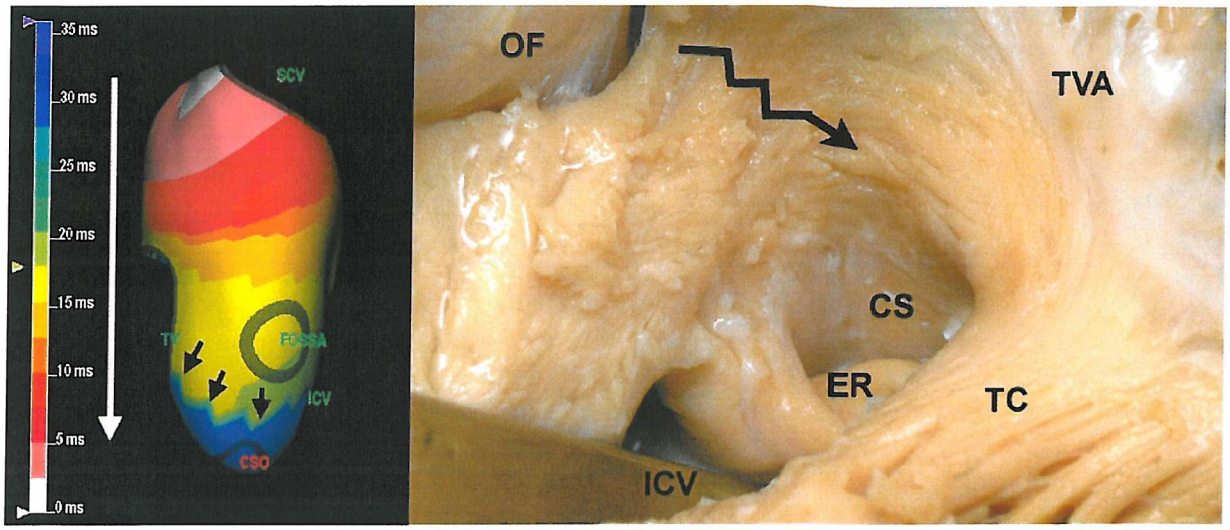

Isochronal map demonstrating anisotropic conduction during sinus rhythm. The right atrial septum is viewed in a left lateral orientation. Activation begins in at the superior caval vein - right atrium junction and spreads from superior to inferior down the septum (white arrows). There is a decrease in conduction velocity at an area level with the superior margin of the coronary sinus os (black arrows). Endocardial dissection demonstrates a band of myocardial fibres extending from posterior to anterior between the oval fossa and coronary sinus to insert into the TVA or turn to enter the cavotricuspid isthmus. Activation descending the septum from superior to inferior crosses this band perpendicular to myofibre orientation (black arrow).

SCV, superior caval vein; TV, tricuspid valve; ICV, inferior caval vein; CSO, coronary sinus os; OF, oval fossa.

Discussion

In the present study, high-density isopotential maps of endocardial activation during sinus rhythm were recorded in the intact, beating heart of 21 anesthetized swine. Endocardial architecture was then examined using dissection techniques. Whereas previous studies suggest a single pattern of right atrial activation during sinus rhythm, the present study reports two distinct patterns, determined by the site of earliest activation, as well as the underlying myocardial architecture. Also unique to the present study is the finding of conduction block or delay during sinus rhythm at the junction between the lateral terminal crest and the smooth posterior wall of the right atrium, in the high anterior septum in the region of the medial terminal crest, within the cavotricuspid isthmus and between the coronary sinus os and the tricuspid valve annulus. Although total right atrial activation times were similar for both activation patterns, the time from earliest activation to P wave onset was significantly shorter for recordings with a superior site of earliest activation.

Previous epicardial mapping studies have described patterns of right atrial activation that begin at the superior caval vein and spread radially through the remainder of the atrium, albeit with some assymetry.[22,28,29] These descriptions bear a similarity to the superior origin pattern recorded in the present study. Using electroanatomic mapping in the human heart, De Ponti et al described right atrial endocardial activation as consisting of 2 wavefronts.[106] The predominant wavefront started in the high lateral right atrium and spread from superior to inferior down the septum and lateral wall before colliding in the cavotricuspid isthmus, similar to the superior origin pattern recorded in the present study. A second wavefront was described that headed superiorly into the superior caval vein. This finding is more consistent with the second pattern of activation described in the present study when the site of earliest activation was on the mid-lateral terminal crest. Under these circumstances activation was initially confined to the terminal crest and pectinate branches until it reached the superior caval vein and low lateral right atrium. The activation maps created in the electroanatomic mapping study by De Ponti et al contained a mean of 89 points collected over many minutes, whereas the non-contact mapping technique used in the present study recorded high density global activation during a single beat. It is possible that the electroanatomic maps represent a composite of the two activation patterns found in the present study resulting from pacemaker shift during the recording process. Alternatively, the differences may arise from the different species studied.

The activation pattern that occurred as a consequence of earliest activation in the mid-lateral TC has also been described in the rabbit heart in separate studies by Sano[35] and Hiraoka.[36]

These authors mapped slow posterior spread from the site of earliest activation with an apparent line of block along the posterior margin of the lateral terminal crest. The slow, posterior spread of conduction may be a consequence of the anisotropic conduction properties of the terminal crest.[107] Although it may be surprising to find conduction block along the terminal crest during sinus rhythm, this structure has been shown to be a barrier to conduction during pacing at slow rates in patients with a history of atrial flutter.[59] In the adult canine heart the spread of activation from the terminal crest to the posterior wall is also blocked.[38] Dissection of this area has shown ingrowth of collagenous septae between myocardial fibres. Connective tissue may also separate the medial border of the terminal crest from the septum.

Conduction delay or block across the cavotricuspid isthmus was seen in 7/21 animals and was particularly pronounced in animals with a lateral site of earliest activation. The myocardial architecture in the isthmus was complex with variation between subjects. The inferior margin of the terminal crest in some animals ended abruptly, with pectinate branches inserting into the tricuspid valve annulus. The remainder of the isthmus contained a high proportion of fatty and fibrous tissue with sparse fibres that were orientated towards the valve annulus. Thus, activation crosses the isthmus perpendicular to the longitudinal orientation of muscle fibres. Previous studies have demonstrated that transverse conduction across pectinate muscle bundles and within the low lateral right atrium may be of slow velocity.[40,107,108]

Regardless of the site of earliest activation, septal depolarisation occurred from superior to inferior. A similar pattern has been described in canine and human hearts.[30,65] In the present study, conduction delay was noted around the coronary sinus os and the oval fossa. This area also displayed variations in endocardial architecture. In a previous study in the porcine heart the complex arrangement of fibres around the Triangle of Koch has been documented. Pacing from different sites around the Triangle of Koch and oval fossa demonstrated areas of non-uniform anisotropy, manifest as lines of slow conduction or block along the posterior border of the Triangle, adjacent to the coronary sinus os.[42] In the present study, this line of block was apparent in 3 animals during sinus rhythm. The more superior septal site of conduction delay corresponded either with the presence of fibres extending from a site inferior to the oval fossa towards the tricuspid valve annulus, or with the medial terminal crest. The perpendicular orientation of fibres with regard to the direction of the wavefront descending the atrial septum would have caused a slowing in conduction velocity.

Global right atrial activation times were similar for lateral and superior origin activation patterns. Of note, the area consistent with the site of the compact atrioventricular node at the apex of the Triangle of Koch was always activated by a wavefront descending the septum.

Thus, more superior sites of impulse origin are likely to have shorter internodal conduction times due to the shorter distance that activation has to travel. Mapping studies of the human heart demonstrating an impulse origin occurring around the superior caval vein have also reported atrioventricular nodal activation occurring from a superior direction by a wavefront descending the septum.[30] However, microelectrode recordings in the excised rabbit heart, in which the site of impulse origin was in the lateral wall, suggest that the lateral terminal crest acted as the preferential internodal conduction route.[36] In the rabbit heart, there was no apparent slowing of conduction across the cavotricuspid isthmus, whereas in this study many subjects showed evidence of conduction delay or block within the isthmus, preventing internodal conduction by this route.

The time from earliest endocardial activation to P wave onset on the surface ECG was shorter in recordings with a superior site of earliest activation. The initial spread of activation was typically rapid and radial, as opposed to a lateral wall site of earliest activation, in which the initial spread was limited to the terminal crest and pectinate branches. The superior site of earliest activation is closer to Bachmann's bundle and would therefore reach the left atrium sooner that spread from a lateral origin. Thus, simultaneous depolarisation of a large enough area of atrial myocardium to produce the onset of the P wave would be expected to occur sooner with a superior origin of the sinus impulse.

Clinical implications

The present study has shown in the porcine heart that areas of conduction block and delay occur even during sinus rhythm. Conduction delay and block may provide the substrate for reentrant arrhythmias. A greater understanding of the spread of activation during sinus rhythm may help to guide future transcatheter or surgical radiofrequency ablation procedures and avoid the pro-arrhythmic effects that palliative surgery for congenital and acquired heart defects may produce. Increased awareness of the spread of atrial activation may also help to guide pacing therapies for the prevention of atrial arrhythmias in the setting of bradycardia, or as a preventive therapy for atrial tachyarrhythmias.

Study limitations

The relationship between endocardial architecture and activation patterns had to be inferred from a comparison of dissection anatomy and the three-dimensional non-contact mapping reconstruction. It was not possible to directly visualize the endocardial architecture during

mapping due to the in-vivo nature of the study. It is therefore possible that the precise site of earliest activation and conduction block or delay may not have been correctly identified.

No epicardial mapping was performed. Although it is possible that epicardial activation patterns could have been different from endocardial patterns, previous combined mapping studies suggest that endocardial and epicardial activation is nearly identicle.[34,47]

It is not possible to state whether areas of apparent conduction block are genuine, or whether they are the result of conduction delay that occurs for long enough for a separate wavefront to approach the area from the opposite direction. For example, apparent conduction block within the cavotricuspid isthmus may have been the result of slow conduction from the lateral to mid-isthmus, with the medial aspect of the isthmus being activated 20-30 ms later by a septal wavefront that has either crossed the posterior wall or descended from the superior septum.

Conclusions

In the porcine heart, the site of earliest activation and underlying endocardial architecture dictates the spread of activation through the right atrium. During sinus rhythm, areas of conduction block or delay may be seen at the junction between the terminal crest and posterior wall, in the cavotricuspid isthmus, and around the margins of the Triangle of Koch. Conduction delay and block is particularly pronounced in recordings with a site of earliest activation in the region of the lateral terminal crest. These sites correspond with areas of myocardial architecture that display sudden changes in the direction of fibre orientation, confirming the role of anisotropic conduction in impulse propagation. A detailed knowledge of the spread of activation during sinus rhythm may help guide future electrophysiological and surgical procedures and provide insights into the development of arrhythmias.

Chapter 5: Left atrial endocardial activation during sinus rhythm and coronary sinus pacing in patients with paroxysmal atrial fibrillation

Chapter abstract

Introduction: Little in known regarding the spread of depolarization through the left atrial endocardium. The present study was designed to record global high-density maps of left atrial endocardial activation during sinus rhythm and coronary sinus pacing.

Methods: Non-contact mapping of the left atrium was performed in 9 patients with paroxysmal atrial fibrillation undergoing pulmonary vein ablation. High-density isopotential and isochronal maps were superimposed on three-dimensional reconstructions of atrial geometry. Mapping was repeated during pacing from up to 5 sites within the coronary sinus.

Results: Earliest left atrial endocardial activation occurred on the posterior septum anterior to the right pulmonary veins in 7 patients and on the anterosuperior septum in 2 patients. A line of conduction block or delay was documented in the posterior wall and inferior septum in every patient. The direction of activation in the left atrial myocardium overlying the coronary sinus was identical to the electrogram sequence in the coronary sinus catheter in only 3/9 patients. During coronary sinus pacing, activation entered the left atrium 41+/-13ms after the pacing stimulus at a site 12+/-10mm from the endocardium directly overlying the pacing electrodes. Lines of conduction block or delay were present in the posterior wall and inferior septum.

Conclusions: In patients with paroxysmal atrial fibrillation, lines of conduction block are present in the left atrium during sinus rhythm and coronary sinus pacing. Electrograms recorded in the coronary sinus infrequently correspond to the direction of activation in the overlying left atrial myocardium.

Introduction

The two previous chapters describe the onset of sinus rhythm and subsequent spread of electrical activation through the right atrium. Recently, more attention has been focused on the left atrium, mainly in an attempt to gain further insight into the mechanisms of atrial fibrillation. Most of these studies have been anatomical, based on dissection techniques. As with the right atrium, the left atrium consists of a smooth-walled venous component, the vestibule of the mitral valve, and a trabeculated appendage. There are usually 4 openings for the pulmonary veins, but otherwise, the structure is simpler than that of the right atrium. The principle muscle bundles are Bachmann's bundle, left septoatrial bundle, and the septopulmonary bundle. The septoatrial and septopulmonary bundles attach to the rim of the oval fossa. There are also small muscle bridges that extend through the left atrioventricular groove to join with the muscular sleeve of the coronary sinus.

Current knowledge of patterns of left atrial activation is limited. Sections of the epicardial surface of the left atrium have been mapped in open-chest subjects using multielectrode plaques. Left atrial activation patterns are often inferred from the electrogram patterns recorded in coronary sinus catheters. Detailed endocardial mapping of the left atrium in the intact, beating heart, has only just begun to be studied.[106] In the present study, non-contact mapping of the left atrium during sinus rhythm and coronary sinus pacing was performed in 9 human subjects undergoing evaluation and treatment for paroxysmal atrial fibrillation.

Methods

Approval was granted by the Local Regional Ethics Committee, and carried out using Southampton University Hospitals' guidelines. All patients gave informed consent for the mapping procedure. Every patient was undergoing electrophysiological study and radiofrequency ablation for paroxysmal atrial fibrillation, believed to arise from ectopic foci within the pulmonary veins. All data for this study was collected prior to ablation therapy or administration of drugs. All antiarrhythmic medication was stopped for 5 days prior to study. No patients were taking amiodarone.

Non-contact mapping of the left atrium was performed in the fasted, non-sedated state. Venous access was gained via the femoral veins and right subclavian vein. The non-contact multielectrode array was positioned in the left atrium via a transseptal approach through the oval fossa. The tip of the multielectrode array was positioned in the left upper pulmonary vein (with the guidewire advanced further within the vein for additional stability) or in the

left atrial appendage. The steerable mapping and ablation catheter was also advanced into the left atrium via a transseptal puncture through the oval fossa, within a Mullens sheath (Daig, Minnetonka, MN). A steerable 20-pole catheter (10 mm inter-bipole distance, 2 mm intra-bipole distance) was positioned in the coronary sinus with the tip advanced to the 2-4 o'clock position when imaged in the left anterior oblique view. Intravenous heparin was infused to maintain the Activated Clotting Time at 350 seconds.

Left atrial geometry was created in the standard fashion. Anatomical structures, including the pulmonary veins, oval fossa, mitral valve annulus and left atrial appendage, were identified using a combination of electrogram characteristics and fluoroscopy.

Non-contact mapping was performed initially during sinus rhythm. In patients 3 to 9, pacing was performed on each of the bipole pairs in turn within the coronary sinus (from the distal pair to the pair at the coronary sinus os) at a cycle length of 600 ms. The position vector from the centre of the multielectrode array to the bipole pairs within the coronary sinus was marked on the left atrial geometry using the locator signal. Pacing amplitude was 1.0 mA above threshold. All data were recorded on optical disk for later analysis. Isopotential maps of left atrial activation during sinus rhythm and pacing were analyzed offline.

Statistical analysis was performed using a personal computer and Statview software. Comparison of mean values between 2 groups was performed using the student t-test. A p value of <0.05 was considered statistically significant. Data are presented as mean +/- standard deviation, unless otherwise indicated.

Results

Data were recorded from 9 patients (7 male, age 46+/-9 years). All patients had paroxysmal atrial fibrillation. No patient had undergone previous cardiac surgery or had significant valvular heart disease. Additional patient characteristics are summarized in Table 1. All patients began the mapping procedure in sinus rhythm.

Table 1. Patient characteristics

Patient	Age (years)	Duration of PAF (months)	Max LA diameter (cm)	Max P wave duration (ms)	Previous Class I/III drugs	Co-morbidity
1	47	25	3.8	124	2	none
2	49	16	3.8	128	2	none
3	54	39	4.5	114	2	hypertension
4	61	31	4.3	134	3	none
5	30	19	3.7	127	2	none
6	38	13	3.9	110	1	none
7	45	27	4.4	130	2	none
8	49	44	4.2	119	2	MVP, mild MR
9	42	28	3.9	123	1	none
Mean +/- SD	46 +/- 9	27 +/- 10	4.1 +/- 0.3	123 +/- 8	2 (median)	

Sinus rhythm

The mean cycle length of sinus rhythm was 744 +/- 170 ms (range 520 – 1077 ms). The mean time from onset of the surface P wave to onset of left atrial activation was 17 +/- 10ms (range –5 to +25 ms). The mean global left atrial activation time was 61 +/- 12 ms.

LA activation patterns during sinus rhythm

The site of earliest left atrial endocardial activation was on the superior posterior interatrial septum, anterior to the ostium of the right upper pulmonary vein in 5 patients, in the mid-posterior septum, anterior to the ostium of the right lower pulmonary vein in 2 patients and on the anterior superior septum in 2 patients. In each case, a single site of origin was recorded. In 5/9 subjects the spread of depolarisation from the site of earliest left atrial endocardial activation encountered a line of conduction block or delay that prevented the direct spread of depolarisation onto the posterior wall. This line was between the right upper and lower pulmonary veins. Depolarisation spread rapidly across the left atrial roof and turned around the right upper pulmonary vein before descending the posterior left atrial wall from superior to inferior (Figure 28). In 2/9 patients, a vertical line of conduction delay was seen in the mid-posterior wall. In the remaining 2 patients, an oblique line of conduction block was seen extending from the mid-posterior wall to the right lower pulmonary vein. Double potentials were recorded along the lines of conduction block.

In all 9 patients, depolarisation was delayed or blocked from spreading inferiorly down the interatrial septum by a horizontal line of conduction block that extended from the right lower pulmonary vein through the oval fossa to the septal margin of the mitral valve. This line of block was continuous with the vertical line of block between the right lower and right upper pulmonary veins, when present (Figure 29). When viewing the left atrium from a left anterior oblique projection, this led to the appearance of a clockwise sequence of activation around the mitral valve.

Relationship between left atrial endocardial activation pattern and coronary sinus electrograms

During sinus rhythm, bipolar electrograms recorded in the coronary sinus in 6/9 patients indicated that activation proceeded from proximal to distal (medial to lateral), although in 2 of these patients the electrograms in the two most distal bipole pairs were simultaneous. The remaining 3/9 patients demonstrated a fusion pattern with earliest electrograms in the proximal and distal poles and subsequent depolarisation spreading towards the middle of the

Figure 28. Isochronal map of sinus rhythm with posterior wall line of block

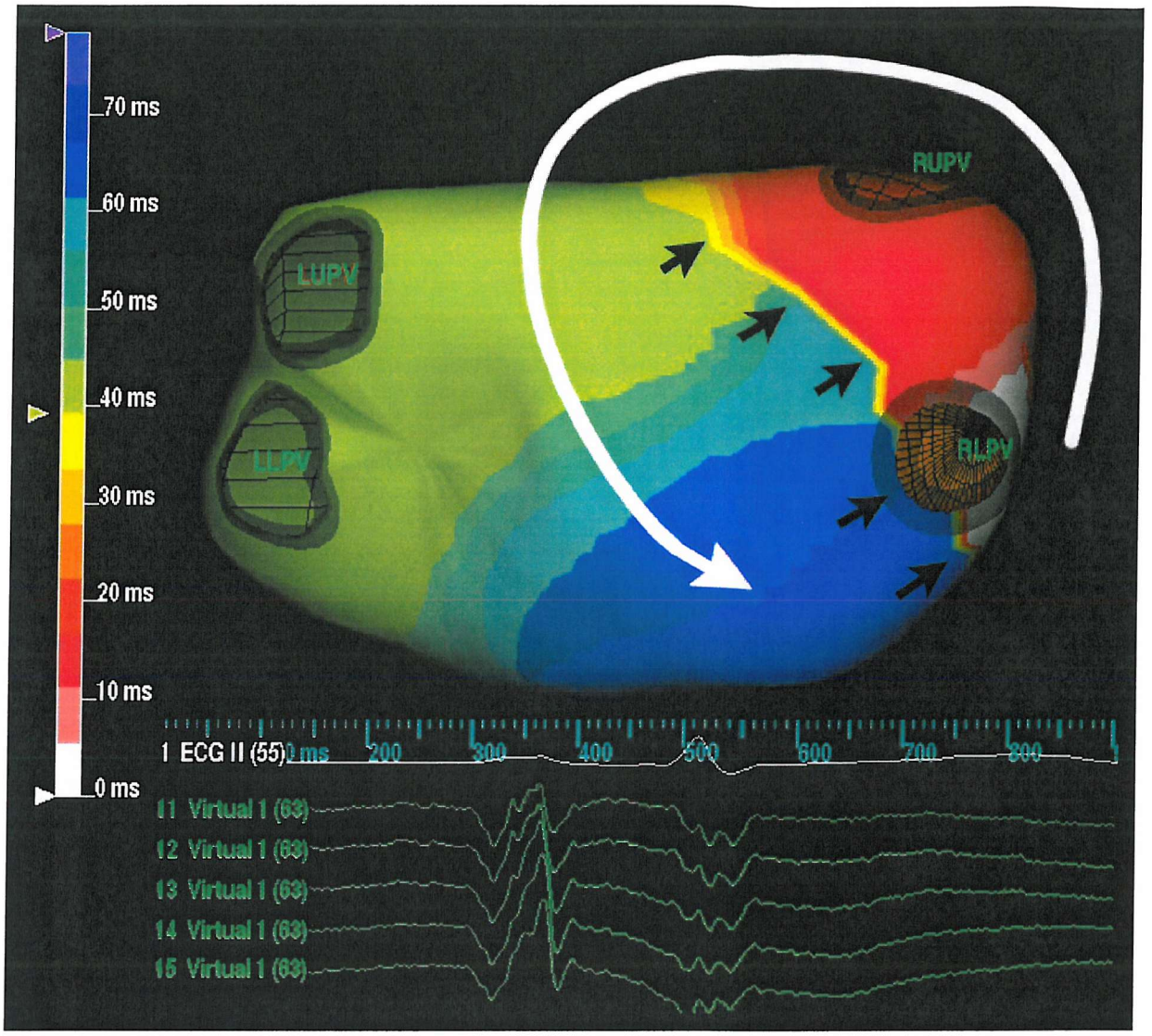

Isochronal map of sinus rhythm. The left atrial geometry is viewed in the equivalent of a right posterior oblique radiographic projection to display the posterior left atrial wall. The earliest site of left atrial endocardial activation occurs on the posterior septum, adjacent to the anterior margin of the RLPV. The colored isochrones depict 6ms intervals. Activation ascends in a superior direction before turning around the RUPV and descending the posterior wall (white arrow). Activation is prevented from crossing onto the posterior wall by a vertical line of conduction block (black arrows). Unipolar virtual electrograms are recorded along the line of conduction block and display double potentials. LUPV, left upper pulmonary vein; LLPV, left lower pulmonary vein; RUPV, right upper pulmonary vein; RLPV, right lower pulmonary vein.

Figure 29. Isochronal map of sinus rhythm with septal line of block

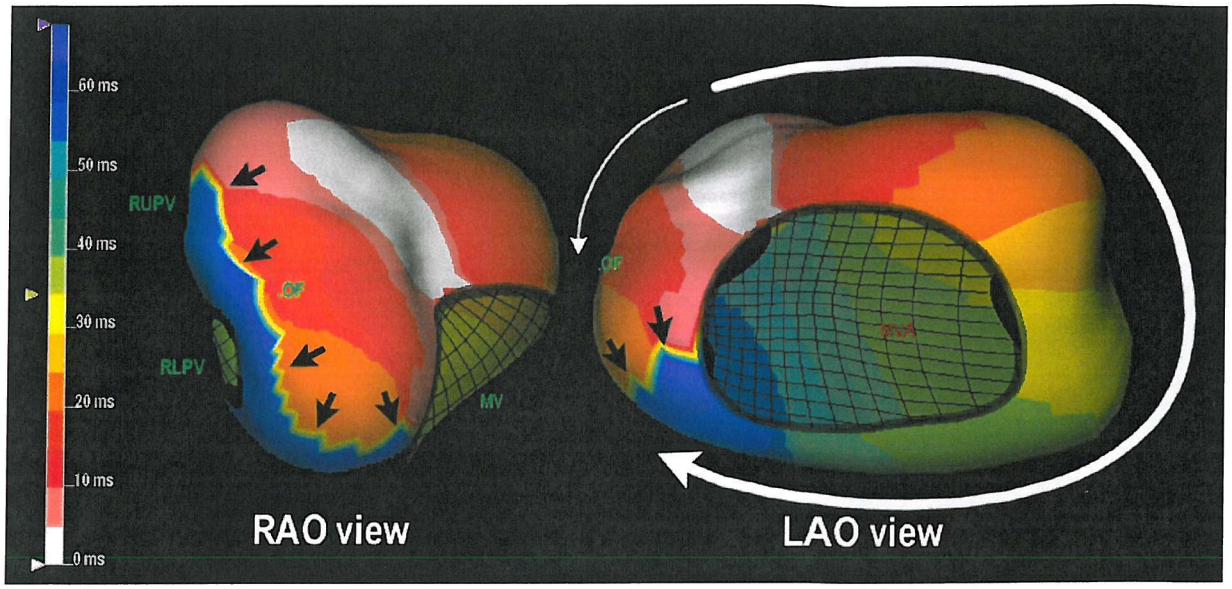

Isochronal maps of sinus rhythm. The left atrial geometry is displayed in right anterior oblique and left anterior oblique radiographic views. The site of earliest left atrial endocardial activation occurs on the superior anterior septum at a site consistent with the left atrial insertion of Bachmann's bundle. Activation initially descends the septum (thin white arrow) where it encounters a line of conduction block that runs between the septal margin of the mitral valve and the orifices of the right pulmonary veins (black arrows). As a consequence, activation rotates around the mitral valve in a clockwise manner when viewed in the LAO orientation (thick white arrow). RUPV, right upper pulmonary vein; RLPV, right lower pulmonary vein; OF, oval fossa; MV, mitral valve

catheter, where the two wavefronts collided. The left atrial myocardium overlying the coronary sinus was activated from the lateral to medial (septal) direction in 4 patients, from medial to lateral in 2 patients, and by the fusion of two separate wavefronts approaching from the lateral and medial directions in 3 patients (Figure 30). Only 3/9 patients had identical coronary sinus and overlying left atrial myocardial activation patterns (Table 2).

Coronary sinus pacing

Coronary sinus pacing was performed in 7/9 patients at a median of 4 (range 3 - 5) sites. Activation entered the left atrium at focal points around the posterior mitral valve or low interatrial septum before spreading through adjacent myocardium. The mean time from pacing stimulus to onset of left atrial endocardial activation was 41 +/- 13 ms (range 15 – 56 ms). More distal pacing sites had shorter stimulus to onset of endocardial activation times (R^2=0.77, p<0.05). The mean global left atrial activation time was 43 +/- 9ms (range 36 - 58ms) and was not related to the pacing site within the coronary sinus (p=0.09).

A median of 3 (range 1 - 4) different sites of earliest left atrial activation was documented in each patient. The mean distance of the site of earliest activation from the endocardium directly overlying the pacing electrodes was 12 +/- 10 mm (range 0 – 32 mm). Only 12/30 sites of earliest endocardial activation occurred at myocardium directly overlying or within 5 mm of the coronary sinus pacing site (Figure 31). In 3 patients, an activation wavefront entered the left atrium at the low anterior septum rather than the posterior mitral valve annulus. In two of these 3 patients this was only seen when pacing was performed from the coronary sinus ostium and it occurred as the sole wavefront. In the third patient, pacing from the mid-CS resulted in earliest activation at a site overlying the posterior mitral valve annulus, with activation entering from the low septum as a second wavefront 17 ms later (Figure 32). It occurred exclusively through the septum when pacing was performed at the coronary sinus os.

Although global left atrial activation times were longer at more lateral sites of entry into the left atrium, this result did not reach statistical significance. Global left atrial activation times during coronary sinus pacing were shorter than during sinus rhythm (42 +/- 7 ms vs. 61 +/- 12 ms, p<0.001).

Figure 30. Isochronal map of sinus rhythm with disparate left atrial and coronary sinus activation sequences

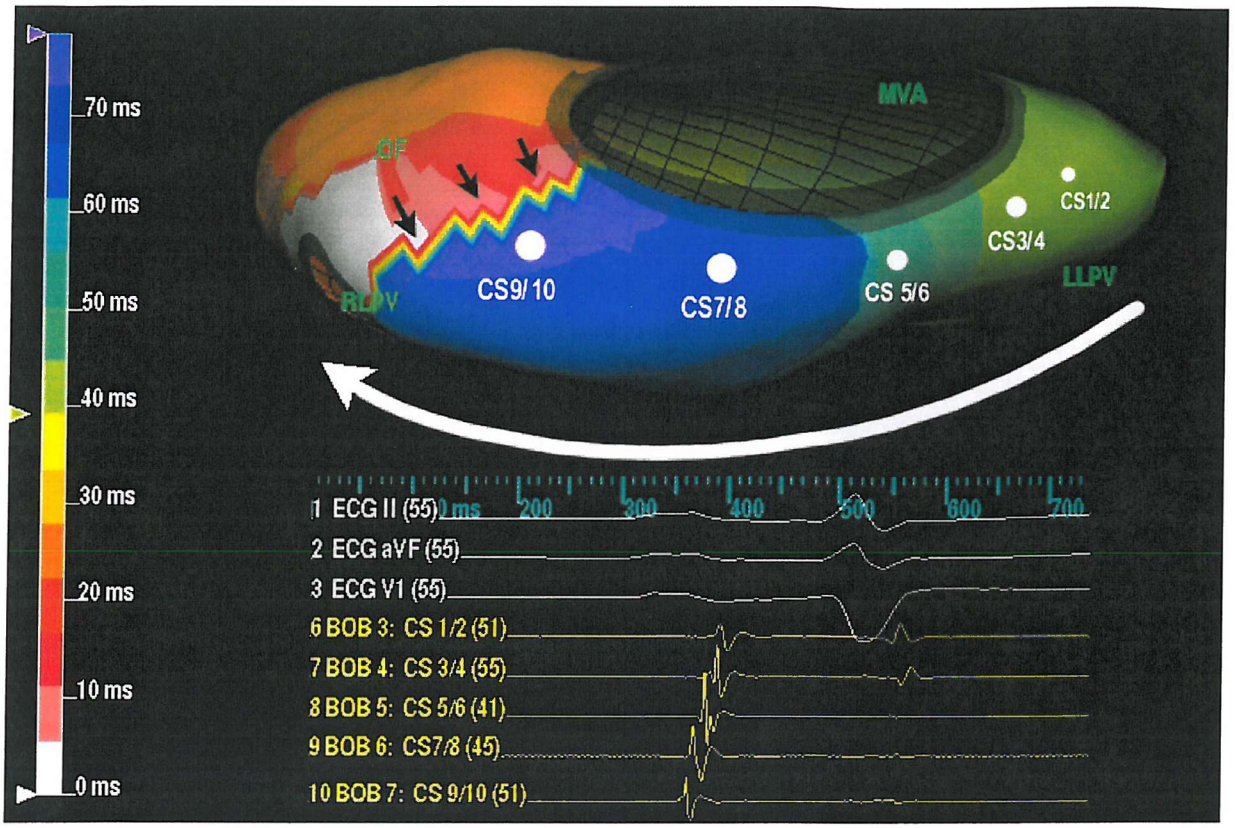

Isochronal map of sinus rhythm. The left atrial geometry is viewed in a left anterior oblique view with caudal tilt to display the left atrial myocardial overlying the coronary sinus. The position vector from the centre of the MEA for each bipole pair within the coronary sinus are marked on the geometry. Earliest left atrial endocardial activation is adjacent to the right lower pulmonary vein (white color) and is prevented from spreading inferiorly and laterally around the lower mitral valve by a line of conduction block (black arrows). As a consequence, activation crosses the left atrial roof from septum to lateral wall and rotates around the mitral valve before activating the myocardium overlying the coronary sinus in a lateral to medial direction (white arrow). Bipolar electrograms from the coronary sinus catheter however display a medial to lateral activation pattern, with earliest activation at the coronary sinus ostium (CS 9/10). RLPV, right lower pulmonary vein; LLPV, left lower pulmonary vein; OF, oval fossa; MVA, mitral valve annulus; CS, coronary sinus.

Table 2. Comparison of coronary sinus electrogram sequence and the isochronal map sequence of activation of endocardium adjacent to the posterior mitral valve annulus

Patient	Coronary sinus electrogram sequence	Posterior mitral valve annulus sequence
1	Prox-dist	Dist-prox
2	Prox-dist	Prox-dist
3	Fused	Dist-prox
4	Prox-dist	Fused
5	Prox-dist	Fused
6	Prox-dist	Dist-prox
7	Fused	Fused
8	Fused	Dist-prox
9	Prox-Dist	Prox-dist

Figure 31. Sites of left atrial onset during coronary sinus pacing

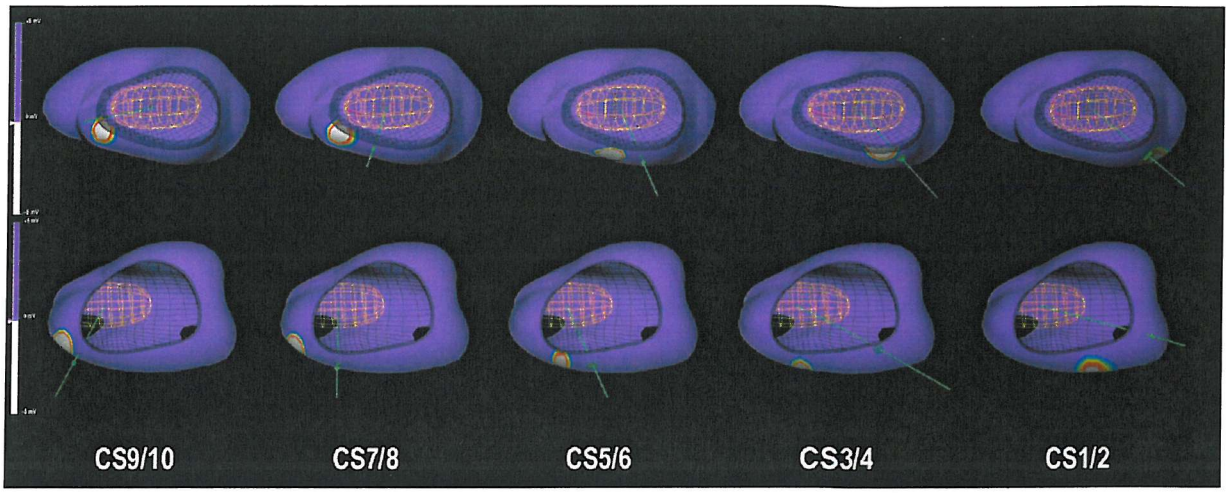

Isopotential maps during coronary sinus pacing. The left atrium is displayed in a left anterior oblique view. The position of the MEA may be viewed in yellow inside the geometry through the mitral valve orifice. The position of the most distal of each bipole pair is indicated by the locator signal, represented by the dot on the green line that extends through the geometry from the centre of the MEA. Each isopotential map is frozen at the time of earliest left atrial activation. Endocardial depolarisation is shown as a white colour against the purple background.

The top 5 images are taken from a patient with a good correlation between pacing site and earliest endocardial activation (3 - 14mm distance on atrial geometry). Four different sites of earliest activation were seen - pacing from CS 7/8 and CS 9/10 shared the same site of earliest atrial activation.

The bottom 5 images are taken from a patient with a poor correlation between pacing site and earliest endocardial activation (8-28mm distance on atrial geometry). Three different sites of earliest activation were seen - pacing from 3/4 plus 5/6, and CS 7/8 plus CS 9/10 shared the same sites of earliest atrial activation.

Figure 32. Isochronal map of coronary sinus pacing

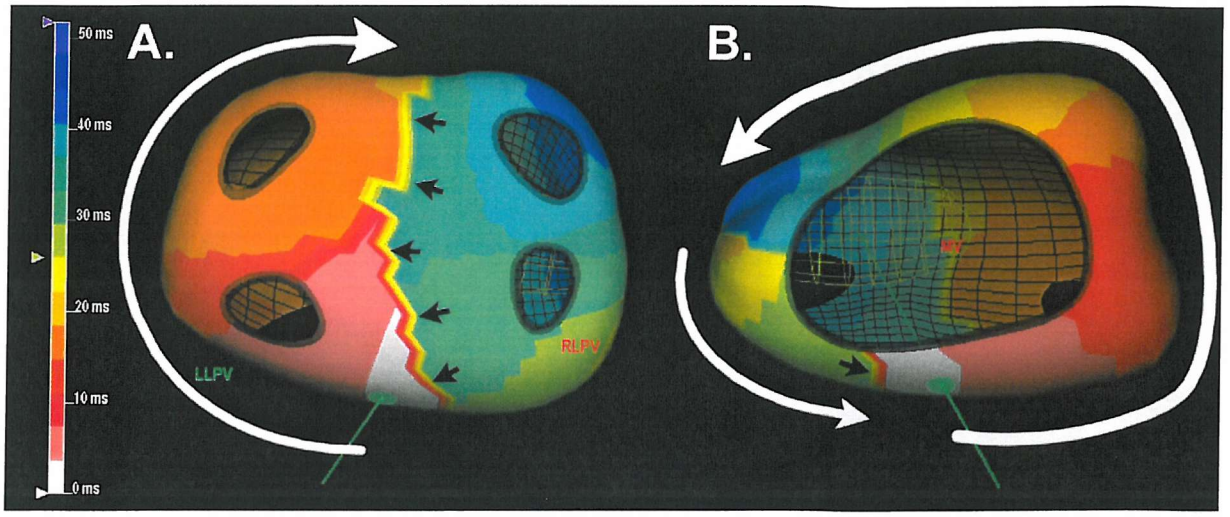

Isochronal maps during pacing from the mid-CS. A: The left atrial geometry is viewed in the equivalent of a right posterior oblique radiographic view to display the posterior left atrial wall. The site of earliest activation (white color) overlies the pacing electrodes (depicted by the green dot on the green locator signal line). Activation spreads laterally and superiorly past the left pulmonary veins (white arrow). It is prevented from spreading medially towards the septum by a vertical line of conduction block that is in the middle of the posterior wall (black arrows). B: The same left atrial geometry is viewed in the equivalent of a left anterior oblique radiographic view. Activation rotates in a counter-clockwise direction around the mitral valve (large white arrow). A second wavefront enters through the septum 17ms after the onset of earliest activation and descends inferiorly until it encounters the previously mentioned line of conduction block from the opposite side than the initial wavefront (small white arrow). RLPV, right lower pulmonary vein; LLPV, left lower pulmonary vein; MV, mitral valve.

Left atrial patterns during coronary sinus pacing

The same conduction barriers that were seen during sinus rhythm were present during coronary sinus pacing. A line of conduction block or delay between the right upper and right lower pulmonary veins was seen in 5/7 patients and a vertical line was present one-third of the way between the right and left-sided veins in the remaining 2 patients (Figure 32). A line a block was also seen along the inferior septum, running between the right lower pulmonary vein and the septal aspect of the mitral valve annulus. When activation emerged solely from a lateral pacing site within the coronary sinus, a counterclockwise spread of depolarisation around the mitral valve was seen. When activation was earliest at a medial site, particularly if a second wavefront emerged through the low septum, 2 separate wavefronts were seen that collided in the medial posterior wall.

Discussion

The present study describes patterns of global left atrial endocardial activation during sinus rhythm and coronary sinus pacing in patients with a history of atrial fibrillation. The site of earliest left atrial activation during sinus rhythm was on the superior interatrial septum anterior to the ostium of the right pulmonary veins or on the anterior limbus of the oval fossa. During coronary sinus pacing, activation entered the left atrium at a single site around the posterior mitral valve annulus. When pacing from a proximal position this was occasionally followed by a second wavefront from the low septum. The site of entry into the left atrium was directly overlying the pacing electrodes in only 12/30 recordings. Lines of conduction block or delay were observed in the mid-posterior wall, between the right upper and right lower pulmonary veins, and between the right lower pulmonary vein and the septal margin of the mitral valve annulus. These lines of conduction block or delay were present during both sinus rhythm and coronary sinus pacing. The pattern of coronary sinus electrograms infrequently matched the activation sequence of the overlying left atrial myocardium.

A previous study of right and left atrial activation patterns during sinus rhythm using multielectrode epicardial plaques described wavefronts crossing from the right to left atrium on the posterior surface beneath the right lower pulmonary vein as well as crossing from right to left in Bachmann's bundle to depolarize the left atrial appendage.[29] In a previously reported non-contact mapping study of pulmonary vein ectopic foci, it was noted that the site of earliest left atrial activation during sinus rhythm was anterior to the right upper pulmonary vein.[109] More recently, De Ponti et al have reported a series of 7 patients without a history of atrial fibrillation in who they performed electroanatomic mapping of the left and right

atria.[106] They described two separate sites of interatrial breakthrough; an anterior site consistent with the left atrial insertion of Bachmann's bundle and a posterior site consistent with the position of the right pulmonary veins. The anterior site predominated and the authors concluded that the posterior wavefront contributed little to global activation. In the present study, the areas of earliest activation were consistent with Bachmann's bundle or interatrial muscular bridges that cross the septal raphe to insert adjacent to the orifices of the right pulmonary veins.[6] All patients demonstrated immediate rapid conduction from medial to lateral across the roof of the left atrium in the direction of fibres within Bachmann's bundle. Bachmann's bundle is an epicardial structure that crosses from the right atrium to left atrium by bridging the septal raphe created by the infolded atrial walls. Both noncontact and electroanatomic mapping record endocardial activation, therefore it is likely that neither mapping technique will record left atrial activation within Bachmann's bundle until it has crossed the septal raphe and has merged with the fibres in the left atrial roof. Thus, the earliest site of activation via this route will appear at the border between the anterosuperior septum and the left atrial roof, as demonstrated in the present study and by De Ponti et al.

If electrical activation crosses the septal raphe through more posteriorly positioned muscle bridges it will appear immediately anterior to the right pulmonary veins. This route was also described by De Ponti et al, who reported that the posterior wavefront had little influence on global left atrial activation.[106] The present study has found that this area is enclosed by posterior and inferior lines of conduction block, therefore activation can only spread in the anterosuperior direction where it immediately merges with the wavefront that crosses through Bachmann's bundle. Whereas De Ponti et al described two separate wavefronts that appeared simultaneously, the present study found a single wavefront in each patient. Differences may be related to mapping techniques or the patient populations studied.

A vertical line of conduction block running from the superior to inferior right pulmonary veins was seen during sinus rhythm and coronary sinus pacing in 5/9 patients. This area coincides with the junction between a band of longitudinal myocardial fibres (the septopulmonary bundle) that lie adjacent to the septum and right-sided pulmonary veins, and a band of circumferential fibres that run perpendicularly towards the lateral left atrium.[6] In addition, every patient demonstrated conduction block or delay at the inferior septum between the right lower pulmonary vein and the septal aspect of the mitral valve annulus. The conduction delay or block witnessed at these sites is likely to result from anisotropic conduction at the junction between these major muscle bundles. Using electroanatomic mapping of left atrial propagation in patients without atrial fibrillation, De Ponti et al described late activation in the posterior wall despite the presence of an interatrial connection

at the right pulmonary veins and early activation in the posterior septum.[106] The authors did not specifically report areas of conduction delay or block, however this is likely to account for the late posterior wall activation and minimal role of the second, posterior wavefront in global left atrial activation described previously.

Anatomical studies have shown that the coronary sinus is covered in a muscular sleeve that is continuous with the right atrium but separated from the left atrium by a layer of fatty tissue.[8] The layer of fatty tissue is bridged by strands of muscle that connect the coronary sinus musculature with the left atrial myocardium. The results in the present study would concur with these findings, suggesting that depolarisation has to spread along the coronary sinus musculature before encountering a muscle bridge that then traverses the fatty layer to insert into the left atrium. The muscle bridges may lie at oblique angles adding to the distance and delay from the pacing site to the site of earliest left atrial activation. Pacing at the most proximal portion of the coronary sinus may result in activation entering the left atrium at the low septum after traveling through right atrial myocardium. Thus, the site of earliest activation is dependent upon the pacing site, the position and orientation of muscle bridges, and the conduction velocities of the muscular components involved.

Previous mapping studies have suggested that there may be dissociation between the left atrium and coronary sinus musculature during coronary sinus pacing or atrial arrhythmias.[63,64] These studies have relied upon interpretation of coronary sinus electrograms with the assumption that sharp potentials correspond to local coronary sinus musculature activation, and low velocity, low amplitude electrograms represent far field signals from the overlying atrial musculature. In the present study, disparate activation patterns were noted during sinus rhythm and coronary sinus pacing in the majority of patients when comparing direct endocardial non-contact mapping and coronary sinus bipolar electrograms.

Clinical implications

Areas of conduction block were present in the left atrium during sinus rhythm and coronary sinus pacing. These lines of block may contribute to the substrate for reentrant arrhythmias, including atrial fibrillation or left atrial flutter. Conduction delay within the atria is more common in patients with a history of atrial fibrillation, although most studies have been limited to right atrial mapping.[110,111] Atrial fibrillation may be triggered by premature beats or a rapidly firing focus typically found in the muscular sleeves of the pulmonary veins.[112] The conduction block or delay in the posterior left atrial wall described in the present study are in

close proximity to the pulmonary veins and may provide the additional component that allows triggers to form reentrant wavelets that in turn degenerate into atrial fibrillation.[113]

Global left atrial conduction times during coronary sinus pacing were more rapid that during sinus rhythm. This may be important when considering multisite pacing strategies for prevention of atrial fibrillation, where the aim is to decrease atrial activation time.[114] The present study also demonstrates that electrograms recorded from the coronary sinus often do not reflect the timing and direction of activation in the overlying left atrium. The interpretation of coronary sinus electrograms during atrial arrhythmias must be treated with caution when used to determine the pattern of macroreentrant circuits or when identifying the site of earliest activation during a focal atrial tachycardia.[64] Indeed, the separation of coronary sinus and left atrial myocardium with interconnecting bridges may even provide the substrate for reentrant arrhythmias.[115]

Study Limitations

All patients had a history of paroxysmal atrial fibrillation. The lines of conduction block or delay may have been part of the substrate for the development of atrial fibrillation, or a consequence of electrical remodeling during the arrhythmia. It is possible that subjects without atrial fibrillation may have different left atrial activation patterns and may not have lines of conduction block. A control population was not included as the policy at our institution was to reserve left atrial non-contact mapping only for treatment of patients with atrial fibrillation and it was not appropriate to subject patients to a transseptal puncture and left atrial non-contact mapping who would not otherwise require it.

Pacing was only performed at one cycle length. The use of premature extrastimuli may have demonstrated additional areas of functional block that exist within the left atrium. In addition, pacing was performed at 1.0 mA above threshold. It is not known whether the pacing stimulus captured local coronary sinus musculature or also captured overlying atrial musculature. However, the stimulus-to-onset of left atrial activation times suggest that only local capture within the vein occurred.

Conclusions

In human patients with a history of paroxysmal atrial fibrillation, earliest left atrial endocardial activation usually occurs anterior to the right upper or lower pulmonary veins.

The subsequent spread of activation follows the longitudinal course of the muscle fibres in Bachmann's bundle across the left atrial roof before spreading down the posterior and lateral walls. Lines of conduction block or delay are present in the posterior wall, most commonly between the right upper and right lower pulmonary veins, extending inferiorly to the mitral valve annulus. These lines of block may also be seen during coronary sinus pacing. There are between 1 and 4 discrete connections between the coronary sinus and the left atrial musculature, which results in disparate activation times and directions. The site of earliest left atrial activation during coronary sinus pacing may be distant from the position of the pacing electrodes. These findings may have relevance to the mechanisms of atrial arrhythmias, including atrial fibrillation, and emphasize the need for caution when interpreting coronary sinus electrograms as indices of left atrial activation during electrophysiological studies.

Chapter 6: Characteristics of Right Atrial Activation During Coronary Sinus Pacing

Chapter abstract

Introduction: Anatomical and electrical connections between the left atrium and right atrium have been described. The relationship between coronary sinus pacing site and right atrial activation has not been examined.

Methods: 15 anesthetized swine underwent high-density non-contact mapping of the right atrium during pacing from up to 5 different sites within the coronary sinus. Isopotential mapping identified the site of earliest right atrial depolarization and the pattern of subsequent activation. Hearts were excised and endocardial dissection performed.

Results: Earliest right atrial activation occurred at the coronary sinus os with proximal coronary sinus pacing sites and Bachmann's bundle at distal pacing sites. The mean depth at which a shift in earliest right atrial activation site occurred was 46+/-13mm (range 21–63mm). Right atrial activation times following earliest activation at the coronary sinus and Bachmann's bundle were 40+/-4ms and 51+/-6ms ($p<0.002$). Conduction delay or block was recorded at the lateral cavotricuspid isthmus, the terminal crest and the Tendon of Todaro. Latest right atrial activation always occurred in the high anterolateral atrium after ascending the anterolateral wall. The lateral right atrium was activated by the wavefront that traversed the posterior wall rather than by the wavefront crossing the cavotricuspid isthmus, even with earliest right atrial activation at the coronary sinus os.

Conclusions: The site of earliest right atrial activation during coronary sinus pacing is dependent upon the pacing depth within the coronary sinus. In the porcine heart, areas of conduction delay influence right atrial activation patterns and timings. These findings may have implications for patients undergoing assessment of radiofrequency ablation of atrial flutter.

Introduction

Pacing from within the coronary sinus is commonly performed during electrophysiological studies. It may be used to assess conduction within the right atrium following cavotricuspid isthmus ablation of atrial flutter.[74] Coronary sinus pacing may also be combined with pacing in the right atrial appendage to prevent atrial fibrillation.[114,116] Little is known about patterns of right atrial activation during coronary sinus pacing.

Anatomical studies have described muscular bridges between the coronary sinus and the left atrium.[6,8,62] The previous study demonstrated that pacing from within the coronary sinus leads to electrical activation entering the posterior left atrium through these muscle bridges at discrete sites around the mitral valve annulus that may be some distance from the pacing electrodes. Areas of conduction delay or block that are probably the result of muscle fibre orientation also affect the subsequent spread of electrical activation through the left atrium. The mouth of the coronary sinus is continuous with right atrial myocardium. There are interatrial connections through Bachmann's bundle, the margins of the oval fossa, and muscle fibres bridging the septal raphe.[6] The coronary sinus and Bachmann's bundle have been described as the principle electrical interatrial connections, but the effect of pacing at different sites within the coronary sinus has not previously been examined.[117]

The present study was designed to examine interatrial conduction and patterns of right atrial activation during pacing at different sites within the coronary sinus in the intact, beating swine heart using high-density non-contact mapping of the right atrium.

Methods

The basic methodology has been described in Chapter 2. The study was carried out in accordance with local guidelines for welfare of animals under an approved Home Office license. General anesthesia was induced in 15 crossbred Large White/Landrace swine (*sus scrofa*) using intravenous alphaxalone/alphadalone, and maintained with inhaled isofluorane. Non-contact mapping was performed using the EnSite 3000 system (Endocardial Solutions Inc., St Paul, MN). The multielectrode array (MEA) was inserted in the mid-RA via a femoral vein. A steerable 4mm tip catheter (Bard, Lowell, MA) was used to construct the right atrial geometry and record electrograms. A 20-pole catheter with 2mm intra-electrode distance, 10mm inter-electrode distance (Bard, Lowell, MA) was positioned with the distal portion in the coronary sinus and proximal portion against the right atrial free wall, such that electrodes 9/10 or 11/12 straddled the coronary sinus os, depending upon how far the catheter

could be advanced. Catheter position was confirmed using injections of radio-opaque contrast. The depth of the distal electrode pairs was taken from the mid-point between the designated electrodes to the mid-point between the electrodes at the coronary sinus os.

Non-contact mapping was performed during pacing from bipole pairs within the coronary sinus, starting at the distal pair and ending with the pair positioned at the coronary sinus os. Pacing cycle length was 450-500ms at 0.5 mV above threshold and 2ms pulse width. Data were recorded on optical disk for subsequent analysis.

The site of earliest activation in the right atrium during pacing was defined as the site where depolarisation first appeared when the color offset (sensitivity) was set at 1 mV with a highpass filter setting of 1 kHz. The cut-off of 1 mV was used to introduce a standard for all animals and to avoid premature mapping of far-field LA activation as it approached the interatrial septum or coronary sinus os. The transition point was defined as the pacing depth at which simultaneous breakout occurred at the coronary sinus os and at an alternative septal structure (Figure 33). If earliest activation shifted from a superior septal site to the coronary sinus os when pacing was steered to a more proximal pair, without the visible occurrence of two individual wavefronts, the transition point was taken as the mid-point between the bipole pairs involved. E.g. if pacing at 56 mm depth resulted in earliest activation at Bachmann's bundle with no breakthrough at the coronary sinus os, and pacing at 42 mm depth resulted in earliest activation at the coronary sinus os and no breakthrough at Bachmann's bundle, the transition point was taken as 49 mm.

The spread of depolarisation from the site of earliest activation through the surrounding myocardium was examined by moving the isopotential map forward in time in 0.83ms intervals. The sensitivity and color offset of the isopotential map were adjusted to allow for the increasing amplitude of the electrical signal. The spread of activation and its relationship to anatomical structures was noted, with particular attention paid to areas of conduction delay or block. Global right atrial activation was then displayed as a single color isochronal map divided into isochrones of 2 - 4ms duration depending upon the total right atrial activation time. Total right atrial activation time was defined as the time from the onset of right atrial endocardial activation to the time that the last site within the right atrium depolarized, as determined by the dV/dt max of the virtual unipolar electrograms at the appropriate sites on the geometry.

Following the mapping procedures, the animals were killed with 50 ml of intravenous Phenobarbital. The hearts were excised and placed in 10% formaldehyde. The endocardium of the RA was peeled off without damaging the myocardial fibres. Watchmaker's forceps

Figure 33. Isopotential maps of onset of right atrial activation

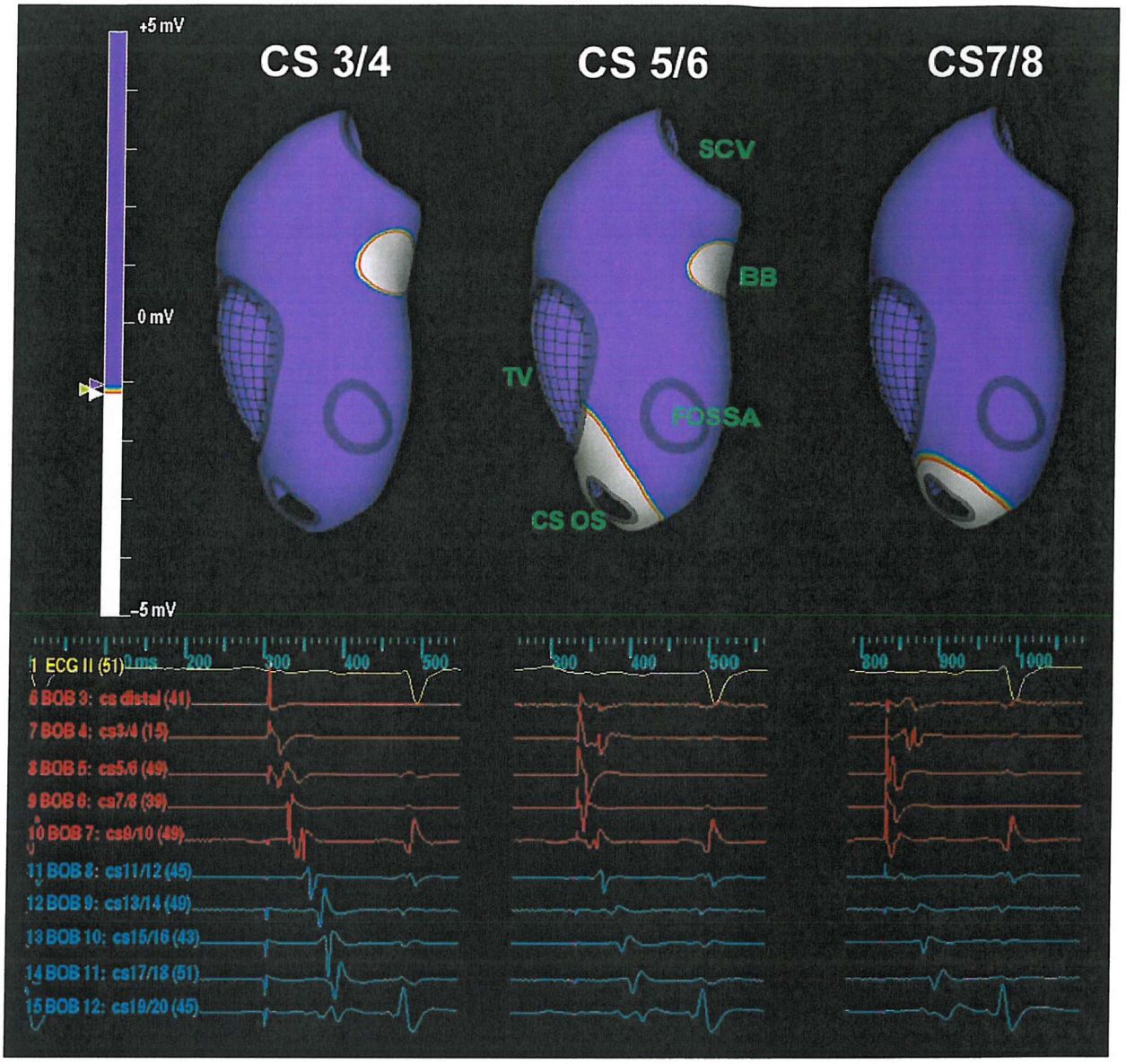

The right atrial geometry is viewed in a left lateral orientation. Depolarisation is shown as a white color against the purple background. When pacing from bipole 3/4 (42mm depth), earliest activation is at Bachmann's bundle. When pacing from bipoles 5/6 (28mm depth) activation breaks through simultaneously at Bachmann's bundle and the coronary sinus os (transition point). When pacing from bipole pair 7/8 (14mm depth) earliest activation is at the coronary sinus os. Electrograms from the 20-pole catheter are displayed below.

CS, coronary sinus; TV, tricuspid valve; SCV, superior caval vein; BB, Bachmann's bundle.

were used to follow the orientation of the fibres. Detailed sketches were made demonstrating the architecture of the endocardial layer of the musculature.

Statistical analysis was performed using a personal computer and Statview software. Comparison of mean values between 2 groups was performed using the student t-test. A p value of <0.05 was considered statistically significant. Data are presented as mean+/-standard deviation, unless otherwise indicated.

Results

Non-contact mapping was performed on 15 animals mean weight 85.5 +/- 4.4 kg. Coronary sinus pacing was performed at a mean cycle length of 478 +/- 42 ms.

Pacing depth vs. site of earliest right atrial activation

Pacing with successful capture was performed to a mean maximum depth of 62 +/- 9 mm (range 42 – 70 mm) within the coronary sinus. In all cases, earliest right atrial activation occurred at two possible sites: the superior septum, consistent with the right atrial insertion of Bachmann's bundle, or at the coronary sinus os (Figure 34). The coronary sinus os was the earliest site of right atrial activation during pacing at proximal sites within the coronary sinus. The transition point occurred at a mean pacing depth of 46+/-13mm (range 21-63mm). Bachmann's Bundle was the earliest site of right atrial activation over a distal coronary sinus length that extended 15+/-10mm (range 0–30mm) beyond the transition point. In two subjects where pacing was possible up to depths of 56mm, right atrial activation occurred exclusively via the coronary os.

Pacing depth vs. stimulus-to-onset right atrial activation time (Figure 35)

Pacing at more proximal sites resulted in a shorter stimulus-to-onset of right atrial activation time ($p<0.001$). A stepwise increase in time interval was noted, apart from at the greatest depth (70mm), where the mean stimulus-to-onset of right atrial activation time was shorter than that at 56mm (66ms vs. 68ms)

Figure 34. Site of earliest right atrial activation for each pacing site within the coronary sinus for each individual subject

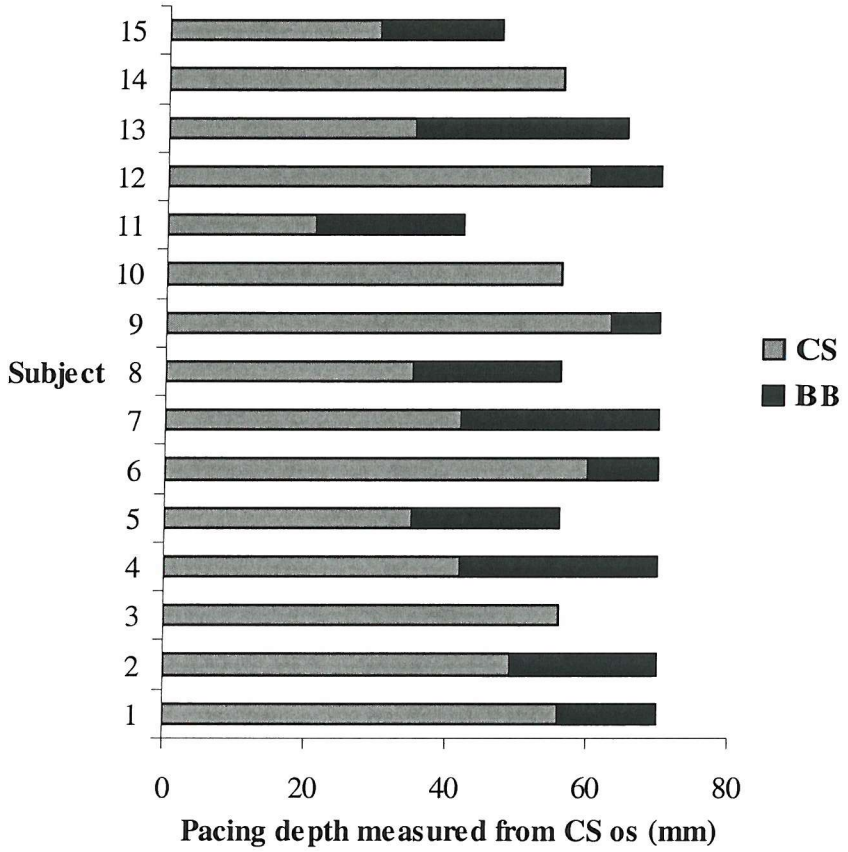

Figure 35. Mean stimulus-to-RA onset time for each pacing site subdivided by site of earliest activation

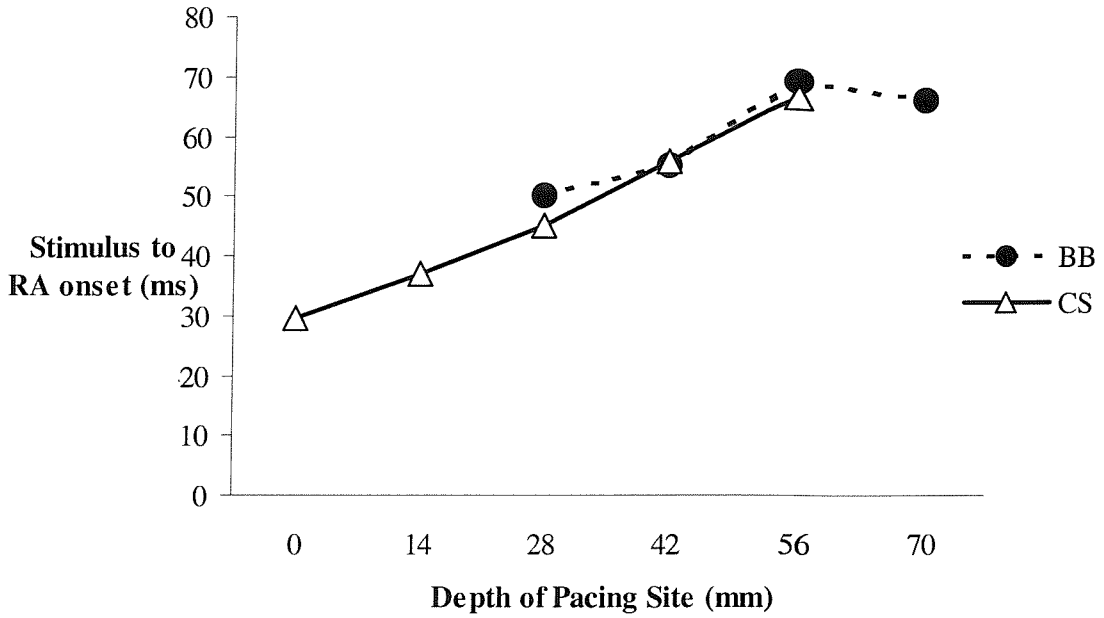

When subdivided by pacing site, the time from pacing stimulus to breakthrough at Bachmann's bundle did not differ significantly whether pacing was performed at 42, 56 or 70 mm from the coronary sinus os (p=0.06). The time from pacing stimulus to breakthrough at the coronary sinus os was significantly shorter at more proximal pacing sites (p<0.001).

Right atrial activation times by earliest activation site

The mean right atrial activation time when the site of earliest activation was Bachmann's bundle was 40 +/- 4ms. The mean right atrial activation time when the site of earliest activation was the coronary sinus was 51 +/- 6 ms (p<0.002).

Right atrial activation patterns

Two distinct right atrial activation patterns were noted, with minor variations between animals. The two patterns were determined by their sites of earliest activation (Figure 36).

Bachmann's bundle

After emerging into the right atrium at the superior septum, the depolarisation wavefront split to cross anteriorly and superiorly into the right atrial appendage and simultaneously descend inferiorly down the septum. A vertical line of conduction block was noted, extending from the superior vena cava a variable length down the posterior wall. The wavefront descending the septum slowed in the area between the tricuspid valve, superior rim of the coronary sinus os and inferior margin of the oval fossa (a site consistent with the position of the Tendon of Todaro), before continuing into the medial aspect of the cavotricuspid isthmus. At the same time, activation crossed the posterior wall, turning around the lower margin of the line of block to simultaneously ascend the lateral wall and enter the lateral cavotricuspid isthmus. The last part of the right atrium to be depolarized was the high anterolateral wall at a site consistent with the junction between the terminal crest and lateral right atrial appendage. This area was always activated by the wavefront that crossed the posterior wall and then ascended the anterolateral wall rather than by the wavefront that entered the medial appendage near the onset of activation, giving the appearance of conduction block or delay within the appendage. The lateral cavotricuspid isthmus always appeared to be activated simultaneously by the wavefront crossing the isthmus from medial to lateral and the wavefront crossing the posterior wall.

Figure 36. Isochronal maps of right atrial activation during coronary sinus pacing

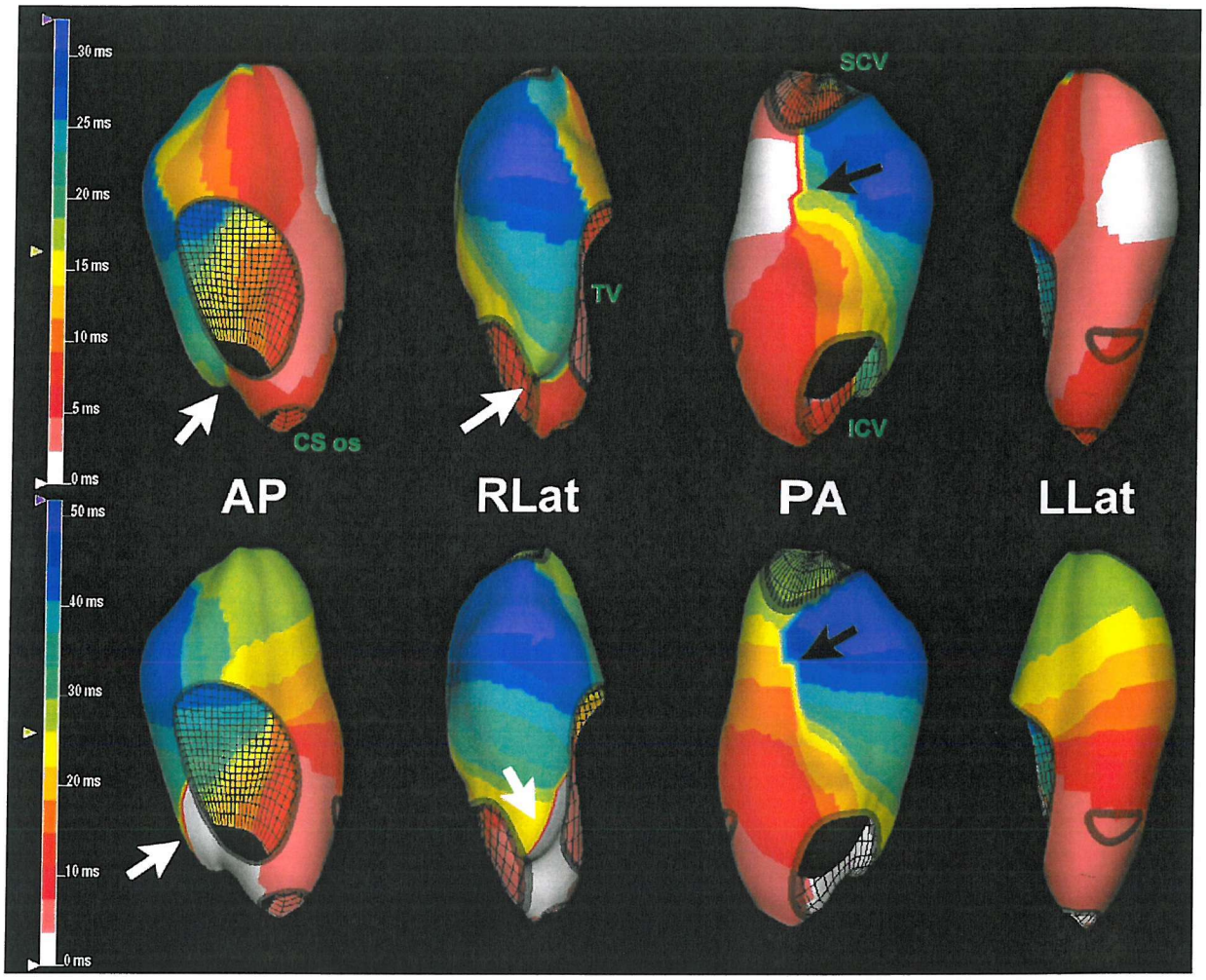

Isochronal maps of right atrial activation. The top row shows 4 views of the right atrium when earliest activation occurred at Bachmann's bundle. The colored isochrones depict 2.4 ms intervals. Activation begins on the superior septum and spreads into the right atrial appendage and inferiorly down the septum. Conduction block is present on the posterior wall (black arrow). The posterior wall wavefront and cavotricuspid isthmus wavefront appear to meet at the low lateral right atrium (white arrow) before ascending the anterolateral wall.

The bottom row shows the same 4 views in the same subject when earliest activation occurred at the coronary sinus os. The colored isochrones depict 3.5 ms intervals. Activation begins at anterior coronary sinus os and rapidly enters the cavotricuspid isthmus. Conduction block occurs at the lateral isthmus (white arrow). Activation ascends the septum and crosses the posterior wall. There is a conduction block in the superior posterior wall (black arrow). The posterior wall wavefront reaches the lateral isthmus and ascends the anterolateral wall approximately 20 ms after the initial isthmus wavefront was blocked.

CS, coronary sinus; TC, tricuspid valve; SCV, superior caval vein; ICV, inferior caval vein

Coronary sinus

Activation emerged from the anterior aspect of the coronary sinus os and headed in two directions; anterolaterally into the medial cavotricuspid isthmus; and superiorly up the septum. The wavefront heading up the septum slowed in the area between the tricuspid valve, superior rim of the coronary sinus os and inferior margin of the oval fossa (a site consistent with the position of the Tendon of Todaro). As the wavefront broadened it spread from the superior septum into the medial right atrial appendage and across the posterior wall. A line of conduction delay or block extending down from the superior caval vein a variable length was present either in the mid-posterior wall or in the lateral wall at a site consistent with the terminal crest. The wavefront crossed the inferior margin of this line of block before spreading superiorly up the anterolateral wall. The last part of the right atrium to be depolarized was the high anterolateral wall, at a site consistent with the junction between the terminal crest and lateral right atrial appendage.

The wavefront leaving the coronary sinus and entering the medial border of the cavotricuspid isthmus was always of low amplitude and slow conduction velocity. In only 1/15 animals studied did activation exit the lateral isthmus and depolarize the anterolateral wall. In the remaining animals, the lateral isthmus and anterolateral wall were activated by the posterior wall wavefront, giving the appearance of a line of conduction block at the lateral cavotricuspid isthmus, with a difference in activation times of 25 +/- 6 ms either side.

Dissection

Anatomical dissection of the RA revealed morphologically normal hearts in every case. The superior caval vein and inferior caval vein entered into the smooth venous component of the right atrium. The posterior wall fibres were orientated vertically, running from the superior caval vein to the inferior caval vein parallel with the terminal crest. The terminal crest appeared as a very prominent muscle bundle that descended the lateral wall giving off thick pectinate branches that spread into the right atrial appendage. At the site where the inferior margin of the terminal crest entered the lateral cavotricuspid isthmus, the most posterior muscle bundle thinned and formed the Eustachian ridge, whereas the anterior bundles and pectinate branches turned ninety degrees to insert into the tricuspid valve annulus. The cavotricuspid isthmus thus consisted of a lattice of muscle fibres interspersed with areas of collagenous tissue. At the lateral margin of the cavotricuspid valve isthmus the fibres were orientated perpendicular to the direction of spread of depolarization (see Chapter 4, Figure 26)

Discussion

In the present study, pacing was performed at different depths within the coronary sinus and subsequent right atrial activation times and patterns were recorded using non-contact mapping. The site of earliest right atrial activation occurred at the coronary sinus os with proximal pacing sites and at the insertion of Bachmann's bundle with more distal pacing sites. Right atrial activation patterns were dependent upon the site of earliest activation and global right atrial activation was faster when activation started at Bachmann's bundle. Conduction block or delay was noted in areas consistent with the lateral terminal crest, the mid-posterior wall and the Tendon of Todaro.

Anatomical studies of the human and canine heart have described muscular connections between the atria occurring through Bachmann's bundle, the coronary sinus musculature, the margins of the oval fossa, and fibres that bridge the septal raphe[2,6,8,62] The coronary sinus has a muscular sleeve that is continuous with the right atrial musculature at its os.[8] The variable length that the muscle sleeve extends into the vein may explain why pacing at 56 and 70 mm depth coronary sinus failed to capture in 2/15 and 8/15 animals respectively. The sleeve is separated from the left atrial myocardium by a fibrofatty cushion, which is traversed by muscular bridges that act as electrical connections between these two structures.[7,8,62]

A prior study utilising electroanatomic mapping in the human right atrium during distal coronary sinus pacing demonstrated earliest right atrial activation at the coronary sinus in 9/11 patients, Bachmann's bundle in 1/11 and at the oval fossa in 1/11 patients.[117] The study was limited by the use of only a single pacing site within the coronary sinus. The present study has shown that the site of earliest right atrial activation varies depending upon the pacing site within the coronary sinus, with considerable inter-subject variation. A number of factors may influence the site of earliest activation, including the pacing depth within the coronary sinus, the position and orientation of the muscular bridges that connect the coronary sinus to the left atrium, and the conduction velocities within the musculature, connecting bridges and left atrial myocardium. The transition from Bachmann's bundle to the coronary sinus os occurred at 46 +/- 13 mm depth. In the 3/15 subjects where the transition point between Bachmann's bundle and the coronary sinus os occurred at pacing depths of 60 – 63 mm, there may have been an absence of distal coronary sinus-left atrial connections, or the connections may have been orientated unfavorably for rapid travel to Bachmann's bundle. In the 2/15 subjects where the transition sites were at 21 and 30 mm depth, earliest activation from more distal pacing sites may have occurred at Bachmann's bundle as a result of slow

conduction within the proximal coronary sinus, connecting bridges immediately adjacent to the pacing site that were orientated favorably towards Bachmann's bundle, and a short left atrial route of conduction. The myocardial fibres surrounding the coronary sinus may be arranged in spirals, resulting in longer conduction over a relatively short longitudinal distance when compared to left atrial conduction.[7]

As expected, the stimulus-to-onset of right atrial activation was longer at deeper pacing sites. The only exception was at 70 mm pacing depth, where the mean time was slightly shorter than at 56 mm pacing depth. At 70mm depth the electrodes were in an anterolateral position and closer to Bachmann's bundle than at 56mm depth, which was more posterolaterally orientated.

In the present study, earliest right atrial endocardial activation did not occur at the oval fossa. Anatomically, the oval fossa is the principle area of right and left septal continuity, with the remaining septal structures composed of the infolded atrial walls separated by fibrofatty tissue that may be bridged by muscle strands.[6] In the canine heart, discordant activation is present on either side of the septum, and the electrical conduits between each side are at the inferior and superior margins, rather than around the fossa.[65] The present study suggests this is also the case in the porcine heart. Alternatively, the orientation of left atrial endocardial fibres may direct activation that enters the left atrium on the posterior mitral valve annulus during coronary sinus pacing in the direction of Bachmann's bundle rather than towards the septum.

The spread of activation through the right atrium encountered conduction delay or block at sites consistent with the Tendon of Todaro and the terminal crest. In Chapter 4, these sites were demonstrated slow conduction or block during sinus rhythm as a consequence of myofibre orientation. These sites have also been previously documented as areas of anisotropy and conduction block during pacing and atrial flutter.[42,53,55,60] During coronary sinus pacing there is slow conduction across the posterior border of the Triangle of Koch. A similar finding was demonstrated in the present study, with rapid spread into the medial isthmus and slower posterior depolarisation when the coronary sinus was the earliest site of activation.[42] In some animals a vertical line of conduction block was seen in the mid-posterior wall. A line of conduction block at this site has previously been reported during atrial flutter in the human heart.[118] Intracardiac echocardiography indicated that the line of block occurred in the sinus venosa region between the oval fossa and terminal crest. In the present study, the activation wavefront that was crossing the posterior wall had to turn around the inferior margin of this line of block. As a consequence, activation subsequently ascended the anterolateral wall from inferior to superior to finish in the high anterolateral right atrium.

When the site of earliest activation was at the coronary sinus os a line of conduction delay or block in the lateral cavotricuspid isthmus was easily identified and the anterolateral wall was clearly activated by the posterior wall wavefront. When earliest activation was at Bachmann's bundle, the posterior wall wavefront arrived at the lateral isthmus at the same time as the medial cavotricuspid isthmus was activated, giving the appearance of a collision of wavefronts and disguising the area of conduction block. Conduction from the coronary sinus os to low lateral right atrium around the posterior inferior caval vein traveled through the smooth venous component, across vertically orientated fibres that descend in the posterior wall. In contrast, conduction around the anterior inferior caval vein through the cavotricuspud isthmus encountered pectinate muscles that were perpendicular to the direction of activation. The terminal crest and pectinate muscles exhibit profound anisotropic properties, with transverse conduction up to 10 times slower than longitudinal conduction.[107] Thus, preferential conduction around the posterior inferior caval vein may be the result of delay or block in the cavotricuspid isthmus rather than unusually rapid spread around the posterior inferior caval vein.

Clinical Implications

During catheter ablation of isthmus-dependent atrial flutter, conduction times across the cavotricuspid isthmus are commonly used to assess the effect of radiofrequency lesions. The present study suggests that in the porcine heart, the fastest conduction from the coronary sinus os to low lateral right atrium takes place around the posterior inferior caval vein rather than through the cavotricuspid isthmus. Thus, following radiofrequency ablation, coronary sinus to low lateral right atrium conduction times may not change even though isthmus block is present. A similar finding has been reported in some human subjects with atrial flutter.[119]

Activation of the anterolateral wall occurred from inferior to superior and the high anterolateral right atrium was the last site to be depolarized, regardless of the pacing site within the coronary sinus and the subsequent site of earliest activation. However, the global right atrial activation time was longer when the coronary sinus os was the earliest site of activation. During the assessment of radiofrequency ablation of atrial flutter, care must be taken to pace from the same coronary sinus catheter electrodes to avoid variations in activation timings that result from changes in interatrial conduction rather than trans-isthmus conduction. Also, in the porcine heart at least, the present study suggests that during coronary sinus pacing the activation sequence in the anterolateral wall would not change after complete, transmural ablation through the cavotricuspid isthmus.

Study limitations

Anatomical landmarks were inferred from fluoroscopic and electrogram characteristics. The precise positions of the tendon of Todaro and terminal crest were speculative, however the combination of a 3-dimensional geometry, the ability to accurately identify of the oval fossa, tricuspid valve, caval veins and coronary sinus, plus subsequent pathological examination and knowledge from previous studies, provided spatial references that allowed for reasonable estimation of the position of these structures. In addition, radiofrequency ablation of the interatrial connections was performed in some animals as part of an alternative study (see Chapter 7). This allowed anatomical confirmation of the breakthrough sites described. However, dissection and pathological examination of the left atrium and coronary sinus was not performed, therefore the anatomical connections between the coronary sinus and left atrium can only be inferred from other animal and human studies.

It was not possible to distinguish between conduction delay and conduction block, particularly at areas of interest such as the cavotricuspid isthmus. Slow conduction through the cavotricuspid isthmus allowed the posterior wall wavefront to reach the low anterolateral right atrium and ascend the anterolateral wall. If there were no posterior wall wavefront, it is possible that activation would eventually emerge from the lateral cavotricuspid isthmus to ascend the anterolateral wall, indicating slow conduction and delay rather than complete block.

Conclusions

In the porcine heart, coronary sinus pacing results in earliest right atrial activation at the insertion of Bachmann's bundle or at the coronary sinus os. The site of earliest activation is determined by the pacing depth, however there is considerable variety between individuals. The site of earliest activation determines right atrial activation patterns and times. Conduction through the cavotricuspid isthmus is delayed or blocked, resulting in activation of the anterolateral wall from inferior to superior by a wavefront that has crossed the posterior wall. Conduction delay may only become apparent during proximal coronary sinus pacing as it is disguised when the site of earliest right atrial activation is at Bachmann's bundle. These findings may have implications for the assessment of radiofrequency ablation in patients with atrial flutter. Further high-density mapping studies in the human heart are warranted.

Chapter 7: Feasibility of transcatheter left atrial disconnection and its effect on the inducibility and maintenance of atrial fibrillation

Chapter abstract

Introduction: An effective, catheter-based treatment for persistent atrial fibrillation remains elusive. This study assessed the feasibility of transcatheter left atrial electrical disconnection and its effect on atrial fibrillation inducibility.

Method: 13 anesthetized swine underwent non-contact mapping of the right atrium during coronary sinus pacing. Sites of earliest right atrial activation were identified using isopotential maps. An ablation catheter was navigated to these sites, and a cluster of radiofrequency lesions applied until earliest activation shifted to a new site. The procedure was repeated until the atria were electrically disconnected. Atrial fibrillation induction was attempted pre- and post-ablation.

Results: Earliest right atrial activation was the coronary sinus os during proximal coronary sinus pacing, and Bachmann's bundle during distal coronary sinus pacing. These two sites were successfully ablated in all 13 animals. Earliest activation then shifted to the oval fossa. Radiofrequency energy was applied at a median of 2.5 (range 1-5) sites around the fossa, then at sites in the Triangle of Koch, septum, cavotricuspid isthmus and posterior wall. Atrial electrical disconnection was achieved in 10/13 animals (5 left atrial electrical disconnection, 3 right atrial electrical disconnection, 2 biatrial electrical disconnection with complete heart block). Following atrial electrical disconnection, the left atrium became electrically silent. Prior to ablation, atrial fibrillation was inducible in every animal. Following atrial electrical disconnection, atrial fibrillation was inducible in 3/10 animals.

Conclusions: Atrial electrical disconnection is feasible using non-contact mapping and radiofrequency energy ablation. Successful electrical disconnection of the atria reduces atrial fibrillation inducibility. This approach is worthy of further evaluation as a management strategy for persistent atrial fibrillation, combined with device therapies.

Introduction

The preceding studies have shown us that the spread of electrical activation between and within the atria is governed by the myocardial architecture. In particular, in the porcine heart the spread of activation from the left to the right atrium during coronary sinus pacing occurs either via Bachmann's bundle or via the os of coronary sinus, depending upon the pacing depth within the coronary sinus. Non-contact mapping was easily able to identify these two electrical connections.

The surgical left atrial isolation procedure was developed two decades ago as a therapeutic option in patients with atrial fibrillation undergoing mitral valve surgery.[77,78] The procedure required extension of the left atriotomy incision together with a cryotherapy lesion of the coronary sinus muscle fibres. Sinus rhythm could be achieved in 72% of patients during follow-up. The risk of thromboembolism remained, however, due to loss of contraction of the isolated left atrium. This operation has been superseded by the Maze procedure, in which atrial compartmentalization prevents atrial fibrillation from sustaining, whilst allowing sinus rhythm to provide coordinated contraction. Attempts to emulate the surgical Maze procedure using transcatheter ablation techniques have been disappointing. Difficulties in creating long, continuous linear lesions, particularly in the left atrium, have resulted in a high arrhythmia recurrence rate and significant procedural complications.

The ideal catheter-based approach for the treatment of atrial fibrillation would combine the simple elegance and success of the electrical disconnection procedure together with a purely right-sided approach. Using non-contact mapping technology, this experiment was designed to investigate the feasibility of performing left atrial electrical disconnection using transcatheter techniques, and examine the effect of this procedure on the inducibility and maintenance of atrial fibrillation.

Methods

The basic methodology was performed as described in the preceding Methods chapter. In brief, the animal subjects were cared for and grown to 75-105 kg in weight. All procedures were performed under general anaesthesia, in accordance with the Home Office Project License. Electrophysiological data were recorded using non-contact mapping techniques. The non-contact mapping catheter multielectrode array was positioned in the centre of the right atrium via the left femoral vein. A 20-pole steerable catheter was positioned in the coronary sinus, such that the catheter tip was in the 2-3 o'clock position when viewed in the

fluoroscopic anteroposterior position, the distal 5 bipolar pairs (electrodes 1-10) were positioned in the coronary sinus, and the proximal 5 bipolar pairs were placed along the floor of the right atrium and up the lateral wall, adjacent to the terminal crest. A 4 mm tip steerable ablation catheter (Stinger, Bard, Lowell, MA) was used for the creation of chamber geometry and labelling of anatomic structures. Following the mapping procedures, the hearts were excised and placed in 10% formaldehyde.

To perform atrial disconnection, continuous pacing at 120 beats per minute was initially directed to a bipole pair within the coronary sinus. Isopotential maps of right atrial activation were reviewed and the site of earliest activation (i.e. where activation entered the right atrial from the left atrium) identified. During continuous coronary sinus pacing the ablation catheter was then guided to the site of earliest activation using the locator signal navigation system. Radiofrequency energy was delivered until re-mapping demonstrated that the site of earliest activation had shifted to an alternative site, indicating successful destruction of the interatrial connection. This sequence was then repeated until coronary sinus pacing failed to conduct to the right atrium via any route. Where earliest right atrial activation occurred at the origin of the coronary sinus, lesions were placed circumferentially 0.5 to 1 cm inside the structure, until it was disconnected from the right atrial chamber. By definition, atrial separation occurred when there was no conduction from the left atrium to the right atrium by any route. An atrium was considered to be isolated if there was no conduction to the alternate atrium nor the ventricles by any route.

A step-wise protocol for the induction of atrial fibrillation was performed at a pacing site in the lateral right atrium and a site in the distal coronary sinus. Up to 3 paced extra-stimuli were followed by high rate incremental atrial pacing. If atrial fibrillation was not induced, 50Hz alternating current was delivered for 5 seconds. This procedure was performed prior to non-contact mapping and then repeated in both atria when atrial separation had been achieved. Following the procedure the animals were terminated and the hearts excised and examined.

Results

Results are summarized in Table 3.

Table 3. Results of left atrial electrical disconnection attempts

Animal	**AF inducible (pre-ablation)**	**Result**	**AV conduction (post-ablation)**	**AF inducible (post-ablation)**
1	LA, RA	Unsuccessful	CHB	-
2	LA	Unsuccessful	Normal	-
3	LA, RA	LA electrical disconnection	RA-V conduction	No
4	LA, RA	RA electrical disconnection	LA-V conduction	LA only
5	LA, RA	Unsuccessful	Normal	-
6	LA, RA	Biatrial electrical disconnection	CHB	No
7	LA	LA electrical disconnection	RA-V conduction	No
8	LA, RA	Biatrial electrical disconnection	CHB	No
9	LA	RA electrical disconnection	LA-V conduction	No
10	LA, RA	RA electrical disconnection	LA-V conduction	LA only
11	LA, RA	LA electrical disconnection	RA-V conduction	No
12	LA, RA	LA electrical disconnection	RA-V conduction	No
13	LA	LA electrical disconnection	RA-V conduction	RA only

AF, atrial fibrillation; AV, atrioventricular; LA, left atrium; RA, right atrium; V, ventricle; CHB, complete heart block

Right atrial mapping during coronary sinus pacing

Isopotential mapping identified the coronary sinus os as the site of earliest right atrial activation during proximal coronary sinus pacing, and a site consistent with Bachmann's bundle on the superior septum as the site of earliest right atrial activation during distal coronary sinus pacing. In all 13 animals these two sites dominated, the switch from one to the other occurring approximately 5 cm into the coronary sinus. At this site it was possible to see simultaneous breakthrough at both sites. Earliest breakthrough at additional sites was not seen until both the coronary sinus connections and the right atrial insertion of Bachmann's bundle had been successfully ablated. Earliest activation then shifted to sites around the oval fossa and the interatrial septum. In some animals, addition areas of earliest activation appeared within the cavotricuspid isthmus and posterior wall at sites that appeared to be away from the interatrial septum.

Radiofrequency ablation

Radiofrequency ablation was initially performed at the coronary sinus os and within the first 2 cm of the coronary sinus. Radiofrequency energy was applied for 90 seconds (maximum power 30W, temperature limited to 55°C). A median of 7 (range 3-12) lesions was required to sever all connections between the coronary sinus and right atrial and shift earliest activation to the right atrial insertion of Bachmann's bundle. Radiofrequency ablation was then performed at Bachmann's bundle, (60 seconds at maximum of 50W, temperature limited to 65°C), identified as the site of earliest activation following successful coronary sinus ablation in every animal. In every case a cluster of lesions covering at least a 1 cm by 0.5 cm area was required (median 6, range 4-7). Radiofrequency ablation lesions were then directed at a median of 2.5 (range 1-5) sites around the margins of oval fossa, the true interatrial septum, the Triangle of Koch, the cavotricuspid isthmus and the posterior wall (Figure 37). Electrical disconnection of the left atrium from the right atrium was achieved in 10/13 subjects: i) 5/10 left atrial electrical disconnection with intact right atrial to ventricular conduction; ii) 3/10 right atrial electrical disconnection with intact left atrium to ventricular conduction; or iii) 2/10 biatrial electrical disconnection with complete heart block. Following successful electrical disconnection of the atria, the right atrium remained in sinus rhythm, whereas the left atrium became electrically silent (Figure 38). Coronary sinus pacing at a shorter cycle length than sinus rhythm confirmed left atrial electrical disconnection (Figure 39).

Figure 37. Breakthrough sites from the left-to-right atrium

Non-contact mapping image of right atrial geometry in an open view. The model of the right atrial chamber has been cut from inferior caval vein to superior caval vein along the posterior wall, and peeled open to expose the entire endocardial surface. Sites of previous radiofrequency energy application are marked as shaded circles. The coloured spot with white centre indicates negative endocardial voltages (i.e. depolarisation) against the purple background (electrically silent or resting myocardium). The image depicts a single frame of the isopotential map, frozen at the time of earliest right atrial activation during coronary sinus pacing. Activation is seen to enter the right atrium at the superior limbus of the oval fossa.

SCV, superior caval vein; ICV, inferior caval vein; CSO, coronary sinus os; TV, tricuspid valve

Figure 38. Sinus rhythm electrograms following left atrial disconnection

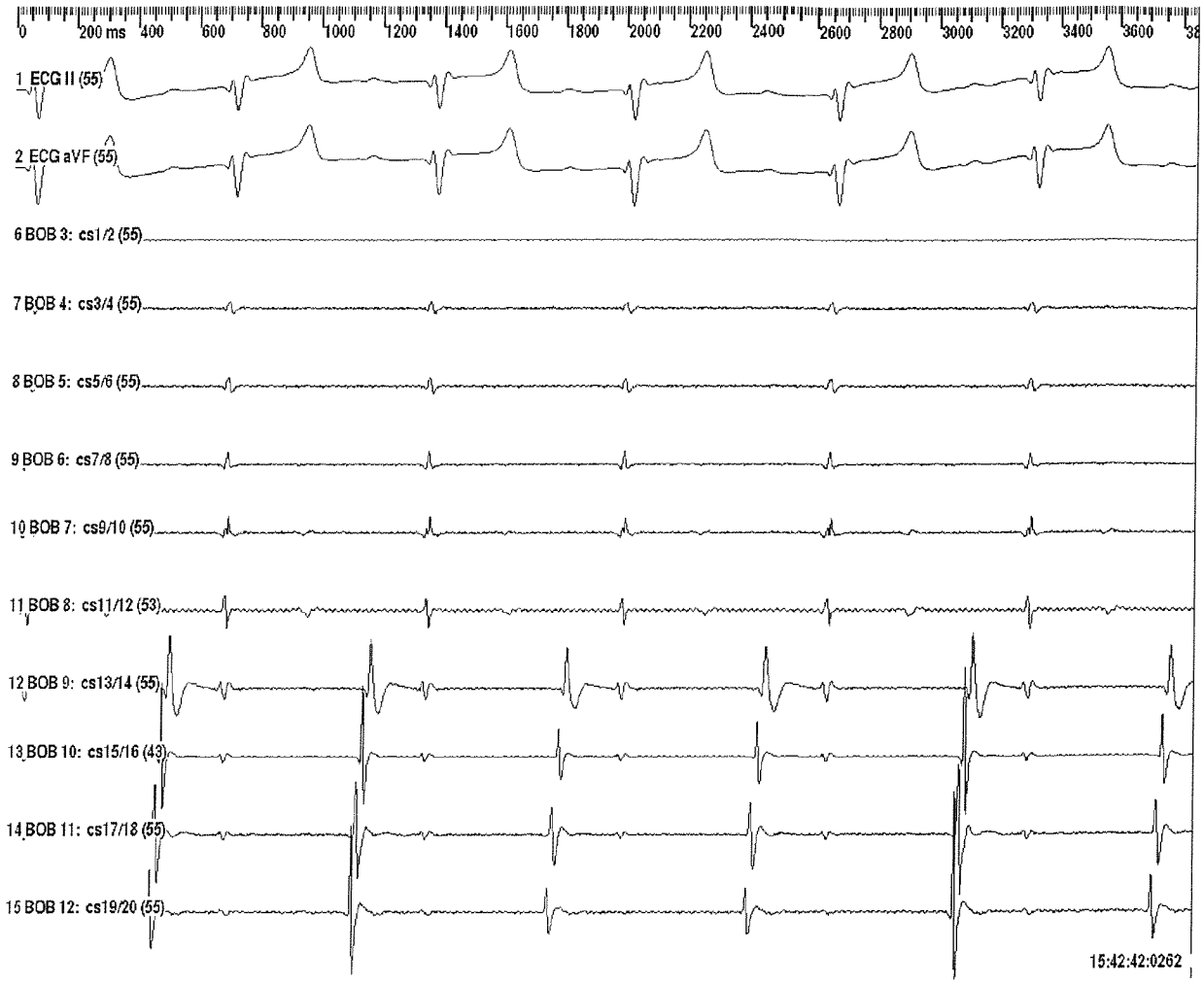

Surface ECG and intracardiac electrogram recordings from the 20-pole catheter. The distal poles (1/2 - 9/10) are in the coronary sinus. The proximal poles (11/12 - 19/20) cross the cavotricuspid isthmus and ascend the lateral right atrial wall. Left atrial electrical disconnection has been performed. Sinus rhythm continues in the right atrium. The left atrium is electrically silent, with far-field potentials recorded from the left ventricle.

Figure 39. Atrial pacing electrograms following left atrial disconnection

Surface ECG and intracardiac electrogram recordings from the 20-pole catheter. The distal poles (1/2 - 9/10) are in the coronary sinus. The proximal poles (11/12 - 19/20) cross the cavotricuspid isthmus and ascend the lateral right atrial wall. Left atrial electrical disconnection has been performed. Distal coronary sinus pacing results in left atrial activation as seen in the distal coronary sinus electrograms. Sinus rhythm continues in the right atrium. Ventricular activation follows right atrial activation.

The three animals with unsuccessful procedures continued to demonstrate earliest activation (as detected by non-contact mapping) occurring around the margin of the oval fossa and anterior interatrial septum, despite exhaustive applications of numerous radiofrequency energy lesions and large areas of necrosis.

Inducibility of atrial fibrillation

Prior to mapping and ablation, atrial fibrillation was inducible with left atrial stimulation in 13/13 animals and right atrial stimulation in 9/13 animals. Re-induction of atrial fibrillation was attempted in the 10 animals with successful atrial electrical disconnection. In 7/10 animals, atrial fibrillation could not be re-induced despite maximal stimulation in either atrium. In the remaining 3 animals, atrial fibrillation was induced with left atrial pacing in 2 cases (both with right atrial electrical disconnection) and right atrial pacing in 1 (with left atrial electrical disconnection). Atrial fibrillation was confined to the atrium in which it was induced and did not conduct to alternate atrium.

Pathological examination

In successful cases, pathological examination revealed evidence of transmural necrosis at the right atrial insertion of Bachmann's bundle, within the proximal portion of the coronary sinus and on the limbus of the oval fossa (Figure 40). The area of necrosis around the fossa and true septum varied considerably between animals and was related to the number of separate breakthrough sites and radiofrequency energy applications.

Discussion

This study has demonstrated that left atrial electrical disconnection is feasible in the porcine heart, using right atrial electrophysiological mapping and RF ablation. Although electrical disconnection of the atria was achieved in 10/13 animals, pure left atrial electrical disconnection with intact right atrium to ventricular conduction was only successful in 5 animals. Atrial electrical disconnection prevented the induction of atrial fibrillation in 7/10 animals. In the 5 cases of successful left atrial electrical disconnection, atrial fibrillation was induced in only 1 animal, with right atrial stimulation.

Figure 40. Pathological specimen following a successful left atrial electrical disconnection procedure

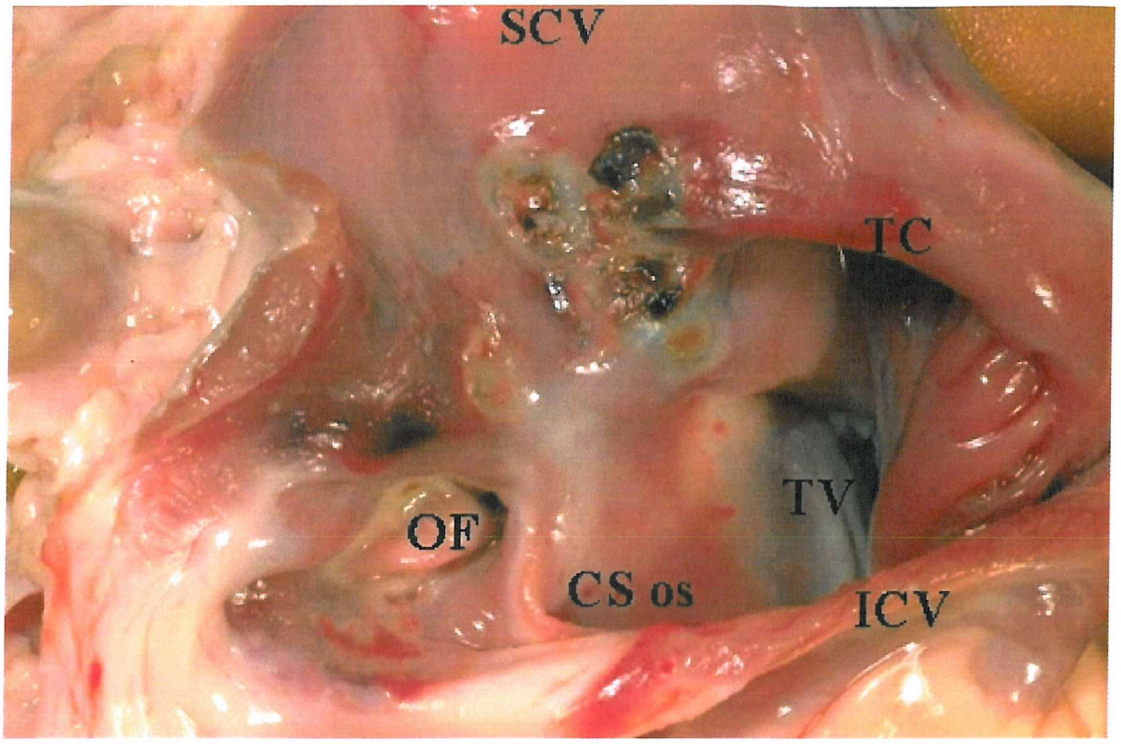

The chamber has been cut from inferior caval vein to superior caval vein along the posterior wall, and peeled open to expose the endocardial surface. A cluster of radiofrequency ablation lesions is seen at the right atrial insertion of Bachmann's bundle, within the oval fossa, and around the margins of the true septum. Further lesions were performed within the proximal portion of the coronary sinus (not visible).

SCV, superior caval vein; ICV, inferior caval vein; coronary sinus os, coronary sinus os; TV, tricuspid valve; OF, oval fossa; TC, terminal crest

Electrical connections between the atria were identified at the coronary sinus os, Bachmann's bundle, and around the margins of the oval fossa. These sites correlate well with known anatomical muscular connections, which have been extensively described by other authors. The muscular cuff surrounding the coronary sinus is continuous with the right atrium and may extend for 2 to 5.5 cm into the vein from the os.[8,62] The muscular cuff is separated from left atrial myocardium by fatty tissue, which is traversed by striated muscle bands providing coronary sinus to left atrium connections. The superior interatrial band (Bachmann's Bundle) originates at the orifice of the superior caval vein or the atriocaval junction.[2] Importantly, the true atrial septum is smaller than originally anticipated, consisting principally of the oval fossa and its immediate muscular inferoanterior rim.[10] It is only at the periphery of the oval fossa that the musculature of the two atria is in continuity. The remainder of the septal wall results from infolding of the right atrial and left atrial walls, separated by a fatty layer. This may explain how in some animals only 2 or 3 radiofrequency applications around the limbus of the oval fossa were capable of severing interatrial connections at this site. Other smaller bundles superiorly and posteriorly may bridge the gap between the infolded septal walls to provide communications between the left atrium and right atrium.[6] This may explain why a high number of radiofrequency ablation lesions were required in some animals, and why electrical connections persisted in 3 animals at the end of the procedure.

Electrophysiological confirmation of the anatomical interatrial connections at the coronary sinus, Bachmann's bundle and oval fossa has been reported previously.[117] In the human heart, distal coronary sinus and left atrial pacing can result in three distinct sites of early right atrial activation The two most common sites are Bachmann's bundle and the coronary sinus os. Earliest right atrial activation at the oval fossa may also be seen in some patients during left atrial pacing. These findings would agree with our report that proximal coronary sinus pacing results in earliest activation of the right atrium at the coronary sinus ostium and distal coronary sinus pacing results in preferential conduction across Bachmann's bundle.

Inoue and Becker have described a left atrium-to-atrioventricular node connection, based on dissection and mapping studies, that lends important support to the observed occurrence of right atrial electrical disconnection and intact left atrium-to-ventricle conduction in 3 animals.[120] Extensive ablation around the Triangle of Koch may have obliterated right atrial inputs to the atrioventricular node, whilst leaving left atrial inputs intact. For true left atrial electrical disconnection to occur, these left-sided inputs must either have been absent, or else ablated during radiofrequency energy application at right atrial or coronary sinus sites. It may be that additional left atrial lesions are required in those with left atrium-to-atrioventricular node connections.

Complete heart block or ablation of right atrial inputs to the atrioventricular node occurred in 5 animals. This may have resulted from unintended ablation of vulnerable conducting tissue due to its proximity to the interatrial connections. Alternatively, there may have been interatrial connections that used nodal pathways, prohibiting atrial electrical disconnection from occurring without additional electrical disconnection of the compact node. In successful cases of left atrial electrical disconnection, the PR interval on the surface ECG increased to >200 msec. This could have resulted from ablation of the principle inputs to the AV node, i.e. the fast pathway with septal ablation, and the slow pathway with lesions around the coronary sinus os.

Reduction in the inducibility of atrial fibrillation may have resulted from a limited form of compartmentalization, with atrial electrical disconnection leading to a halving of the area of continuous atrial myocardium. In the normal swine hearts used in this study, this reduction in area may have been enough to prevent the critical number of reentrant circuits required for atrial fibrillation from being able to sustain and maintain the arrhythmia, even for a few seconds. Atrial fibrillation was easier to induce in the left atrium, and in 2 animals remained inducible but confined to the left atrium. Other workers have reported the relative inefficacy of right atrial versus left atrial linear lesions in reducing atrial fibrillation, leading them to the suggestion that the left atrium is the principle driver behind the initiation and maintenance of atrial fibrillation.[121]

There has been considerable effort to reproduce the surgical Maze approach using transcatheter endocardial radiofrequency ablation. Despite the use of advanced mapping systems, atrial fibrillation recurrence rates may be as high as 94%.[87] Procedure times are long and there are risks of thromboembolism and cardiac tamponade with left-sided approaches. Transcatheter left atrial electrical disconnection may offer a more simple, right-sided approach with greater efficacy.

In this study, the left atrium became electrically silent in every case of successful electrical disconnection. If this technique became applicable for human use it would require additional therapy with biatrial pacing to maintain coordinated left atrial contraction. Biatrial pacing with right atrial and coronary sinus leads has been studies previously, and may have a role in the prevention of atrial fibrillation in its own right.[114,122,123] The combination of atrial electrical disconnection and biatrial pacing may have a synergistic effect on reducing the frequency and duration of atrial fibrillation episodes, whilst removing the thromboembolic risk of a non-contractile left atrium. However, should either atrium continue to fibrillate, anticoagulation may still be required.

Study Limitations

This study was performed on swine hearts, and consequently may not apply to the human heart. It is anticipated that left atrial electrical disconnection using non-contact mapping and radiofrequency ablation in the human right atrium would be feasible for a number of reasons. The human right atrium is more spherical than the tall, narrow, tubular swine atrium, and has a broad-based atrial appendage, facilitating catheter manipulation and activation mapping. Also, identification of the compact node and His bundle is easier in the human heart due to a greater familiarity with atrial anatomy.

The technique is dependent upon the ability to perform pacing from sites within the coronary sinus during sinus rhythm. This study has not examined the feasibility of atrial electrical disconnection whilst the subject is in atrial fibrillation. In addition, the induction of atrial fibrillation using burst pacing or alternating current delivery in the swine heart may not reflect the mechanism of initiation and maintenance of patients with persistent atrial fibrillation. Thus, although induction of atrial fibrillation in the normal swine heart may be prevented, this may not be the case in a diseased human heart. However, the procedure has demonstrated that it is possible to confine rapid left atrial activation (from coronary sinus pacing) to the left atrium, avoiding a rapid ventricular response and maintaining synchrony between the right atrium and ventricles. The study did not assess the ease of inducibility, but rather whether atrial fibrillation was inducible or not. Prior to ablation, the majority of animals had atrial fibrillation induced by rapid atrial pacing in either atrium; after successful atrial electrical disconnection, atrial fibrillation could not be induced in 7/10 animals despite aggressive stimulation with AC delivery to the left or right atrium. However, the primary study aim was to test the feasibility of a left atrial electrical disconnection procedure, rather than the effect on the inducibility of atrial fibrillation.

Atrial electrical disconnection was achieved in only 10/13 subjects. Failure occurred in 3 of the first 5 subjects to undergo the procedure. There was a learning curve involving the interpretation of non-contact mapping data and application of radiofrequency energy around the oval fossa. Pathological examination demonstrated that only a small number of applications around the rim of the oval fossa, where the left and right atrial myocardium is continuous as it folds back on itself, were required to sever this connection. The large number of radiofrequency lesions applied around this site in the earlier procedures may have contributed to the high incidence of complete heart block. The effect of ablation of the anatomical inputs to the AV node is also not well defined. Refinement of the procedure, based on greater anatomical and electrophysiological knowledge of the interatrial connections, should be undertaken before embarking on transcatheter left atrial electrical disconnection in the human heart

Conclusions

It is possible to achieve atrial electrical disconnection in the anesthetized swine heart using transcatheter radiofrequency ablation and non-contact mapping. Atrial electrical disconnection reduced atrial fibrillation inducibility from 100% to 30% of animals with successful procedures. Transcatheter atrial electrical disconnection may be a therapeutic option for patients with poorly controlled paroxysmal or persistent atrial fibrillation that are not eligible for ablation of ectopic foci in the pulmonary veins. The right-sided approach avoids the need for transseptal puncture and left atrial ablation. The addition of a biatrial permanent pacemaker with a coronary sinus lead would ensure coordinated left atrial contraction during sinus rhythm as well as the additional antiarrhythmic effects of the pacing modality. If atrial fibrillation should recur in an isolated left atrium, right atrial and ventricular rhythm would still be governed by the sinus node. Further studies are required to reduce the incidence of complete heart block and to examine the effect in the feasibility of this procedure in the human heart.

Chapter 8: Thesis conclusion

This thesis examined the relationship between atrial architecture and electrical activation using non-contact mapping. An extensive review on the literature pertaining to atrial anatomy and its relationship to the origin and subsequent spread of the sinus impulse was discussed. Although a great deal of knowledge was available that described sinus node function, pacemaker shift, the anisotropic nature of myocardial architecture and the role of anatomical structures, the limitations of the electrophysiological mapping techniques available have, to date, prevented detailed descriptions of the onset and spread of depolarization through the left and right atria in the intact beating heart. It is also apparent that the influence of a common diagnostic and therapeutic maneuvre, coronary sinus pacing, on atrial activation patterns had not been fully described. It was anticipated that a greater understanding of the spread of the sinus and paced impulse, and its relationship to underlying myocardial anatomy, would contribute to the design of a therapeutic procedure for the treatment of abnormal atrial rhythms such as atrial fibrillation.

Many previous studies have documented pacemaker shift within and beyond the sinus node during changes in sinus rhythm cycle length. However, the majority of these studies were performed on isolated sections of heart using microelectrode techniques, or in open-chest subjects using multielectrode plaques. In the modern era of electrophysiological procedures endocardial mapping is used to identify impulse origin and the spread of electrical activation. In abnormal conditions, such as inappropriate sinus tachycardia, it has been demonstrated that many sites in the high lateral right atrium show similar activation times, making identification of the impulse origin and the anatomical sinus node very challenging. The study in Chapter 3 of this thesis is the first to describe high density, global endocardial activation of the onset of sinus rhythm and sinus tachycardia over a range of heart rates. During sinus rhythm and sinus tachycardia, earliest endocardial depolarisation arose from one of 2 to 5 sites in a region consistent with the location of the terminal crest. Some sites lay beyond the histological margins of the sinoatrial node. As the cycle length shortened the site of earliest endocardial depolarisation either remained static or shifted 5-55mm in a cranial or caudal direction in an unpredictable manner. Contrary to the previous reports (that were based on very limited mapping techniques with a single multipolar catheter) only a minority of subjects demonstrated a stepwise shift in the origin of earliest endocardial depolarisation in a cranial direction with faster heart rates. Depolarisation entered the endocardium over a diffuse area at cranial sites and a more focal point at caudal sites, a pattern that could be consistent with the multicentric origin of the sinus impulse, but also may be a consequence of the subendocardial position of the head of the sinus node and the subepicardial position of its

tail. These findings suggest that endocardial activation mapping using single catheters may be an inadequate technique for guiding ablation of inappropriate sinus tachycardia, in which destruction of the cranial portion of the sinus node is believed to reduce the resting heart rate and prevent inappropriate tachycardia. Indeed, recent clinical studies suggest that an anatomical approach rather than an activation-guided approach is more efficacious.

A review of the literature regarding the spread of the electrical impulse through the atria reveals that the debate over the presence of specialised conduction tracts has largely been resolved with the improvement of histological and electrophysiological mapping techniques that indicate that such tracts do not exist. The work by Spach and many others has introduced the concept of anisotropic conduction, where the spread of electrical activation is influenced by myocardial fibre orientation. It has been proposed that it is the arrangement of muscle fibres that leads to the preferential spread of depolarisation in certain directions throughout the atria. The study in Chapter 4 is one of the first to describe global high-density patterns of activation in right atrial endocardium in the intact beating heart. Subsequent endocardial dissection reveled the role of fibre arrangement. In the porcine heart at least, the site of earliest activation and underlying endocardial architecture dictates the spread of activation through the right atrium. During sinus rhythm, areas of conduction block or delay may be seen at the junction between the terminal crest and posterior wall, in the cavotricuspid isthmus, and around the margins of the Triangle of Koch, all areas where myocardial fibre arrangement was perpendicular o the direction of activation. Conduction delay and block at these sites was particularly pronounced in recordings with a site of earliest activation in the region of the lateral terminal crest. No previous study has demonstrated the presence of areas of delay or block that result from anisotropic properties of the atrial architecture.

There is very limited data available in the literature on left atrial activation patterns, largely because of the inaccessibility of the chamber, particularly to high-density mapping. The high incidence of atrial fibrillation, together with its associated morbidity and mortality, has aroused a great interest in the underlying mechanisms of this arrhythmia. Left atrial anatomy and the spread of electrical activation may play a significant role in the initiation and maintenance of atrial fibrillation. With this in mind, the study in Chapter 5 undertook to examine left atrial endocardial activation patterns during sinus rhythm and coronary sinus pacing. Non-contact mapping in the human heart revealed that earliest left atrial endocardial activation usually occurred anterior to the right upper or lower pulmonary veins. The subsequent spread of activation followed the longitudinal course of the muscle fibres in Bachmann's bundle across the left atrial roof before spreading down the posterior and lateral walls. Lines of conduction block or delay were present in the posterior wall, most commonly

between the right upper and right lower pulmonary veins, extending inferiorly to the mitral valve annulus. These lines of block were also seen during coronary sinus pacing. Between 1 and 4 discrete connections were present between the coronary sinus and the left atrial musculature, resulting in disparate activation times and directions. The site of earliest left atrial activation during coronary sinus pacing was often distant from the position of the pacing electrodes. The ability to directly record left atrial activation at the same time as coronary sinus activation reinforces the conclusions of two recent studies that there may be dissociation between the coronary sinus and left atrium. There is a need for caution when interpreting coronary sinus electrograms as indices of left atrial activation during electrophysiological studies. Conduction block or delay within the left atrium may also provide a substrate for reentry, thus perpetuating atrial fibrillation.

In Chapter 6 the effect of coronary sinus pacing on right atrial activation was examined. A previous human study described electrical connections between the left and right atrium as occurring at the coronary sinus, oval fossa and Bachmann's bundle. This study did not assess the influence of pacing depth within the coronary sinus. The findings in Chapter 5 have already indicated that the spread of activation through the left atrium depends upon the pacing depth within the coronary sinus, number and position of coronary sinus to left atrium muscular connections, and areas of conduction block or delay within the left atrium. Mapping in the porcine right atrium revealed that coronary sinus pacing results in earliest right atrial activation at the insertion of Bachmann's bundle or at the coronary sinus os. The site of earliest activation was determined by the pacing depth, however there was considerable variety between individuals. The site of earliest activation determined right atrial activation patterns and times. In common with findings in Chapter 4, conduction through the cavotricuspid isthmus was delayed or blocked. This led to activation of the anterolateral wall from inferior to superior by a wavefront that has crossed the posterior wall. Conduction delay was only apparent during proximal coronary sinus pacing as it was disguised when the site of earliest right atrial activation was at Bachmann's bundle. A recent study in human subjects undergoing radiofrequency ablation of atrial flutter has revealed that rapid conduction around the posterior inferior caval vein may mimic trans-isthmus conduction, even after the creation of a complete line of conduction block. The results from Chapters 4 and 6 suggest that in the porcine heart there is delay or block in conduction through the cavotricuspid isthmus during sinus rhythm and during coronary sinus pacing and that the fastest route from medial to lateral cavotricuspid isthmus is around the posterior isthmus. Thus, the porcine heart may not be the most appropriate model to use when investigating atrial flutter mechanisms or therapies.

The review of the literature also discussed the many potential therapies that have been attempted for the treatment of atrial fibrillation. The greatest success in preventing atrial fibrillation has been with surgical therapies such as the left atrial isolation and the Maze procedures. Unfortunately there are many drawbacks with the surgical approach, not in the least the need for open-heart surgery. Attempts to emulate the maze procedure using transvenous radiofrequency ablation techniques have been disappointing. The realisation that non-contact mapping is easily able to identify the different sites of electrical conduction between the left and right atrium during coronary sinus pacing, together with a review of the literature detailing the anatomical basis of interatrial connections, led to a renewed interest in the concept of left atrial isolation. In Chapter 7 the feasibility of a transvenous, right atrial catheter-based ablation technique of left atrial disconnection was attempted. The effect of such a procedure on atrial fibrillation induction was also assessed. It was possible to achieve atrial electrical disconnection in the swine heart in 10/13 animals studied however, left atrial disconnection was achieved in only 5 of these 10. Atrial electrical disconnection reduced atrial fibrillation inducibility from 100% to 30% of animals with successful procedures. It is important to note that a right-sided approach avoids the need for transseptal puncture and left atrial ablation, reducing potential complications. The addition of a biatrial permanent pacemaker with a coronary sinus lead would ensure coordinated left atrial contraction during sinus rhythm as well as the additional antiarrhythmic effects of the pacing modality. If atrial fibrillation should recur in an isolated left atrium, right atrial and ventricular rhythm would still be governed by the sinus node.

Thesis Limitations

The limitations of each individual study are discussed in the preceding chapters. Overall, four of the 5 studies were performed in the porcine heart. Although this enabled excision of the heart and pathological examination, it is not known how applicable the findings are to the human subject. Conversely, in Chapter 5, left atrial mapping was performed in the human heart and the findings were discussed in relation to prior published anatomical studies because direct pathological correlation was not possible. Even when dissection was available, the relationship between endocardial architecture and activation patterns had to be inferred from a comparison of dissection anatomy and the three-dimensional non-contact mapping reconstruction. It was not possible to directly visualize the endocardial architecture during mapping due to the in-vivo nature of the study. It is therefore possible that the precise site of earliest activation and conduction block or delay demonstrated in the studies may not have been correctly identified.

It is not possible to state whether areas of apparent conduction block are genuine, or whether they are the result of conduction delay that occurs for long enough for a separate wavefront to approach the area from the opposite direction. For example, apparent conduction block within the cavotricuspid isthmus in Chapters 4 or 6 may have been the result of slow conduction from the lateral to mid-isthmus, with the medial aspect of the isthmus being activated 20-30 ms later by a septal wavefront that has either crossed the posterior wall or descended from the superior septum.

In Chapter 7 the methodology did not examine the feasibility of atrial electrical disconnection whilst the subject was in atrial fibrillation. In addition, the induction of atrial fibrillation using burst pacing or alternating current delivery in the swine heart may not have reflected the mechanism of initiation and maintenance of patients with persistent atrial fibrillation. To be applicable to a broad population of patients, many who have chronic atrial fibrillation, further studies are required.

Final conclusion

This thesis has demonstrated that non-contact mapping can provide highly detailed three-dimensional maps of atrial activation during sinus and paced rhythm. These maps have been related to endocardial dissection and, combined with previous knowledge, confirm that the spread of electrical activation is determined by the orientation of the underlying muscle architecture. Analysis of the earliest onset of right atrial activation has shown that the relationship between site of activation and heart rate is variable and unpredictable. This suggests that clinical ablation therapy of inappropriate sinus tachycardia should be anatomically guided rather than by activation mapping. Areas of function block are present in the porcine right atrium even during sinus rhythm. These areas, together with the site of earliest activation, define the subsequent pattern of right atrial activation. The human left atrium also displays areas of conduction delay and block during sinus rhythm and coronary sinus, at least in patients with a history of atrial fibrillation. There is electrical dissociation between the coronary sinus and left atrial myocardium, confirming the reported findings of previous anatomical studies. The depth of coronary sinus pacing determines at which site activation enters the right atrium from the left side of the heart and the subsequent right atrial activation pattern. Using this knowledge a transvenous, right atrial procedure for performing left atrial disconnection was devised. The procedure, when successful, was capable of reducing the inducibility of atrial fibrillation. Further studies in the human subject should be undertaken to determine whether similar results may be obtained, and to continue the search

for an effective therapy for atrial fibrillation with minimal associated morbidity and mortality.

References

1. Anderson RH, Ho SY. The anatomy of the heart. Pamphlet: 1997. Pubs: Johnson and Johnson Medical

2. Wang K, Ho SY, Gibson DG, Anderson RH. Architecture of atrial musculature in humans. Br Heart J 1995;73(6):559-565.

3. Cabrera JA, Sanchez-Quintana D, Ho SY, Anderson RH. The architecture of the atrial musculature between the orifice of the inferior caval vein and the tricuspid valve: the anatomy of the isthmus. J Cardiovasc Electrophysiol 1998;9:1186-1195.

4. Sanchez-Quintana D, Davies DW, Ho SY, Oslizlok P, Anderson RH. Architecture of the atrial musculature in and around the triangle of Koch: its potential relevance to atrioventricular nodal reentry. J Cardiovasc Electrophysiol 1997;8(12):1396-1407.

5. Koch W. Weiter Mitteilungen uber den Sinusknoten der Herzens. Verhandlungen der Deutschen Pathologische Anatomie 1909;13:85-92.

6. Ho SY, Sanchez-Quintana D, Cabrera JA, Anderson RH. Anatomy of the left atrium: implications for radiofrequency ablation of atrial fibrillation. J Cardiovasc Electrophysiol 1999;10(11):1525-1533.

7. von Ludinghausen M, Ohmachi N, Boot C. Myocardial coverage of the coronary sinus and related veins. Clin Anat 1992;5:1-15.

8. Chauvin M, Shah DC, Haissaguerre M, Marcellin L, Brechenmacher C. The anatomic basis of connections between the coronary sinus musculature and the left atrium in humans. Circulation 2000;101(6):647-652.

9. Sweeney LJ, Rosenquist GC. The normal anatomy of the atrial septum in the human heart. Am Heart J 1979;98(2):194-199.

10. Anderson RH, Webb S, Brown NA. Clinical anatomy of the atrial septum with reference to its developmental components. Clin Anat 1999;12(5):362-374.

11. Anderson RH, Ho SY. The architecture of the sinus node, the atrioventricular conduction axis, and the internodal atrial myocardium. J Cardiovasc Electrophysiol 1998;9:1233-1248.

12. Opthof T. The mammalian sinoatrial node. Cardiovasc Drugs Ther 1988;1(6):573-597.

13. Keith A, Flack M. The form and nature of the muscular connections between the primary division of the vertebrate heart. J Anat Physiol 1907.

14. Tawara S. Das Reitzleitungssystem des Saugeteirherzen. Jena: G Fischer, 1906.

15. Anderson KR, Ho SY, Anderson RH. Location and vascular supply of sinus node in human heart. Br Heart J 1979;41(1):28-32.

16. He BM, Tan YX, Cheng M, Cui YQ. The surgical anatomy of the sinoatrial node. Surg Radiol Anat 1991;13(2):123-128.

17. Purkinje JE. Mikroskopisch-neurologische Beobactungen. Arch Anat Physiol Wiss Med 1845;281.

18. Wenckebach KF. Beitrëge zur Kenntnis der menschlichen Herztätigkeit. Arch Anat Physiol 1907;1.

19. Thorel C. Uber die supraventrikularen abschnitte des sog. Reizleitungssysyems. Verh Dtsch Ges Pathol 1910;14:71-90.

20. Bachmann G. Inter-auricular time interval. Am J Physiol 1916;41:309-358.

21. James TM. The connecting pathways between the sinus node and A-V node and between the right and left atrium in the human heart. Am Heart J 1963;66:498.

22. Paes de Carvalho A, de Mello WC, Hoffman BF. Electrophysiological evidence for specialized fibre types in rabbit atrium. Am J Physiol 1959;196:483-488.

23. Meredith J, Titus JL. The anatomic connections between sinus and A-V node. Circulation 1968;37:566-579.

24. Anderson RH, Ho SY, Smith A, Becker AE. The internodal atrial myocardium. Anat Rec 1981;201(1):75-82.

25. Lewis T, Meakins J, White PD. The excitatory process in the dog's heart. Part I: The auricles. Phil Trans Roy Soc B 1914;205:375.

26. Eyster JAE, Meek WJ. Experiments on the origin and conduction of the heart beat: IX. Sinoventricular conduction. Am J Physiol 1922;61:130-137.

27. Trautwein W, Zink K. Pflüger's Arch ges Physiol 1952;256:68.

28. Durrer D, Dam Rv, Freud GE, Janse MJ, Meijler FL, Arzbaecher RC. Total excitation of the isolated human heart. Circulation 1970;41(6):899-912.

29. Canavan TE, Schuessler RB, Boineau JB, Corr PB, Cain ME, Cox JL. Computerized global electrophysiological mapping of the atrium in patients with Wolff-Parkinson-White syndrome. Ann Thorac Surg 1988;46:223-231.

30. Chang BC, Schuessler RB, Stone CM, Branham BH, Canavan TE, Boineau JP, Cain ME, Corr PB, Cox JL. Computerized activation sequence mapping of the human atrial septum. Ann Thorac Surg 1990;49(2):231-241.

31. Waldo AL, Bush HI, Gelband H, Zorn GL, Vitikainen KJ, Hoffman BF. Effects on the canine P wave of discrete lesions in the specialized atrial tracts. Circ Res 1971;39:452.

32. Wagner ML, Lazzara R, Weiss RM, Hoffman BF. Specialized conducting fibres in the interatrial band. Circ Res 1966;18:502-518.

33. Spach MS, King TD, Barr RC, Boaz DE, Morrow MN, Herman-Giddens S. Electrical potential distribution surrounding the atria during depolarization and repolarization in the dog. Circ Res 1969;23:857-873.

34. Goodman D, van der Steen A, van Dam RT. Endocardial and epicardial activation pathways of the canine right atrium. Am J Physiol 1971;220:1-11.

35. Sano T, Yamagishi S. Spread of excitation from the sinus node. Circ Res 1965;16:423.

36. Hiraoka M, Adaniya H. Function of atrial preferential conduction routes under normal and abnormal conditions. J Electrocardiol 1983;16(2):123-132.

37. Hayashi H, Lux RL, Wyatt RF, Burgess MJ, Abildskov JA. Relation of canine atrial activation sequence to anatomic landmarks. Am J Physiol 1982;242(3):H421-H428.

38. Spach MS, Lieberman M, Scott JG, Barr RC, Johnson EA, Kootsey JM. Excitation sequences of the atrial septum and the AV node in isolated hearts of the dog and rabbit. Circ Res 1971;29:156-172.

39. Spach MS, Miller WT, Geselowitz DB, Barr RC, Kootsey JM, Johnson EA. The discontinuous nature of propagation in normal canine cardiac muscle. Evidence for recurrent discontinuities of intracellular resistance that affect the membrane currents. Circ Res 1981;48:39-54.

40. Spach MS, Miller WT, Dolber PC, Kootsey JM, Sommer JR, Mosher CEJr. The functional role of structural complexities in the propagation of depolarization in the atrium of the dog. Circ Res 1982;50:175-191.

41. Dolber PC, Spach MS. Structure of canine Bachmann's bundle related to propagation of excitation. Am J Physiol 1989;257(5 Pt 2):H1446-H1457.

42. Hocini M, Loh P, Ho SY. Anisotropic conduction in the triangle of Koch of mammalian hearts: Electrophysiologic and anatomic correlations. J Am Coll Cardiol 1998;31:629-636.

43. Horibe H. Studies on the spread of the right atrial activation by means of intracellular microelectrode. Jap Circ J 1961;25:583.

44. Miyauchi A. Electrical events in specialized muscle fibres of a mammalian right atrium. S-A node. Jap Heart J 1962;3:357.

45. Bleeker WK, Mackaay AJ, Masson-Pevet M, Bouman LN, Becker AE. Functional and morphological organization of the rabbit sinus node. Circ Res 1980;46(1):11-22.

46. Boineau JB, Schuessler RB, Mooney CR. Multicentric origin of the atrial depolaization wave: the pacemaker complex. Relation to dynamics of atrial conduction, P-wave changes and heart rate control. Circulation 1978;58:1036-1048.

47. Boineau JB, Schuessler RB, Hackel DB, Miller CB, Brockus CW, Wylds AC. Widespread distribution and rate differentiation of the atrial pacemaker complex. Am J Physiol 1980;239:H406-H415.

48. Boineau JB, Canavan TE, Schuessler RB, Cain ME, Corr PB, Cox JL. Demonstation of a widely distributed pacemaker complex in the human heart. Circulation 1988;77:1221-1237.

49. Bromberg BI, Hand DE, Schuessler RB, Boineau JP. Primary negativity does not predict dominant pacemaker location: implications for sinoatrial conduction. Am J Physiol 1995;269(3 Pt 2):H877-H887.

50. Spach MS, Barr RC, Serwer GA, Kootsey JM, Johnson EA. Extracellular potentials related to intracellular action potentials in the dog Purkinje system. Circ Res 1972;30:505-519.

51. Kalman JM, Lee R, Fisher WB, Chin M, Ursell PC, Stillson CA, Lesh MD, Scheinman MM. Radiofrequency catheter modification of sinus pacemaker function guided by intracardiac echocardiography. Circulation 1995;92:3070-3081.

52. Lee RJ, Kalman JM, Fitzpatrick AP, Epstein LM, Fisher WG, Olgin JE, Lesh MD, Scheinman MM. Radiofrequency catheter modification of the sinus node for 'inappropriate' sinus tachycardia. Circulation 1995;92:2919-2928.

53. Cosio FG, Arribas F, Barbero JM, Kallmeyer C, Goicolea A. Validation of double-spike electrograms as markers of conduction delay or block in atrial flutter. Am J Cardiol 1988;61(10):775-780.

54. Olgin JE, Kalman JM, Fitzpatrick AP, Lesh MD. Role of right atrial endocardial structures as barriers to conduction during human type I atrial flutter. Activation and entrainment mapping guided by intracardiac echocardiography. Circulation 1995;92(7):1839-1848.

55. Olgin JE, Kalman JM, Lesh MD. Conduction barriers in human atrial flutter: of electrophysiology and anatomy. J Cardiovasc Electrophysiol 1996;7(11):1112-1126.

56. Olshansky B, Okumura K, Henthorn RW, Waldo AL. Characterization of double potentials in human atrial flutter: studies during transient entrainment. J Am Coll Cardiol 1990;15(4):833-841.

57. Tanoiri T, Komatsu C, Ishinaga T. Study on the genesis of double potentials recorded in the high right atrium in atrial flutter and its role in the reentry circuit of atrial flutter. Am Heart J 1991;121:57-61.

58. Yamashita T, Inoue H, Nozaki A, Sugimoto T. Role of anatomic architecture in sustained atrial reentry and double potentials. Am Heart J 1992;124(4):938-946.

59. Tai CT, Chen SA, Chen YJ, Yu WC, Hsieh MH, Tsai CF, Chen CC, Ding YA, Chang MS. Conduction properties of the Crista Terminalis in patients with typical atrial flutter: Basis for a line of block in the reentrant circuit. J Cardiovasc Electrophysiol 1998;9(8):811-819.

60. Arenal A, Almendral J, Alday JL, Villacastin J, Ormaetxe JM, Sande JLM, Perez-Castellano N, Gonzalez S, Ortiz M, Delcan JL. Rate-dependent conduction block of the crista terminalis in patients with typical atrial flutter. Circulation 1999;99:2771-2778.

61. Schumacher B, Jung W, Schmidt H, Fischenbeck C, Lewalter T, Hagendorff A, Omran H, Wolpert C, Luderitz B. Transverse conduction capabilities of the crista terminalis in patients with atrial flutter and atrial fibrillation. J Am Coll Cardiol 1999;34(2):363-373.

62. Antz M, Otomo K, Arruda M, Scherlag BJ, Pitha J, Tondo C, Lazzara R, Jackman WM. Electrical conduction between the right atrium and the left atrium via the musculature of the coronary sinus. Circulation 1998;98(17):1790-1795.

63. Kasai A, Anselme F, Saoudi N. Myocardial connections between left atrial myocardium and coronary sinus musculature in man. J Cardiovasc Electrophysiol 2001;12(9):981-985.

64. Ndrepepa G, Zrenner B, Schneider M, Schreieck J, Karch M, Schomig A, Schmidt C. Dissociation between coronary sinus and left atrial conduction in patients with atrial fibrillation and flutter. J Cardiovasc Electrophysiol 2001;12(6):623-628.

65. Sun H, Velipasaoglu EO, Wu DE, Kopelen HA, Zoghbi WA, Spencer WH, Khoury DS. Simultaneous multisite mapping of the right and the left atrial septum in the canine intact beating heart. Circulation 1999;100:312-319.

66. Cosio FG, Lopez-Gil M, Goicolea A, Arribas F. Electrophysiologic studies in atrial flutter. Clin Cardiol 1992;15(9):667-673.

67. Cosio FG, Goicolea A, Lopez-Gil M, Arribas F. Catheter ablation of atrial flutter circuits. Pacing Clin Electrophysiol 1993;16:637-642.

68. Lesh MD, Van Hare GF, Epstein LM, Fitzpatrick AP, Scheinman MM, Lee RJ, Kwasman MA, Grogin HR, Griffin JC. Radiofrequency catheter ablation of atrial arrhythmias. Circulation 1994;89:1074-1089.

69. Shah D, Jais P, Haissaguerre M, Chouairi S, Takahashi A, Hocini M, Garrigue S, Clementy J. Three-dimensional mapping of the common atrial flutter circuit in the right atrium. Circulation 1997;96:3904-3912.

70. Jais P, Haissaguerre M, Shah DC, Chouairi S, Clementy J. Regional disparities of endocardial atrial activation in paroxysmal atrial fibrillation. Pacing Clin Electrophysiol 1996;19(II):1998-2003.

71. Roithinger FX, Sippensgroenewegen A, Karch MR, Steiner PR, Ellis WS, Lesh MD. Organized activation during atrial fibrillation in man: endocardial and electrocardiographic manifestations. J Cardiovasc Electrophysiol 1998;9(5):451-461.

72. Adam M, Fischetti D, Montenero AS. A typical pattern of activation in the right atrium during paroxysmal atrial fibrillation: the washing-machine phenomenon. Cardiologia 1999;44(1):63-68.

73. Kumagai K, Khrestian C, Waldo AL. Simultaneous multisite mapping studies during induced atrial fibrillation in the sterile pericarditis model. Circulation 1997;95(2):511-521.

74. Cauchemez B, Haissaguerre M, Fischer B, Thomas O, Clementy J, Coumel P. Electrophysiological effects of catheter ablation of inferior vena cava-tricuspid annulus isthmus in common atrial flutter. Circulation 1996;93(2):284-294.

75. Cox JL, Canavan TE, Schuessler RB, Cain ME, Lindsay BD, Stone C, Smith PK, Corr PB, Boineau JB. The surgical treatment of atrial fibrillation. II. Intraoperative electrophysiologic mapping and description of the electrophysiologic basis of atrial flutter and atrial fibrillation. J Thorac Cardiovasc Surg 1991;101(3):406-426.

76. Haissaguerre M, Jais P, Shah DC, Takahashi A, Hocini M, Quiniou G, Garrigue S, Le Moroux A, Metayer P, Clementy J. Spontaneous initiation of atrial fibrillation by ectopic beats originating in the pulmonary veins. N Engl J Med 1998;339(10):659-666.

77. Williams JM, Ungerleider RM, Lofland GK, Cox JL. Left atrial isolation: New technique for the treatment of supraventricular arrhythmias. J Thorac Cardiovasc Surg 1980;80:373-380.

78. Graffigna A, Pagani F, Minzioni G, Salerno J, Vigano M. Left atrial isolation associated with mitral valve operations. Ann Thorac Surg 1992;54:1093-1098.

79. Cox JL, Boineau JB, Schuessler RB, Kater KM, Ferguson TB, Jr., Cain ME, Lindsay BD, Smith JM, Corr PB, Hogue CB, Lappas DG. Electrophysiologic basis, surgical development, and clinical results of the Maze procedure for atrial flutter and atrial fibrillation. Adv Card Surg 1995;6:1-67.

80. Cox JL, Boineau JB, Schuessler RB, Jaquiss RB, Lappas DG. Modification of the Maze procedure for atrial flutter and atrial fibrillation: 1. Rationale and surgical results. J Thorac Cardiovasc Surg 1995;110:473-484.

81. Nitta T, Lee R, Schuessler RB, Boineau JB, Cox JL. Radial approach: a new concept in surgical treatment for atrial fibrillation. I. Concept, anatomic and physiologic bases and development of a procedure. Ann Thorac Surg 1999;67:27-35.

82. Elvan A, Huang X, Pressler M, Zipes DP. Radiofrequency catheter ablation of the atria eliminates pacing-induced sustained atrial fibrillation and reduces connexin 43 in dogs. Circulation 1997;96(5):1675-1685.

83. Tondo C, Sherlag BJ, Otomo K, Antz M, Patterson E, Arruda M, Jackman WM, Lazzara R. Critical atrial site for ablation of pacing-induced atrial fibrillation in the normal dog heart. J Cardiovasc Electrophysiol 1997;8(11):1255-1265.

84. Mitchell MA, McRury ID, Haines DE. Linear atrial ablations in a canine model of chronic atrial fibrillation: morphological and electrophysiological observations. Circulation 1998;97:1176-1185.

85. Jais P, Shah DC, Takahashi A, Hocini M, Haissaguerre M, Clementy J. Long-term follow-up after right atrial radiofrequency catheter treatment of paroxysmal atrial fibrillation. Pacing Clin Electrophysiol 1998;21(II):2533-2538.

86. Schwartzman D, Kuck KH. Anatomy-guided linear atrial lesions for radiofrequency catheter ablation of atrial fibrillation. Pacing Clin Electrophysiol 1998;21:1959-1978.

87. Ernst S, Schluter M, Ouyang F, Khanedani A, Cappato R, Hebe J, Volkmer M, Antz M, Kuck KH. Modification of the substrate for maintenance of idiopathic human atrial fibrillation: efficacy of radiofrequency ablation using nonfluoroscopic catheter guidance. Circulation 1999;100(20):2085-2092.

88. Garg A, Finneran W, Mollerus M, Birgersdotter-Green U, Fujimura O, Tone L, Feld GK. Right atrial compartmentalization using radiofrequency catheter ablation for management of patients with refractory atrial fibrillation. J Cardiovasc Electrophysiol 1999;10(6):763-771.

89. Jais P, Shah DC, Haissaguerre M, Takahashi A, Lavergne T, Hocini M, Garrigue S, Barold SS, Le MP, Clementy J. Efficacy and safety of septal and left-atrial linear ablation for atrial fibrillation. Am J Cardiol 1999;84(9A):139R-146R.

90. Pappone C, Oreto G, Lamberti F, Vicedomini G, Loricchio ML, Shpun S, Rillo M, Calabro MP, Conversano A, Ben-Haim SA, Cappato R, Chierchia S. Catheter ablation of paroxysmal atrial fibrillation using a 3D mapping system. Circulation 1999;100(11):1203-1208.

91. Natale A, Leonelli F, Beheiry S, Newby K, Pisano E, Potenza D, Rajkovich K, Wides B, Cromwell L, Tomassoni G. Catheter ablation approach on the right side only for

paroxysmal atrial fibrillation therapy: long-term results. Pacing Clin Electrophysiol 2000;23(2):224-233.

92. Gepstein L, Evans SJ. Electroanatomical mapping of the heart: Basic concepts and implications for the treatment of cardiac arrhythmias. Pacing Clin Electrophysiol 1998;21:1268-1278.

93. Gandhi SK, Bromberg BI, Rodefeld MD. Lateral tunnel suture line variation reduces atrial flutter after the modified Fontan operation. Ann Thorac Surg 1996;61:1299.

94. Crick SJ, Sheppard MN, Ho SY, Anderson RH. Anatomy of the pig heart: comparisons with normal human cardiac structure. J Anat 1998;193:105-119.

95. Bharati S, Levine M, Huang SK, Handler B, Parr GV, Bauernfeind R, Lev M. The conduction system of the swine heart. Chest 1991;100(1):207-212.

96. Kadish A, Hauck J, Pederson B, Beatty G, Gornick CC. Mapping of atrial activation with a non-contact, multielectrode catheter in dogs. Circulation 1999;99:1906-1913.

97. Schilling RJ, Peters NS, Davies DW. Simultaneous endocardial mapping in the human left ventricle using a non-contact catheter: Comparison of contact and reconstructed electrograms during sinus rhythm. Circulation 1998;98:887-898.

98. Gornick CC, Adler SW, Pederson B, Hauck J, Budd J, Schweitzer J. Validation of a new noncontact catheter system for electroanatomic mapping of left ventricular endocardium. Circulation 1999;99(6):829-835.

99. West TC. Ultramicroelectrode recording from the cardiac pacemaker. J Pharmacol Exp Ther 1955;115:283-290.

100. Bouman LN, Gerlings ED, Biersteker PA. Pacemaker shift within the sino-atrial node during vagal stimulation. Pflüger's Arch ges Physiol 1968;302:255-267.

101. Boineau JB, Schuessler RB, Roeske WR, Autry LJ, Miller CB, Wylds AC. Quantitative relationship between sites of atrial impulse origin and cycle length. Am J Physiol 1983;245:H781-H789.

102. Randall WC, Talano JV, Kaye MP. Cardiac pacemakers in absence of the SA node: responses to exercise and autonomic blockade. Am J Physiol 1978;234:H465-H470.

103. Marrouche NF, Beheiry S, Tomassoni G, Cole C, Bash D, Dresing T, Saliba W, Abdul-Karim A, Tchou P, Schweikert R, Leonelli F, Natale A. Three-dimensional nonfluoroscopic mapping and ablation of inappropriate sinus tachycardia. Procedural strategies and long-term outcome. J Am Coll Cardiol 2002;39(6):1046-1054.

104. Man KC, Knight BP, Tse HF, Pelosi F, Michaud GF, Flemming M, Strickberger A, Morady F. Radiofrequency catheter ablation of inappropriate sinus tachycardia guided by activation mapping. J Am Coll Cardiol 2001;35(2):451-457.

105. Ren JF, Marchlinski FE, Callans DJ, Zado ES. Echocardiographic lesion characteristics associated with successful ablation of inappropriate sinus tachycardia. J Cardiovasc Electrophysiol 2001;12(7):814-818.

106. De Ponti R, Ho SY, Salerno-Uriarte JA, Tritto M, Spadacini G. Electroanatomic Analysis of Sinus Impulse Propagation in Normal Human Atria. J Cardiovasc Electrophysiol 2002;13:1-10.

107. Spach MS, Heidlage JF. The stochastic nature of cardiac propagation at a microscopic level: Electrical description of myocardial architecture and its application to conduction. Circ Res 1995;76:366-380.

108. Yamashita T, Oikawa N, Inoue H, Murakawa Y, Nakajima T, Usui M, Ajiki K, Ohkawa S, Sugimoto T. Slow abnormal conduction in the low right atrium: Its anatomic basis and relevance to atrial reentry. Am Heart J 1994;127:353-359.

109. Hindricks G, Kottkamp H. Simultaneous noncontact mapping of left atrium in patients with paroxysmal atrial fibrillation. Circulation 2001;104(3):297-303.

110. Platonov PG, Yuan S, Hertervig E, Kongstad O, Roijer A, Vygovsky AB, Chireikin LV, Olsson SB. Further evidence of localized posterior interatrial conduction delay in lone paroxysmal atrial fibrillation. Europace 2001;3(2):100-107.

111. Omori I, Inoue D, Shirayama T, Asayama J, Katsume H, Nakagawa M. Prolonged atrial activity due to delayed conduction in the atrium of patients with paroxysmal atrial fibrillation. Heart Vessels 1991;6(4):224-228.

112. Haissaguerre M, Jais P, Shah DC, Takahashi A, Hocini M, Quiniou G, Garrigue S, Le Mouroux A, Le Metayer P, Clementy J. Spontaneous initiation of atrial fibrillation by ectopic beats originating in the pulmonary veins. New Engl J Med 1998;339(10):659-666.

113. Jalife J, Berenfeld O, Skanes A, Mandapati R. Mechanisms of atrial fibrillation: mother rotors or multiple daughter wavelets, or both? J Cardiovasc Electrophysiol 1998;9(8 Suppl):S2-12.

114. Papageorgiou P, Anselme F, Kirchhof CJ, Monahan K, Rasmussen CA, Epstein LM, Josephson ME. Coronary sinus pacing prevents induction of atrial fibrillation. Circulation 1997;96(6):1893-1898.

115. Olgin JE, Jayachandran JV, Engesstein E, Groh W, Zipes DP. Atrial macroreentry involving the myocardium of the coronary sinus: a unique mechanism for atypical flutter. J Cardiovasc Electrophysiol 1998;9(10):1094-1099.

116. Delfaut P, Saksena S, Prakash A, Krol RB. Long-term outcome of patients with drug-refractory atrial flutter and fibrillation after single- and dual-site right atrial pacing for arrhythmia prevention. J Am Coll Cardiol 1998;32(7):1900-1908.

117. Roithinger FX, Cheng J, Sippensgroenewegen A, Lee RJ, Saxon LA, Scheinman MM, Lesh MD. Use of electroanatomic mapping to delineate transseptal atrial conduction in humans. Circulation 1999;100(17):1791-1797.

118. Friedman PA, Luria D, Fenton AM, Munger TM, Jahangir A, Shen WK, Rea RF, Stanton MS, Hammill SC, Packer DL. Global right atrial mapping of human atrial flutter: the presence of posteromedial (sinus venosa region) functional block and double potentials: a study in biplane fluoroscopy and intracardiac echocardiography. Circulation 2000;101(13):1568-1577.

119. Scaglione M, Riccardi R, Calo L, Di DP, Lamberti F, Caponi D, Coda L, Gaita F. Typical atrial flutter ablation: conduction across the posterior region of the inferior

vena cava orifice may mimic unidirectional isthmus block. J Cardiovasc Electrophysiol 2000;11(4):387-395.

120. Inoue S, Becker AE. Posterior extensions of the human compact atrioventricular node: a neglected anatomic feature of potential clinical significance. Circulation 1998;97(2):188-193.

121. Roithinger FX, Steiner PR, Goseki Y, Sparks PB, Lesh MD. Electrophysiologic effects of selective right versus left atrial linear lesions in a canine model of chronic atrial fibrillation. J Cardiovasc Electrophysiol 1999;10(12):1564-1574.

122. Gilligan DM, Fuller IA, Clemo HF, Shepard RK, Dan D, Wood MA, Ellenbogen KA. The acute effects of biatrial pacing on atrial depolarization and repolarization. Pacing Clin Electrophysiol 2000;23(7):1113-1120.

123. Yu WC, Tsai CF, Hsieh MH, Chen CC, Tai CT, Ding YA, Chang MS, Chen SA. Prevention of the initiation of atrial fibrillation: mechanism and efficacy of different atrial pacing modes. Pacing Clin Electrophysiol 2000;23(3):373-379.

Publications arising from the Thesis

Betts TR, Ho SY, Sanchez-Quintana D, Roberts PR, Anderson RH, Morgan JM. Characteristics of Right Atrial Activation During Coronary Sinus Pacing. J Cardiovasc Electrophysiol 2002;13(8):794-800

Betts TR, Roberts PR, Morgan JM. Feasibility of a Left Atrial Electrical Disconnection Procedure for Atrial Fibrillation Using Transcatheter Radiofrequency Ablation. J Cardiovasc Electrophysiol 2001;12(11):1278-83

Betts TR, Roberts PR, Ho SY, Morgan JM. High-density endocardial mapping of the onset of sinus rhythm and sinus tachycardia. Pacing Clin Electrophysiol 2003; 26[Pt. I]:1–9

Betts TR, Ho SY, Sanchez-Quintana D, Roberts PR, Anderson RH, Morgan JM. Three-dimensional mapping of right atrial activation during sinus rhythm and its relationship to endocardial architecture. J Cardiovasc Electrophysiol 2002; 13(11): 1152-1159

Abstracts presented at national and international meetings

TR Betts, PR Roberts, SA Allen, JM Morgan. Feasibility of a left atrial isolation procedure using transcatheter radiofrequency ablation. British Cardiac Society, Manchester, 2001

TR Betts, SY Ho, D Sanchez-Quintana, PR Roberts, RH Anderson, JM Morgan. The relationship between myocardial architecture and activation patterns in the right atrium. North American Society of Pacing and Electrophysiology, Boston, 2001

TR Betts, PR Roberts, JM Morgan. Feasibility of a transcatheter left atrial isolation procedure to treat atrial fibrillation. North American Society of Pacing and Electrophysiology, Boston, 2001

TR Betts, PR Roberts, DC Smith, S Allen, JM Morgan. Site of earliest sinus node activity during sinus rhythm and sinus tachycardia. Cardiostim, Nice, 2000

TR Betts, PR Roberts, S Allen, JM Morgan. Earliest Sites of Sinus Node Activation at Varying Rates of Sinus Rhythm and Sinus Tachycardia. North American Society of Pacing and Electrophysiology, Washington, 2000

TR Betts, SY Ho, D Sanchez-Quintana, PR Roberts, DC Smith, RH Anderson, JM Morgan. The relationship between right atrial endocardial architecture and intra atrial conduction. European Society of Cardiology, Amsterdam, 2000

TR Betts, PR Roberts, DC Smith, S Allen, JM Morgan. Site of sinus node pacemaker activity at varying heart rates. British Cardiac Society, Glasgow, 2000